

BUCKLING BEHAVIOR OF REINFORCED CONCRETE

PLATE MODELS

by

Abdoulaye Yaya SECK

B.S., Ecole Nationale d'Ingenieurs

de Bamako, MALI, West Africa, 1974

A MASTER'S THESIS

submitted in partial fulfillment of the
requirements for the degree

MASTER OF SCIENCE

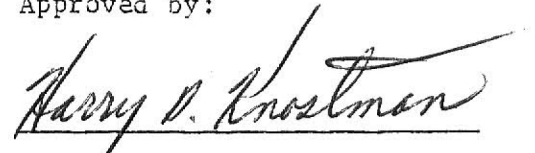
Department of Civil Engineering

KANSAS STATE UNIVERSITY

Manhattan, Kansas

1983

Approved by:


Major Professor

LD
2668
TY
1983
S42
C.2

List of Figures -----	iii
List of Tables -----	vi
CHAPTER 1 INTRODUCTION -----	1
1.1 General Comments -----	1
1.2 Literature Survey -----	2
1.3 Motivation, Scope, and Objectives of this Study -----	4
CHAPTER 2 MODELING ANALYSIS OF TEST STRUCTURE -----	6
2.1 Material Similitude Requirements -----	6
2.2 Steel Reinforcement -----	8
2.3 Concrete Pumpability -----	8
CHAPTER 3 CRITICAL LOAD -----	9
3.1 Experimental Values of the Buckling Load -----	9
3.2 Analytical Determination of the Buckling Load -----	11
CHAPTER 4 EXPERIMENTAL PROCEDURE -----	16
4.1 Equipment Investigation -----	16
4.2 Description of Structural Model -----	17
4.2.1 Structural Model Characteristics -----	17
4.2.2 Microconcrete Reinforcement -----	18
4.3 Construction of Model -----	23
4.3.1 Formwork and Site Preparation -----	23
4.3.2 Microconcrete Preparation and Form Pumpability -	24
4.3.3 Form Removing and Concrete Curing Process -----	27
4.4 Test Cylinders -----	27
4.5 Test Frame and Test Panel Preparation -----	34
4.6 Apparatuses and Testing Procedure -----	36

CHAPTER 5	REVIEW AND DISCUSSION OF TEST RESULTS -----	45
5.1	General Comments -----	45
5.2	Analytical Method -----	45
5.3	Experimental Method -----	47
5.4	Comparison and Discussion of Results -----	48
CHAPTER 6	SUMMARY, CONCLUSION, AND RECOMMENDATIONS -----	51
6.1	Summary -----	51
6.2	Conclusions -----	52
6.3	Recommendations -----	53
BIBLIOGRAPHY	-----	112
APPENDIX A	COMPUTER PROGRAM -----	114
APPENDIX A	NOTATION -----	116

LIST OF FIGURES

<u>Figure</u>		<u>Page</u>
4.1	Completed Form -----	19
4.2	Moyno Open Throat Pump -----	19
4.3	Stress-Strain Curve for Reinforcement -----	22
4.4	Stress-Strain Curve for Plates 1,2,3,4 -----	29
4.5	Stress-Strain Curve for Plates 8,9,10,11 -----	30
4.6	Stress-Strain Curve for Plates 12,16 -----	31
4.7	Stress-Strain Curve for Plates 5,6,7,17 -----	32
4.8	Stress-Strain Curve for Plates 15,20 -----	33
4.9	Plate Thickness Measurement Device -----	37
4.10a	Plate Average Thickness Values -----	38
4.10b	Plate Average Thickness Values -----	39
4.11	Plate "Beam-Case" Deflection Measurement Device -----	37
4.12	Gage Locations on Test Plate -----	40
4.13	Simply-Supported Test Plate -----	41
4.14	Test Plate With Two Double Clip Angles -----	41
5.1	Typical Behavior of Plate When Subjected to Plate or Column Type Buckling Load -----	57
5.1a	Load vs. Strain, Plate 1, Gages 1 & 2 -----	58
5.1b	Load vs. Strain, Plate 1, Gages 3 & 4 -----	59
5.1c	Load vs. Strain, Plate 1, Gages 5 & 6 -----	60
5.1d	Deflection Profiles for Plate 1 -----	61
5.2a	Load vs. Strain, Plate 2, Gages 1 & 2 -----	62
5.2b	Load vs. Strain, Plate 2, Gages 3 & 4 -----	63
5.2c	Load vs. Strain, Plate 2, Gages 5 & 6 -----	64
5.2d	Deflection Profiles for Plate 2 -----	65
5.3a	Load vs. Strain, Plate 3, Gages 1 & 2 -----	66
5.3b	Load vs. Strain, Plate 3, Gages 3 & 4 -----	67
5.3c	Load vs. Strain, Plate 3, Gages 5 & 6 -----	67
5.3d	Deflection Profiles for Plate 3 -----	68

LIST OF FIGURES (continued)

<u>Figure</u>	<u>Page</u>
5.4a Load vs. Strain, Plate 4, Gages 1 & 2 -----	69
5.4b Load vs. Strain, Plate 4, Gages 3 & 4 -----	69
5.4c Load vs. Strain, Plate 4, Gages 5 & 6 -----	70
5.4d Deflection Profiles for Panel 4 -----	71
5.5a Load vs. Strain, Plate 5, Gages 1 & 2 -----	72
5.5b Load vs. Strain, Plate 5, Gages 3 & 4 -----	72
5.5c Load vs. Strain, Plate 5, Gages 5 & 6 -----	73
5.5d Deflection Profiles for Panel 5 -----	74
5.6a Load vs. Strain, Plate 6, Gage 2 -----	75
5.6b Load vs. Strain, Plate 6, Gages 3 & 4 -----	75
5.6c Load vs. Strain, Plate 6, Gage 6 -----	76
5.6d Deflection Profiles for Panel 6 -----	77
5.7d Deflection Profiles for Plate 7 -----	78
5.8d Deflection Profiles for Panel 8 -----	79
5.9d Deflection Profiles for Panel 9 -----	80
5.10a Load vs. Strain, Plate 10, Gages 1 & 2 -----	81
5.10b Load vs. Strain, Plate 10, Gages 3 & 4 -----	82
5.10c Load vs. Strain, Plate 10, Gages 5 & 6 -----	83
5.10d Deflection Profiles for Plate 10 -----	84
5.11d Deflection Profiles for Plate 11 -----	85
5.12d Deflection Profiles for Plate 12 -----	86
5.14a Load vs. Strain, Plate 14, Gages 1 & 2 -----	87
5.14b Load vs. Strain, Plate 14, Gages 3 & 4 -----	87
5.14c Load vs. Strain, Plate 14, Gages 5 & 6 -----	88
5.14d Deflection Profiles for Plate 14 -----	89
5.15a Load vs. Strain, Plate 15, Gages 1 & 2 -----	90

LIST OF FIGURES (continued)

v

<u>Figure</u>	<u>Page</u>
5.1 Typical Behavior of Plate When Subjected to Plate or Column-Type Buckling Loads -----	57
5.15b Load vs. Strain, Plate 15, Gages 3 & 4 -----	90
5.15c Load vs. Strain, Gages 5 & 6, Plate 15 -----	91
5.15d Deflection Profiles for Plate 15 -----	92
5.16a Load vs. Strain, Plate 16, Gages 1 & 2 -----	93
5.16b Load vs. Strain, Plate 16, Gages 3 & 4 -----	94
5.16c Load vs. Strain, Plate 16, Gages 5 & 6 -----	95
5.16d Deflection Profiles for Plate 16 -----	96
5.17a Load vs. Strain, Plate 17, Gages 1 & 2 -----	97
5.17b Load vs. Strain, Plate 17, Gages 3 & 4 -----	97
5.17c Load vs. Strain, Plate 17, Gages 5 & 6 -----	98
5.17d Deflection Profiles for Plate 17 -----	99
5.18d Deflection Profiles for Plate 18 -----	100
5.19a Load vs. Strain, Plate 19, Gages 1 & 2 -----	101
5.19b Load vs. Strain, Plate 19, Gages 3 & 4 -----	101
5.19c Load vs. Strain, Plate 19, Gages 5 & 6 -----	102
5.19d Deflection Profiles for Plate 19 -----	103

LIST OF TABLES

<u>Table</u>	<u>Page</u>
4.1 Pump Specifications -----	20
4.2 Mix -----	21
4.3 Plate Pouring Dates and Slump ASTM C143 Test -----	25
4.4 Cylinder Test Log -----	28
4.5 Strain Gage Properties -----	42
4.6 Panel Support Conditions -----	43
5.1 Values of Critical Load P_{crT} (ACI) Using Theoretical Panel Thickness -----	104
5.2 Values of P_{crT} (ACI) Using Actual Panel Thickness -----	104
5.3 Cylinder Compressive Load-Strain Data From Five Batches -----	105
5.4 Theoretical Values of Critical Load (P_{crT}) Using Design Panel Thickness -----	106
5.5 Theoretical Values of Critical Load (P_{crA}) Using Actual Panel Thickness -----	107
5.6 Evaluation of Experimental Buckling Load ($P_{cr E_i}$) Using Different Approaches -----	108
5.7 Identification of the Buckling Loads -----	109
5.8 Buckling Ratio Results -----	110
5.9 Values of the Modulus of Elasticity of Concrete Based on Different Formulas -----	111

**THIS BOOK
CONTAINS
NUMEROUS PAGES
WITH THE ORIGINAL
PRINTING BEING
SKEWED
DIFFERENTLY FROM
THE TOP OF THE
PAGE TO THE
BOTTOM.**

**THIS IS AS RECEIVED
FROM THE
CUSTOMER.**

ACKNOWLEDGMENTS

The author is greatly acknowledged to his advisor, Dr. Harry D. Knostman, for his guidance and incredible assistance no matter the time, during the elaboration of this research.

Sincere thanks are extended to Dr. Stuart E. Swartz for his treasureous contribution and guidance, and to Dr. Robert Snell, Head of the Department of Civil Engineering for his tuition waiver support, to Dr. Peter B. Cooper, Cecil H. Best and Wayne W. Williams for their contributions in my studies at Kansas State University.

Sincere appreciation is extended to Russell Gillespie and Gerry Pons for their assistance in the Civil Engineering Design Shop.

Special appreciation is extended to Peggy Selvidge and Lori Meyer for typing this thesis.

Deep gratitude is addressed to my country and the African-American Institute in New York, New York for providing me sponsored guidance and a total financial support until the completion of my degree.

To my wife Penda, my Mom, my brothers and sisters, I dedicated this work for all of you.

CHAPTER 1

INTRODUCTION

1.1 General Comments

Structural reinforced concrete plates have recently become more widely used as components of common structures such as folded plates, T-beams, box girders and especially as shear and bearing wall in the building industry. In current practice, the plates are generally supported monolithically along all sides, as in folded plates or box girders, or may be supported with small restraint against rotation, as in precast panels for walls (17). The latter is the most commonly used.

For buckling analysis of precast wall panels, the loaded edges are generally assumed to be supported and the unloaded edges free. Such concrete may be subjected to compressive stresses of considerable magnitude. Thus, the possibility of plate buckling may occur. Depending upon how the unloaded edges are supported, the plate will buckle into single or biaxial curvature.

This report presents the fabrication procedure and the results of testing a series of twenty reinforced concrete plates in uniaxial compression.

1.2 Literature Survey

Very little work has been done in the historical development of the buckling of reinforced concrete plates. The only work in this domain was by Ernst in 1953 (8) who tested small mortar panels which were simply supported along the loaded edges and elastically restrained along the other edges by steel channels. Yokel and Dickers (16) performed buckling tests on masonry walls where the column type buckling governed with regard to the support conditions.

A recent paper presented by Swartz, Rosebraugh and Berman (17), shows the results of a series of tests on rectangular reinforced concrete panels simply-supported on all edges, and subjected to uniaxial compression. All panels showed a plate type buckling before they failed. It was recorded that the initial buckling capacities of the panels were lower than their final load-carrying capacities. The methods used to determine the critical load will be discussed in chapter 3.

The ACI Building Code 318-77 (6), which used a column type formula for estimating wall stresses, is more conservative than that proposed by the ACI Wall Committee 533 (7) which recommends and suggests design procedures to be used for precast wall panels not indicated or given in ACI 318-77 (6). An attempt will be made to verify this empirical design method with experimental results. Because of our desirability of going to smaller models, some of the ACI specifications were not met. The Laboratory work, the equipment size, and the reasonable conception of making test specimens, required the use of small scale models for determining the response of concrete structures to collapse and predicting the prototype behavior. Also, the scale factor used to scale down the aggregate gradation of the prototype structure led this study to the use of microconcrete.

Munoz (13) tested ten panels of size 24 in. long, 12 in. wide, and 0.25 in. thick. All panels were simply-supported at top and bottom edges with three support conditions at the long vertical edges and one steel ratio. The panels simply-supported along the vertical edges showed a plate type buckling as in the prototype and good agreement with the theoretical buckling strength was reached. However, the panels with clip angles along the long sides displayed a column type buckling also expected in the prototype, but the buckling capacity predicted did not agree well with the experimental results, partly because the equation

was not used properly.

1.3 Motivation, Scope, and Objectives of this Study

The essential motivation of this study was to run more tests to collect experimental datas. There has been little attempt to investigate the proposed design equations, and to compare them with the experimental values. The availability of high strenght concrete and of the greater quality control on mix design make possible the production of thinner plates for precast construction so that failure due to buckling should be considered.

The scope of this report included the different steps involved in the fabrication and the testing in uniaxial compression of twenty precast microconcrete wall panel models. The size of the model was determined to be 24 in. long, 12 in. wide and 0.25 in. thick. All the tested structure models were simply-supported at top and bottom. Three types of support conditions along the vertical edges were considered, simply-supported, two clip angles at mid-heigh, and free edges. An axial load was applied uniformily. In addition, three different steel ratios were used for the reinforcement systems.

Finally, the objectives of this study were to investigate

the method of making the microconcrete plates with wire reinforcing using superplasticizer in the mix proportions and the testing of the models to see whether they could be used to predict the buckling load of the prototype. Analytical predictions and experimental values of the buckling load are presented in this report for comparison.

CHAPTER 2

MODELING ANALYSIS OF TEST STRUCTURE

There have been several useful techniques developed in direct modeling of reinforced concrete structural systems. High compatibility is required between the model and the prototype materials. The fabrication of the microconcrete panel depends on three major considerations which are the materials similitude, a suitable steel reinforcement and the pumpability of concrete.

2.1 Material Similitude Requirements

The basic similitude requirements for the design of structural models have been treated by Zia, White, and Vanhorn (19). A direct structural model may be used to predict the overall prototype responses even though certain details of the behavior may not have been reproduced. Yet, it is necessary that all linear dimensions of the model be scale down from the corresponding dimensions of the prototype by a linear scale factor ratio. It is recommended that model materials be used as

similar as possible to prototype materials. Preliminary material tests are essential for the successful applications of direct model analysis in reinforced concrete structures. Because of uncertainties concerning failure criteria, particular attention should be devoted to carefully matching material stress-strain characteristics of both microconcrete model and the prototype structures (1).

In Reference (14), Sabnis through his work, has shown that it is not possible to model by merely scaling the individual components, e.g., coarse aggregates, cement, and admixtures according to laws of similitude. No limitation is imposed on the selection of model concrete as long as the overall physical properties of the model material such as the stress-strain curve and the failure envelope are similar to those of the prototype concrete. For instance, compressive strength, tensile strength and shrinkage characteristics might be modeled (5), keeping in mind that tensile strengths tend to become relatively greater as the scale of the mix is reduced while small amounts of water reduce shrinkage but wetter mixes are easier to place. References (1,9,11,19) also complement the paper presented by Sabnis (14).

2.2 Steel Reinforcement

The problem of providing suitable reinforcement in small scale direct models of reinforced concrete structures is examined in detail by Harris, Sabnis and White (9). Deformed model reinforcement is needed to best simulate the behavior of prototype structural concrete reinforced by deformed bars. Careful choice of model reinforcement, combined with the proper annealing processes, will result in reinforcing of suitable strength properties for each particular model study (19,5,6,1).

2.3 Concrete Pumpability

A method of analysis is presented by Anderson (2) to gage the relative pumpability of a given concrete mixture. The flow of concrete in a pumpline has been described as "plug flow" whereby the concrete slides on a thin film of mortar along the pipewall. A testing and evaluation program for optimum pumpability of concrete was also conducted by Best and Lane, Browne and Bamforth, and Houghton (3,4,10) to determine significant parameters relative to pumping concrete mixture. The effects of numerous variables on the pumping characteristics of concrete were investigated, including water-cement ratio; mortar volume; air content; slump; and the admixtures.

CHAPTER 3

CRITICAL LOAD

Certain formulas and approaches have been developed to determine the critical load of a structure. These equations contain parameters which depend on the structural geometry, boundary conditions, loading and material characteristics. One experimental approach and three theoretical methods of analysis will be discussed in this report. Comparison will be made between the values of buckling load obtained experimentally and those predicted by the column type formulas, plate type formulas, or ACI Journal reduced formula of July 1971 (7).

3.1 Experimental Evaluation of the Buckling Load

Three methods of determining the experimental critical load were considered in this study.

The method used by Miknail and Guralnick(18,12) to find the buckling load is based on the behavior of strain gages mounted on the plate in the direction of the applied load, on opposite

faces at the location nearest the center of the bulged surface. The buckling load was taken as the last load prior to the decrease in the strain on the tension side of the plate, while the strain on the compressive side increased more rapidly. When this critical load could be determined, it was used as the experimental buckling load for comparison with the design buckling load of the tested plates.

Another method of determining the critical buckling load was to consider the lateral deflection profile curves (18). The critical load was taken as the last load at which the displacements of the dial gages were read before failure occurred. This method was used only when the information from the strain gages was not available.

The last of the experimental methods for evaluating the buckling load was the averaged strain method. In Reference (15), Souza, Fok and Walker have described the averaged strain technique which is a purely experimental method of determining the critical load of a test specimen. The method consists of plotting the averaged strain against load of two strain gages mounted back to back. A graph with two distinctly linear portions is usually obtained, the junction of which is taken to be a measure of the critical load. In other words, the critical load is the junction of the two distinct slopes of the curve.

However, the accuracy of this technique relies on the fact that the linear position of the post-buckling path is located ambiguously. If the test has to be terminated prematurely, due perhaps to the failure of the specimen, an erroneous result might be obtained. Furthermore, this technique does not take into account the initial imperfection, which tends to blur the division of the position of the graph (15). According to the authors, serious doubts must be cast on the validity of this interpretation.

3.2 Analytical Determination of the Buckling Load

The predicted buckling load was calculated using three different formulas selected according to the support conditions.

Whenever the long edges support condition was two clip angles or free, the panel buckles as a column. Therefore, the critical load may be calculated using the Euler's Formula:

$$P_{cr} = \frac{n^2 \pi^2 EI}{L^2} \text{-----Eq.(3.1)}$$

where E = Tangent Modulus for Concrete,

I = Moment of Inertia about bending axis,

L = unsupported length of panel,

n = number of waves panel deflects.

The critical load is also :

$$P_{cr} = A_c f_{cr} + A_s E_s \epsilon_{cr} \quad \text{-----Eq. (2.2)}$$

where

A_c, A_s = Areas of Concrete and Steel, respectively,

E_s = Modulus of Elasticity of Steel,

f_{cr} = Critical Stress in Concrete,

ϵ_{cr} = Critical Strain in Concrete.

Figure 3.1 shows the plate proportions and the direction of the applied load:

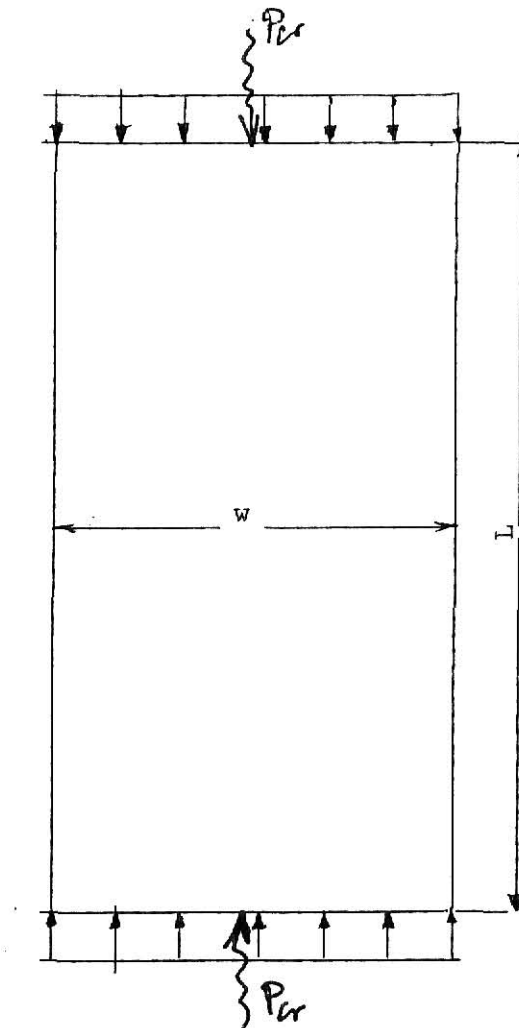


Figure 3.1 Applied Load on Test Panel

The stress-strain curve for the microconcrete is assumed to be a second order parabolic equation, of the form,

$$f_c = A_1 \epsilon_c + B_1 \epsilon_c^2 + C_1 \text{ --- Eq. (3.3a)}$$

The solution of this equation as presented by Munoz (13) defines:

- i. the concrete parabolic formula,

$$f_c = 0.85 f'_c (2e - e^2), \text{ --- Eq. (3.3b)}$$

where $e = \frac{\epsilon_c}{\epsilon_o}$ and ϵ_o is the strain at ultimate stress.

- ii. the critical stress for concrete,

$$f_{cr} = 0.85 f'_c \left[2 \frac{\epsilon_{cr}}{\epsilon_o} - \left(\frac{\epsilon_{cr}}{\epsilon_o} \right)^2 \right] \text{ --- Eq. (3.3c)}$$

- iii. the Tangent Modulus for concrete as the slope of the stress-strain curve at any point,

$$E_T = \frac{df_c}{d\epsilon_c} = \frac{1.7 f'_c}{\epsilon_o} \left[1 - \frac{\epsilon_c}{\epsilon_o} \right] \text{ --- Eq. (3.4)}$$

By substitution of Eq. (3.4) into (3.1), then equating with Eq. (3.2) and collecting terms, one obtains,

$$\frac{n^2 \pi^2 I}{L^2} \cdot \frac{1.7 f'_c}{\epsilon_o} \left[1 - \frac{\epsilon_{cr}}{\epsilon_o} \right] = A_c \left[f'_c \left(2 \frac{\epsilon_{cr}}{\epsilon_o} - \left(\frac{\epsilon_{cr}}{\epsilon_o} \right)^2 \right) \right] + A_s E_s \epsilon_{cr} \text{ --- Eq. (3.5)}$$

The value of ϵ_{cr} determined in Eq. (3.5), is then entered into Eq. (3.3c) to calculate the critical stress f_{cr} . With these values, the buckling load, which is also the critical load of the panel due to column action, is evaluated by Eq. (3.2).

When the panel buckles as a plate, the use of a simplified design formulas has been proposed by Swartz and Rosebraugh in Reference (16).

The critical load is calculated according to the following:

The buckling strain is defined as

$$\epsilon_{cr} = e_{cr} \epsilon_o \text{ - - - - - Eq. (3.6)}$$

where,

$$e_{cr} = 1 + \frac{1}{2} (B - \sqrt{4 + B^2}) \text{ - - - - - Eq. (3.7)}$$

For laboratory work the concrete buckling is defined as

$$f_{cr} = 0.425 f'_c B (-B + \sqrt{4 + B^2}) \text{ - - - - - Eq. (3.8)}$$

where,

$$B = \frac{\pi^2}{6\epsilon_o(1-\rho)} \left[\frac{1}{\ell} + \ell \right]^2 \left(\frac{t}{w} \right)^2$$

$$\ell = \frac{L}{w} \text{ if } \frac{L}{w} < 1;$$

$$\ell = 1 \text{ if } \frac{L}{w} \geq 1;$$

The plate buckling load is then defined as

$$P_{cr} = C_s w(t) [f_{cr}(1-\rho) + E_s \epsilon_{cr} \rho]; \text{ for } \epsilon_{cr} \leq \epsilon_y, \text{ - - - - - Eq. (3.10)}$$

or,

$$P_{cr} = C_s w(t) [f_{cr}(1-\rho) + f_y \rho]; \text{ for } \epsilon_{cr} > \epsilon_y. \text{ - - - - - Eq. (3.10a)}$$

where C_s , factor of safety = 1 for laboratory experiments

t = thickness of panel,

w = width of panel,

ρ = steel ratio.

The value of B determined in Eq. (3.9), is used to calculate f_{cr} , e_{cr} and ϵ_{cr} in Eq. (3.8), (3.7) and (3.6) respectively. The critical load due to plate action is then evaluated using Eq. (3.10) or (3.10a).

From ACI Code Specifications (6) for wall buckling the nominal

axial load strength (P_{nw}) of a wall according to Section 14.2.3, is

$$\phi P_{nw} = 0.55 \phi f'_c A_g \left[1 - \left(\frac{L}{40t} \right)^2 \right] \text{ --- Eq. (14.1)}$$

For experimental analysis, this formula becomes

$$P_{nw} = f'_c A_g \left[1 - \left(\frac{L}{40t} \right)^2 \right] \text{ --- Eq. (14.1a)}$$

However, Specification 14.2.5 limits the thickness to height or width ratio to not less than 1:25,

$$\frac{t}{L} \text{ or } \frac{t}{w} \geq \frac{1}{25} .$$

For the present microconcrete panels, this ratio is:

$$\frac{1}{4 \times 12} = \frac{1}{48} \text{ which is less than } \frac{1}{25} .$$

Therefore, according to ACI Specification 14.2.5, the model panels cannot carry any load (6). From Euler's Formula,

$$P_{cr} = n^2 \frac{\pi^2 EI}{L^2} \text{ --- Eq. (3.1)}$$

and from ACI Specification 8.5.1,

$$E = 33w_c^{1.5} \sqrt{f'_c} \text{ --- Eq. (3.11)}$$

where, w_c = unit weight of concrete

$$I = \frac{1}{12} (w) (t)^3 \text{ --- Eq. (3.12)}$$

Defining the critical stress as $F_a = P_{cr}/A_g$, where $A_g = w \cdot t$ and substituting Eqs. (3.11) and (3.12) into Eq. (3.1) and taking $n = 1$, one obtains

$$F_a = \frac{\pi^2 33}{12} w_c^{1.5} \sqrt{f'_c} \left[\frac{t}{L} \right]^2 = (27.14) w_c^{1.5} \sqrt{f'_c} \left[\frac{t}{L} \right]^2 \text{ --- Eq. (3.13)}$$

which is approximately the formula proposed in the July 1971 ACI Journal (7)

$$F_a = 22.22 w_c^{1.5} \sqrt{f'_c} \left[\frac{t}{L} \right]^2 \text{ --- Eq. (3.13a)}$$

CHAPTER 4

EXPERIMENTAL PROCEDURE

4.1 Equipment Investigation

The research commenced with the location, cleaning, repair and modification of four forms constructed by Munoz who gave details on their design and construction in Reference (13). Each form is composed of a sheet of plywood serving as stiffener for the mold, as anchorage for the reinforcement and on which are bolted two plexiglass plates of the same size. An opening is designed on the top plexiglass plate to receive a rectangular funnel that is connected to the hose at the time of pumping. Three plexiglass edge strips are located between the two plates to maintain a uniform distance of 0.25 in.(6.4mm). These strips had holes drilled at 1 in. (25.4 mm) intervals at the center of the thickness to fit the reinforcement.

One cracked plexiglass plate form was repaired, and openings on two of the forms previously designed to have a double male brass fitting(13), were modified to have a rectangular opening. Also, the forms were improved to accept different spacings for the reinforcement. Two sets of side strips with holes drilled at 0.5 in.(25.4 mm), and 2.0 in. (50.4 mm) intervals were fabricated for that purpose. A phototgraph of a complete form is shown in Figure 4.1.

A Moyno Open Throat Pump Model 2J4 in Figure 4.2, stationed at the cooling tower location, was used to place the microconcrete into the form providing uniform discharge without pulsation, turbulence or agitation. The pump can handled suspended particules less than 0.3 in.(8mm) in diameter. The pump specifications are described in Table 4.1.

4.2 Description of Structural Model

4.2.1 Structural Model Characteristics

The size of the structural model was determined to be 24 in.(610mm) long, 12 in.(305mm) wide, and 0.25 in.(6.4mm) thick. An improved microconcrete mix design developed for the cooling tower research was used for the purpose and prepared at the Civil Engineering Laboratory on different dates with the

proportion mentioned in Table 4.2.

The Chemical set retarder was used to prevent an early setting of the concrete, while the Pump Aid HEC 400, which behaved as plasticizer, assured better concrete workability and fluid properties when operating the pumping machine. Type 1 cement was mixed with aggregate whose maximum size passed a No. 16 sieve. The final mix design had a water-cement ratio of 0.5, an aggregate-cement ratio of 2, a unit weight of 135 lbs. per cu. ft (21.2 KN/m³), and an average slump of 8.6 in.(218.44mm).

4.2.2 Microconcrete Reinforcement

After testing a series of different wires, a galvanized wire of 3/64 in. (0.047 in. = 1.19mm) with an average yield strength of 65,896 psi (454.48 MPa) obtained at the University Physical Plant, was selected and placed in two perpendicular directions. The wire which came in a roll had to be cut to a convenient length and straightened by loading each piece to yielding before placing in form. Three major different spacings of reinforcement of 2.0, 1.0 and 0.50 in. (50.8, 25.4, and 12.7 mm) were used giving steel ratios of 0.0035, 0.0070 and 0.0140, respectively. The properties of the reinforcement wire are shown in Table 4.2, and the stress-strain curve in Figure 4.3.

ILLEGIBLE DOCUMENT

**THE FOLLOWING
DOCUMENT(S) IS OF
POOR LEGIBILITY IN
THE ORIGINAL**

**THIS IS THE BEST
COPY AVAILABLE**

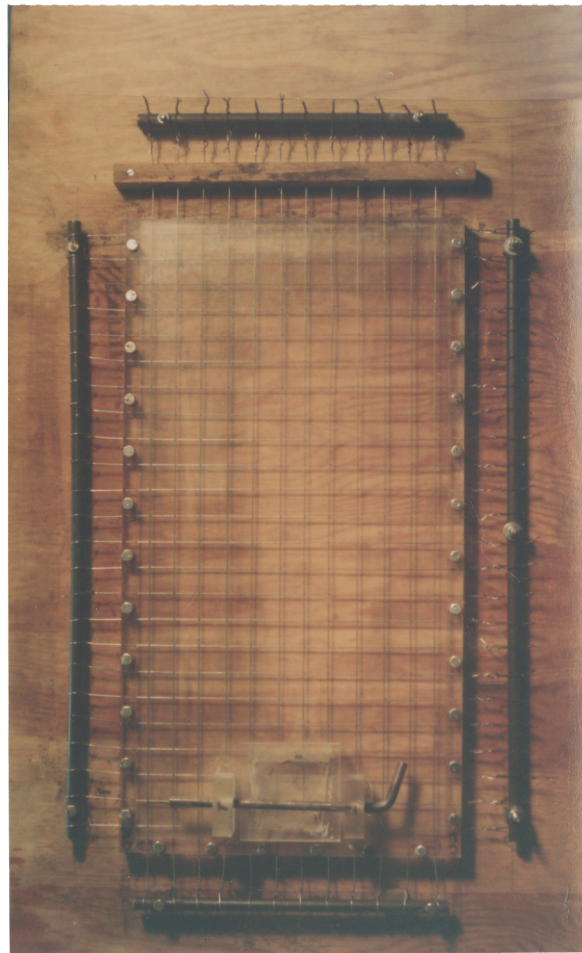


Figure 4.1 Completed Form

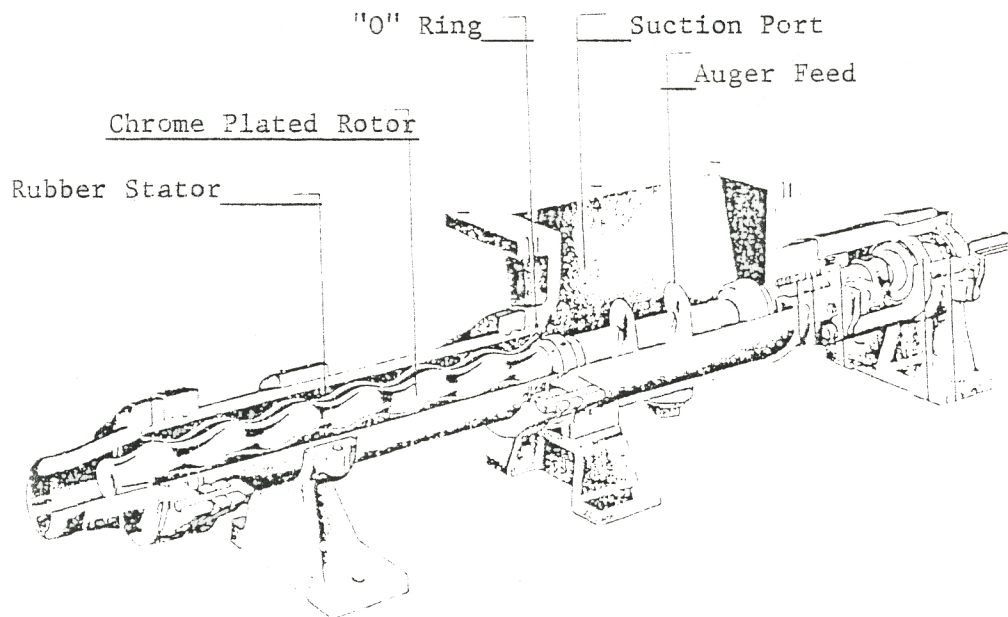


Figure 4.2 Moyno Throat Pump

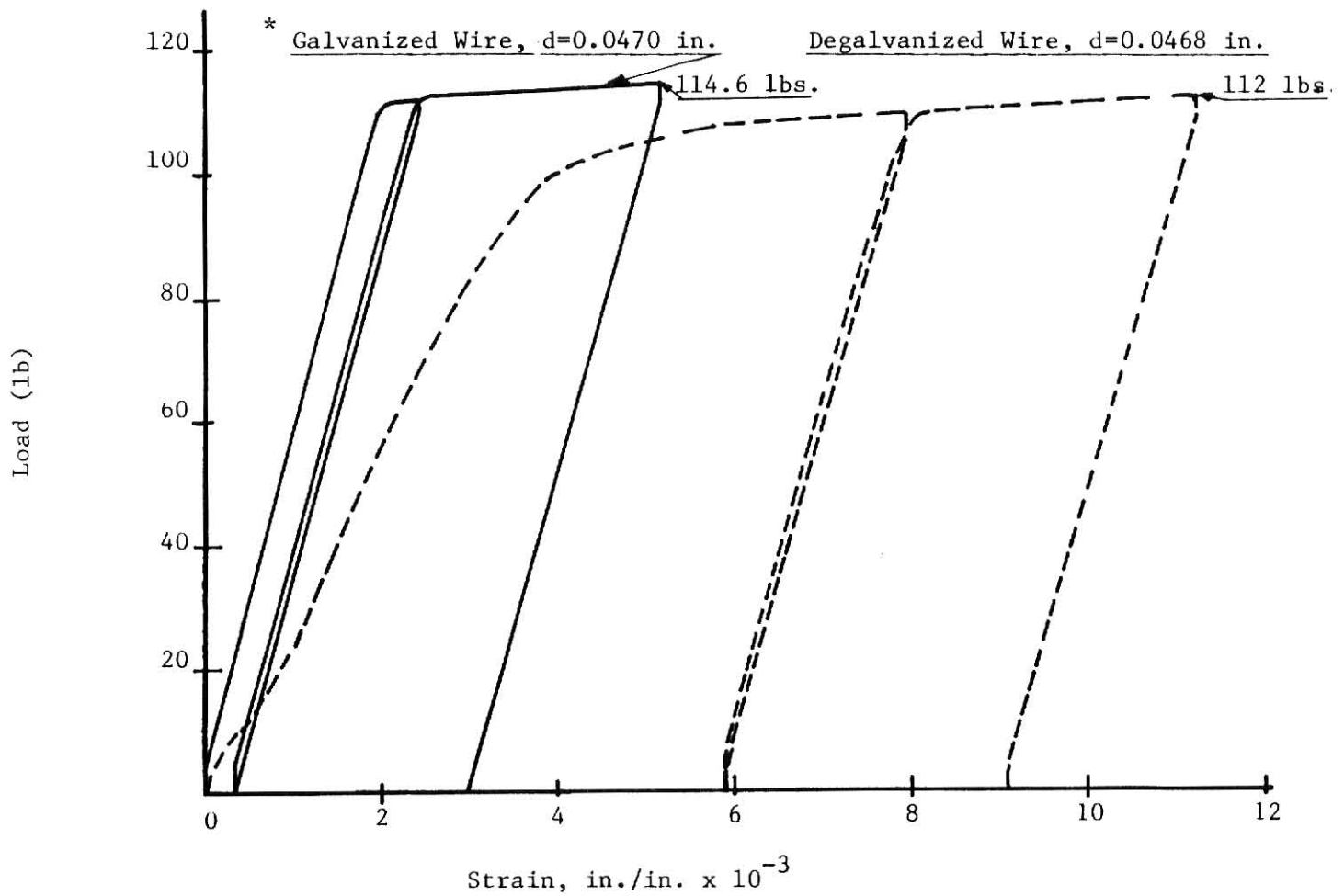


Figure 4.3 Stress-Strain Curve for Reinforcement

* For Galvanized Wire:

$$\Delta P = 80 \text{ lbs.}$$

$$\delta = \frac{8.2}{10} \times 0.004 = 32.80 \times 10^{-4} \text{ in.}$$

$$d = 0.047 \text{ in.}, A_s = 0.00173 \text{ in}^2$$

$$\Delta \sigma = \frac{80 \text{ lbs.}}{0.00173} = 46,240 \text{ psi}$$

$$\Delta \epsilon = \frac{\delta}{l_{\text{gage}}} = \frac{\delta}{2} = 16.40 \times 10^{-4} \text{ in./in.}$$

$$E = \frac{\Delta \sigma}{\Delta \epsilon} = \frac{46,240}{16.40 \times 10^{-4}} = 28.20 \times 10^6 \text{ psi}$$

4.3 Construction of Model

4.3.1 Formwork and Site Preparation

The following steps were considered in the model construction:

- 1- The inner surfaces of plexiglass plates were coated with a bond breaking compound (grease) to prevent adhesion of concrete to plexiglass.
- 2- Prior to positioning the reinforcement, a sheet of plastic were placed over the surface of the bottom plexiglass to prevent reinforcement from contacting oil.
- 3- The reinforcement systems was placed in the mold. A new technique was developed for positioning and holding the wires to the support systems through the middle of the 0.25 in. (6.35mm) thick plexiglass edge strips. When the reinforcement wire was in place, the sheet of plastic was removed.
- 4- The upper plexiglass plate was fastened to the bottom plate and to the plywood by bolts previously dipped into grease.

Prior to mixing the concrete, the hose equipped with the funnel was connected to the pump. Within the vicinity,

the miscellaneous tools such as pans, trowels, steel rod, test cylinder forms were located for their immediate used.

4.3.2 Microconcrete Preparation and Form Pumpability

The microconcrete was prepared in the Civil Engineering Concrete Laboratory. Standard ASTM tests were made to determined the properties of the concrete mix. Table 4.3 shows different pouring dates and ASTM slump test results. The steps involved in mixing the microconcrete were described by Munoz in Reference (13). Once ready, the microconcrete was carried to the pumping machine stationed at the cooling tower location.

The first trial pumping attempt on June 24, 1982 failed due to the segregation of the water from the sand and cement and the hose length. Indeed, due to the excess of microconcrete into the pump hopper and the absence of plasticizer, the solide particles and the water were separated and the mix pumped through the 25 feet (7620 mm) long hose set before reaching the mold. The sand and the cement settled around the pump auger feed. Hence, the 0.40 cu. ft (0.0113 cu. meter) mix was unusable and it took about three hours to clean out the pump and the hose of concrete.

The second experimental pumping attempt on July 1st,

Table 4.3 Plate Pouring Dates and Slump ASTM C143 Test

Date of Pouring	Number of Plates	Batch Slump in.(mm)	Spacing of 3/64 in. diam. wire in.(mm)	Steel Ratio
01 July, 82*	2	-	0	0
21 July, 82	4	8.0 (203.2)	1.0 (25.4)	0.007
01 Sept, 82	2	9.0 (228.6)	1.0 (25.4)	0.007
-----	2	9.0 (228.6)	1/2 (12.7)	0.014
06 Oct, 82	2	9.0 (228.6)	1/2 (12.7)	0.014
-----	2	9.0 (228.6)	0	0
25 Oct, 82	2	8.5 (215.9)	1/2 (12.7)	0.014
28 Oct, 82	2	8.75 (222.25)	2.0 (50.8)	0.0035
01 Nov, 82	2	8.5 (215.9)	2.0 (50.8)	0.0035
04 Nov, 82	2	8.5 (215.9)	2.0 (50.8)	0.0035

* Second Pumping Trial

1.0 in. = 25.4 mm

1982 was satisfactory when the hose length was reduced to 12 feet (3657.6 mm) and the pump aid HEC 400 was added to the mix design. The pump aid HEC 400 kept the water from separating from the sand and cement. In addition, the pump was primed by pumping water and a small quantity of cement through the system prior to placing the concrete into the hopper. Small amounts of mix were added to the mixture of water and cement until a continuous flow of concrete was obtained through the hose. The pump was then shut off and the hose connected to the first form. The mold was filled while in a vertical position with concrete flowing thru the rectangular funnel connected to the plate opening. The pump was shut off again after the form was filled. The mold was placed in a horizontal position with the funnel engaged into the form. The opening into the top plexiglass was covered with a capping system after the funnel was disconnected from the mold and inserted into the next mold ready to be pumped. After vibrating, small amounts of concrete were added to the top edge of some of the forms. Two unreinforced plates were successfully pumped during this trial. One at a time, after filling the last mold of each set of forms on different dates, the 3 in. x 6 in. (76.2 mm x 152.4 mm) concrete test cylinders were made following standard specifications and then, transported in a cart to the concrete Laboratory, as well as the entire molds.

4.3.3 Form Removing and Concrete Curing Process

Each test specimen and cylinder were cured for twenty four hours in the molds. After this initial curing period, each reinforcement wire was cut and the bolts were loosened. The plates were removed from the mold and the specimens along with the bottom plexiglass plate and the edge strips were marked and put in the moisture room. The three edge strips and the bottom plexiglass were removed the next day. Then, the test specimens were placed with the long edges on the floor in the curing room for at least 28 days before they could be tested. Next, the molds were cleaned out and prepared for another set of plates fabrication. A total of 20 plates were fabricated as indicated in Table 4.3.

4.4 Test Cylinders

The compressive strengths of the 3 in. x 6 in. (76.2 mm x 152.4 mm) concrete cylinders are displayed in Table 4.4 according to their ages and mixed batches. The cylinders were tested using the 75,000 lbs (337.5 kN) Baldwin-Southwark compression test machine.

The uniaxial stress-strain curves for cylinders from five batches were determined and plotted in Fig. 4.4 thru 4.8. These cylinders were tested the same day as the last plate of that

Table 4.4 Cylinder Test Log

Casting Date	Testing Date	Failure Stress psi (MPa)	Age At Test Days
24 June, 82	19 Aug, 82	6,170 (42.55)	55
1 July, 82	19 Aug, 82	6,430 (44.34)	49
1 July, 82	19 Aug, 82	6,360 (43.86)	49
21 July, 82	19 Feb, 83	7,300 (50.20)	213
21 July, 82	19 Aug, 82	5,370 (37.03)	28
21 July, 82	3 Dec, 82	6,930 (47.79)	135
*21 July, 82	9 Dec, 82	7,700 (53.10)	141
1 Sept, 82	29 Sept, 82	4,030 (27.72)	28
1 Sept, 82	15 Feb, 83	8,080 (55.58)	167
*1 Sept, 82	15 Feb, 83	7,780 (53.51)	167
6 Oct, 82	26 Jan, 83	6,920 (47.60)	112
6 Oct, 82	26 Jan, 83	6,220 (42.78)	112
6 Oct, 82	27 Jan, 83	6,500 (44.71)	113
*6 Oct, 82	27 Jan, 83	7,240 (49.80)	113
25 Oct, 82	2 Nov, 82	3,180 (21.87)	7
25 Oct, 82	26 Nov, 82	4,810 (33.08)	31
*25 Oct, 82	11 Feb, 83	6,730 (46.30)	109
28 Oct, 82	26 Nov, 82	4,170 (28.70)	28
28 Oct, 82	26 Nov, 82	4,100 (28.22)	28
1 Nov, 82	6 Dec, 82	4,740 (32.60)	35
1 Nov, 82	19 Feb, 83	5,230 (36.00)	110
4 Nov, 82	6 Dec, 82	4,600 (31.62)	32
4 Nov, 82	15 Feb, 83	6,080 (41.80)	103
4 Nov, 82	19 Feb, 83	5,230 (35.98)	107
*1 Nov, 82	9 May, 83	6,370 (43.93)	190

5930 psi = Mean

524.6 psi = Standard Deviation

8.84% = Coefficient of Variation

* From Cylinder Stress-Strain Test Datas

1 psi = 0.006897 MPa

1 psi = 6.9 KPa

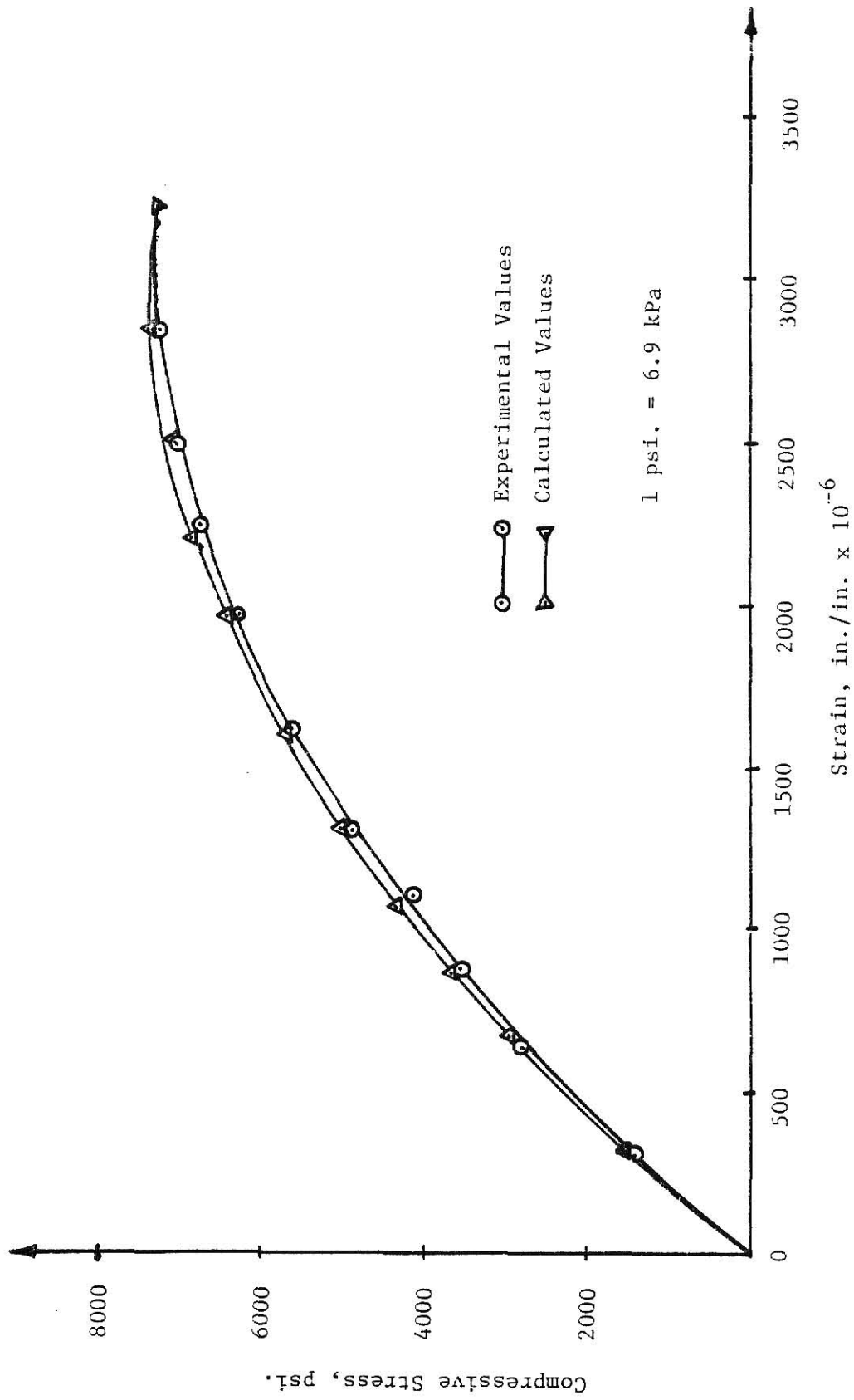


Figure 4.4 Stress-Strain Curve for Plates 1,2,3,4

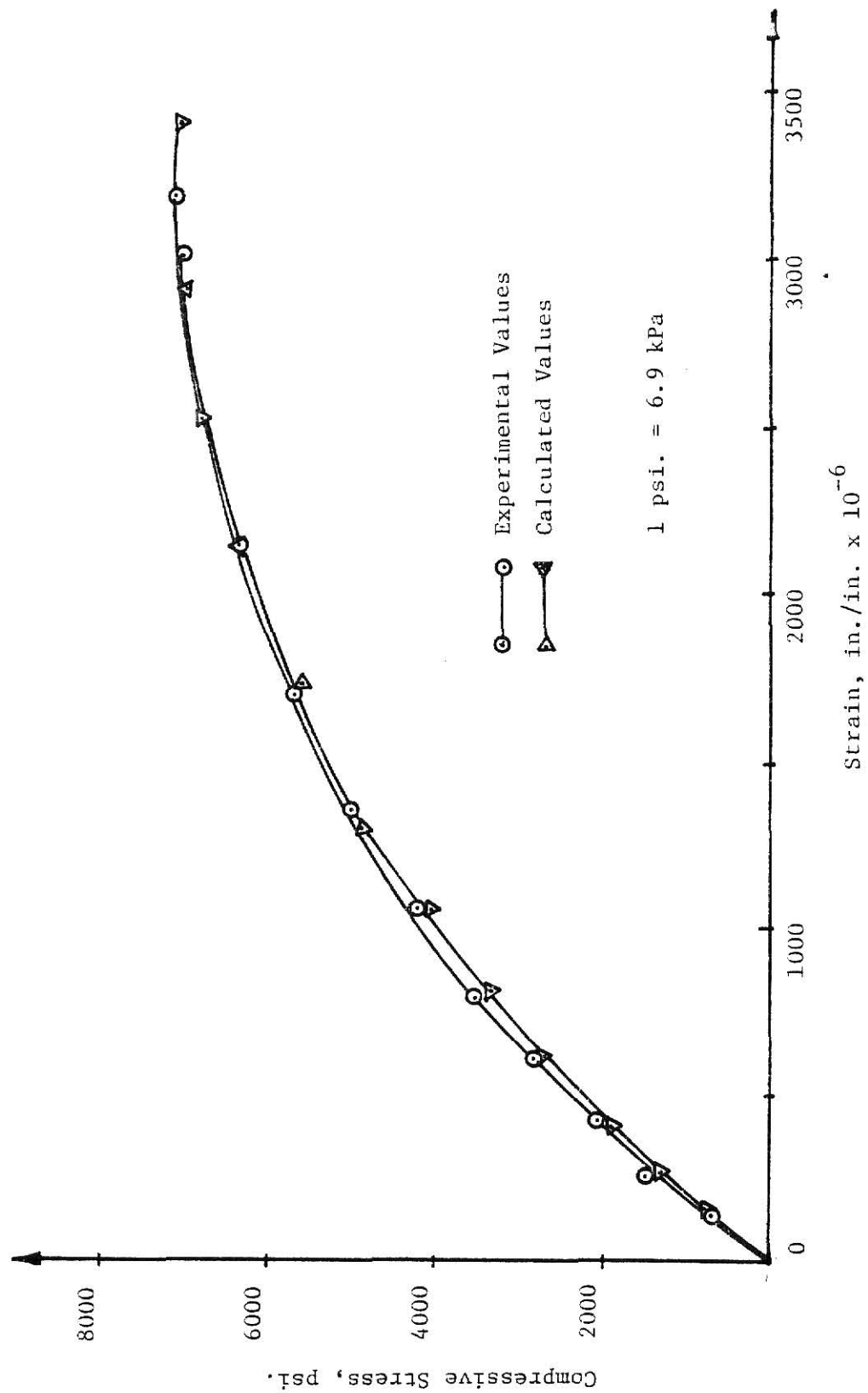


Figure 4.5 Stress-Strain Curve for Plates 8,9,10 11

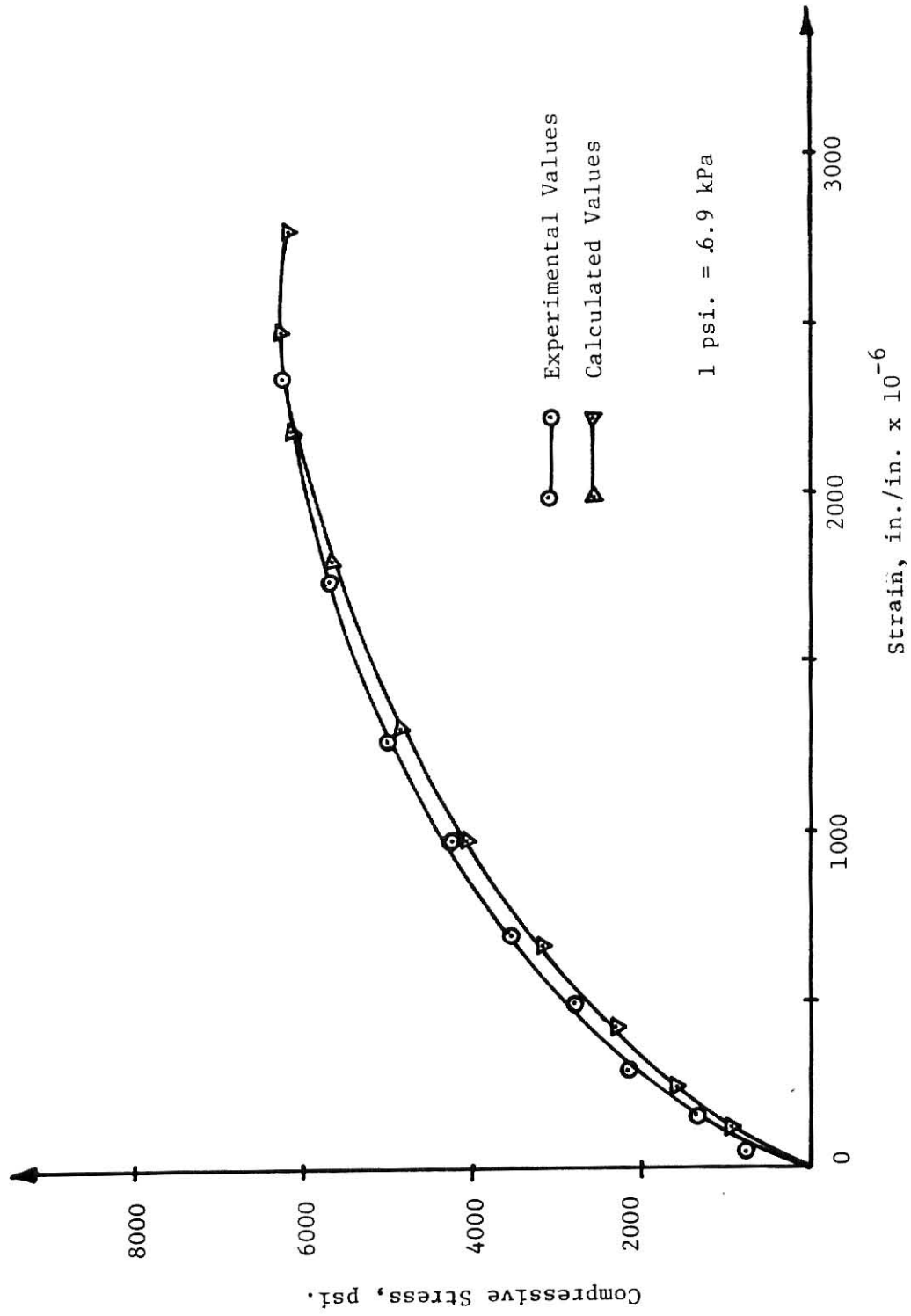


Figure 4.6 Stress- Strain Curve for Plates 12,16

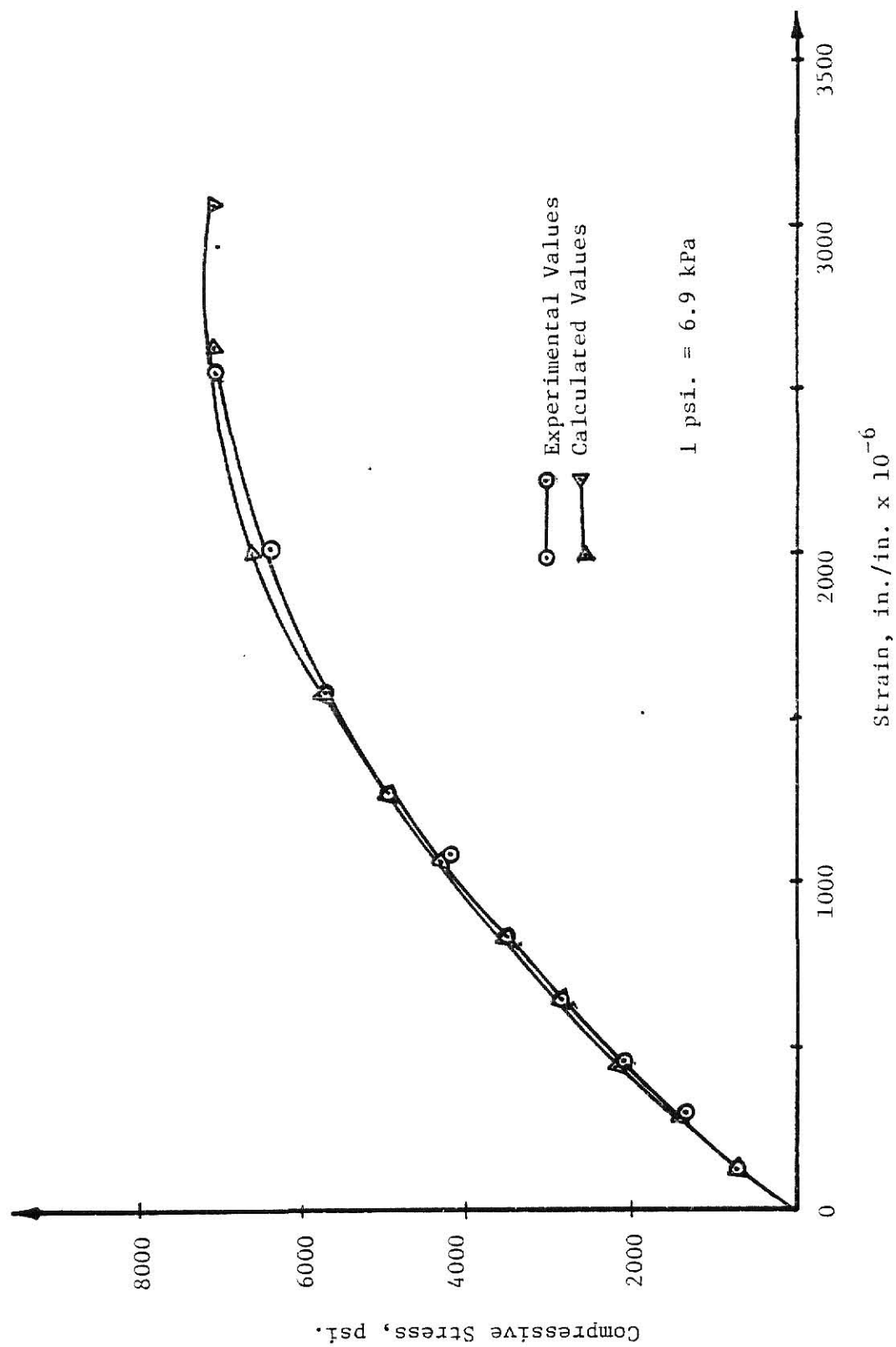


Figure 4.7 Stress-Strain Curve for Plates 5,6,7,17

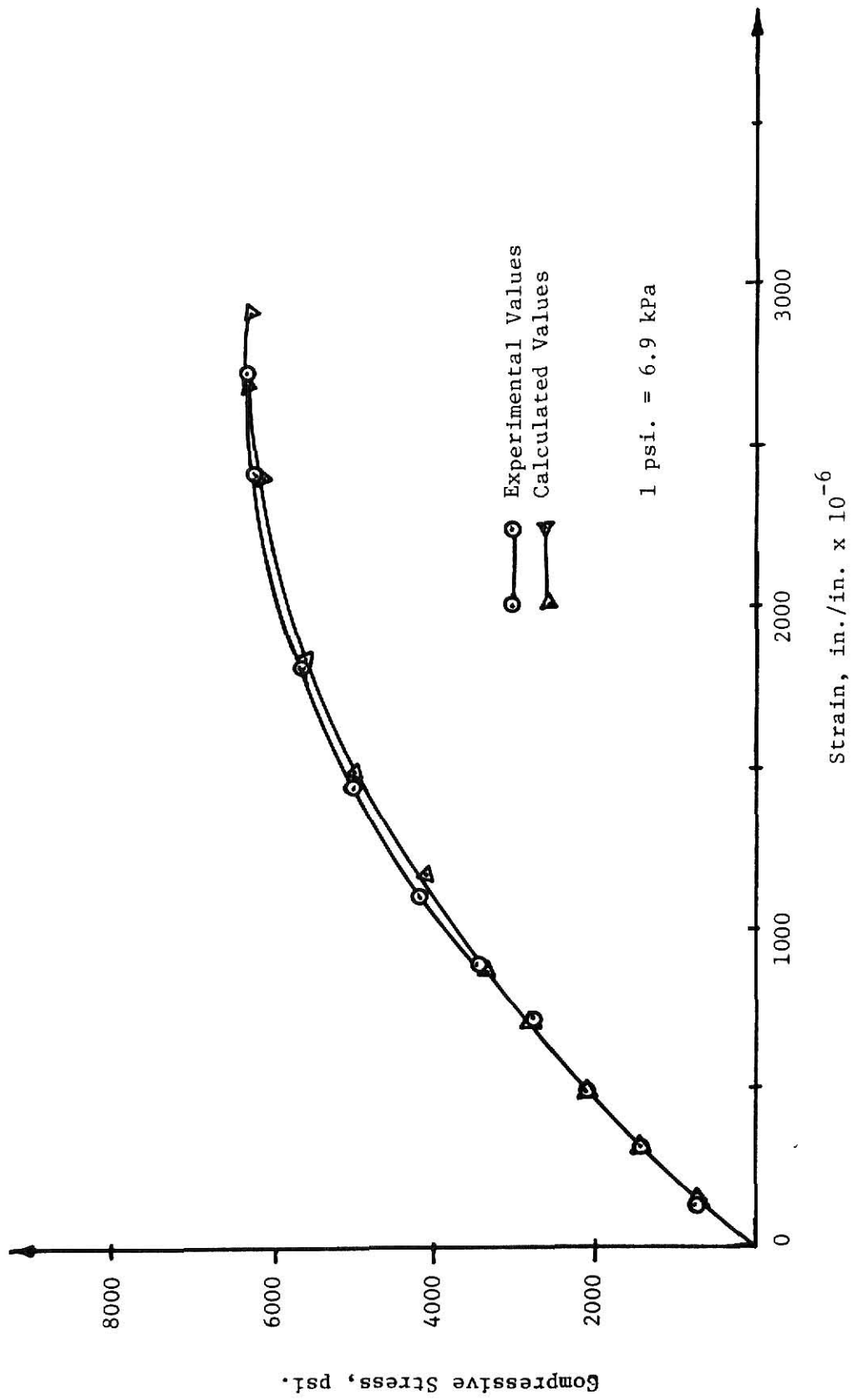


Figure 4.8 Stress-Strain Curve for Plates 15,20

particular batch.

4.5 Test Frame and Test Panel Preparation

The test Frame designed by Munoz (13) was set up for each concrete plate edge support condition. So that double clip angle supports would be easily mounted to the frame, a couple of holes were drilled in the side rails of the test frame at the location of the plate midheight. A new method was developed to fix the dial gage support to the test frame. After each test, the test frame simply supporting elements were cleaned out and regreased if necessary.

The first plate was tested on November 4th, 1982. To prepare the plate for testing, it was removed from the moist room to dry at least three days prior to the testing schedule. After cleaning the plate and smoothing the edges by grinding the remaining fragments of wires, a grid pattern of 3 in. (76.2 mm) squares were located on it. Twenty one readings were taken to determine the average thickness fabrication of each plate by using the convenient device shown in Figure 4.9. Two Soil Test LC-10 dial gages were used for that purpose and Figures 4.10.a and 4.10.b displayed different values of the average thickness of each plate.

Also, a new device was set up to measure the deflection of the plate when simply-supported and subjected to a uniform load of 10 lbs (4.536 kg) over a 2 in. (50.8 mm) width. A Soil Test LC-10 dial gage was used to evaluate the deflection at three locations across the plate width as indicated in Fig. 4.11.

Six strain gages were mounted onto twelve plates at different dates, glued, wired, coated, and protected following standard techniques. They were oriented parallel to the long direction at 0.5 in. (12.7 mm) from the centerline in the direction of the applied load. Also, they were placed at the same location on opposite faces in order to measure the corresponding surface tension or compression strain. Precautions were taken to prevent the electric wires from peeling of the strain gages. Then, the plate was carefully inserted into the test frame.

Seven Soil Test LC-10 dial gages were conveniently fixed on the test frame and placed in contact with the plate in order to measure the deflection of the center line.

Finally, the plate strain leads were connected to the Strainert Strain Indicator ready for testing. Location for strain and deflection measurements are shown in Figure 4.12 and the type and properties of the strain gage on Table 4.5.

4.6 Apparatuses and Testing Procedure

The 20,000 lbs (90 kN) Riehle Compressive Testing Machine and the 300,000 lbs (1350 kN) Southwark-Emery C.T.M. were used for testing the plates. The top and bottom edges of the test plates were always simply-supported while three types of support conditions were considered along the long sides; simply-supported, pair of clip angles at midspan and free edges. Along with the proper support conditions, the dial gages were mounted and secured to the test frame that was then placed in the correct position at the testing machine. Figures 4.13, 14, and Table 4.6 display the type of support conditions for each plate. The strain gage leads were then connected to the Vishay/Ellis-20 (V/E-20 A) Strain Indicator.

The steps involved in the testing procedure were:

- 1- Initialize strain and dial gages data, then rebalance to zero;
- 2- Apply load to desire level and maintain so;
- 3- Record strain and dial data after each incremental increase of load until failure.

The stress-strain data was obtained by going through the

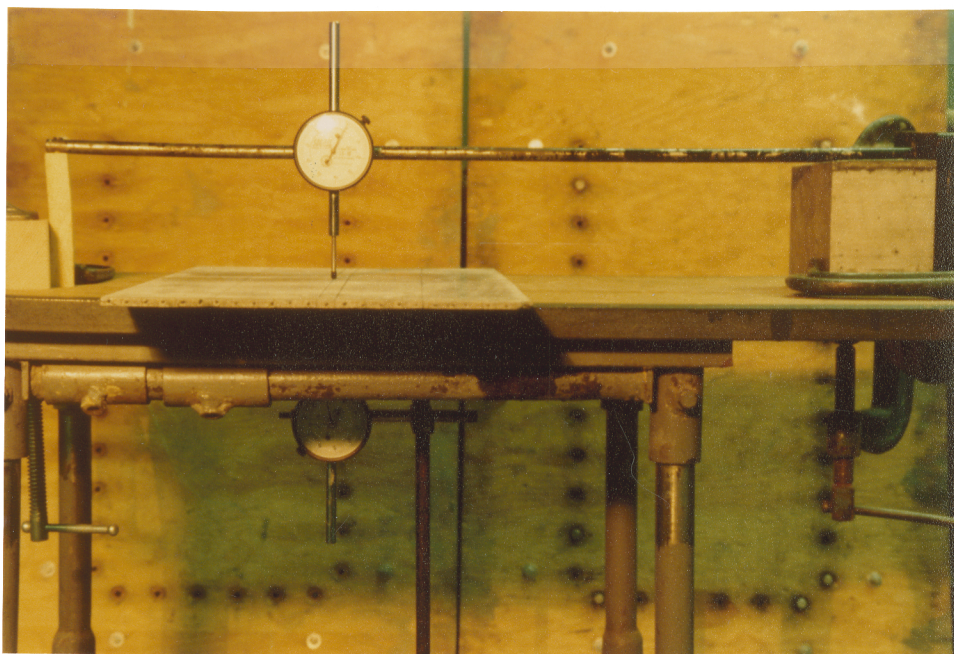


Figure 4.9 Plate Thickness Measurement Device

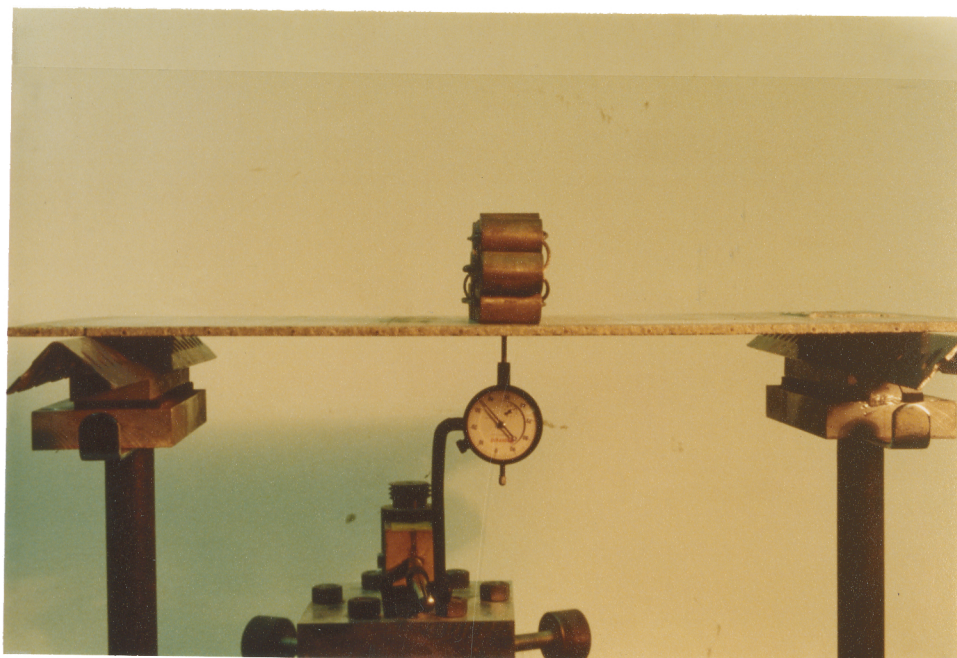


Figure 4.11 Plate "Beam-Case" Deflection Measurement Device

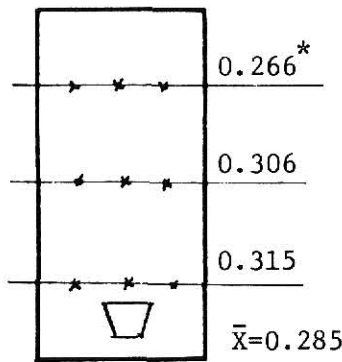


Plate #1, Opening at B.
s=1.0 in.

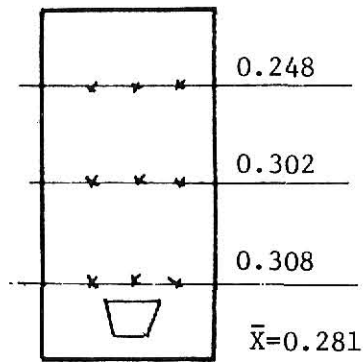


Plate #2, Opening at B.
s=1.0 in.

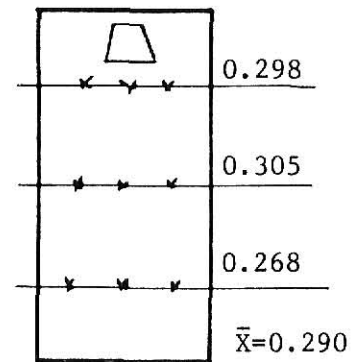


Plate #3, Opening at T.
s=1.0 in.

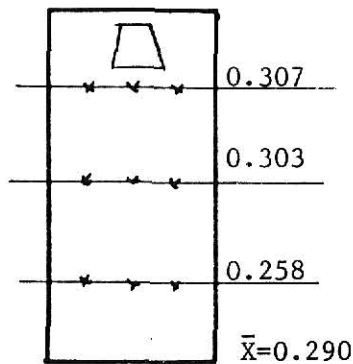


Plate #4, Opening at T.
s=1.0 in.

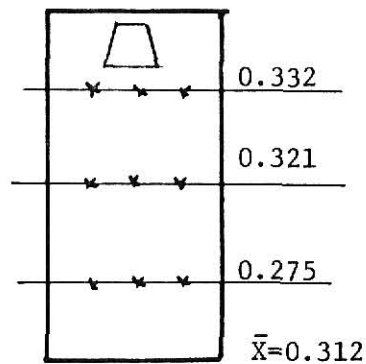


Plate #5, Opening at T.
s=1/2 in.

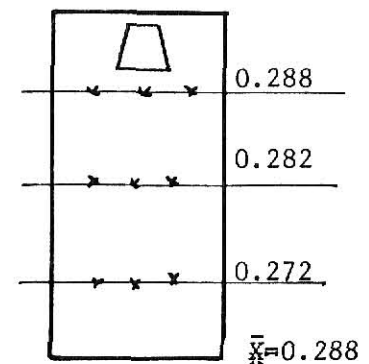


Plate #6, Opening at T.
s=1/2 in.

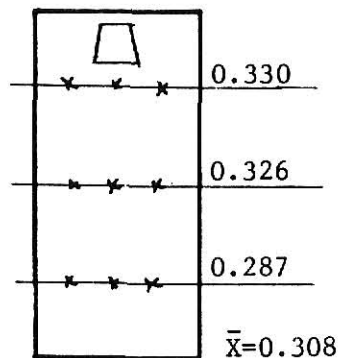


Plate #7, Opening at T.
s=1.0 in.

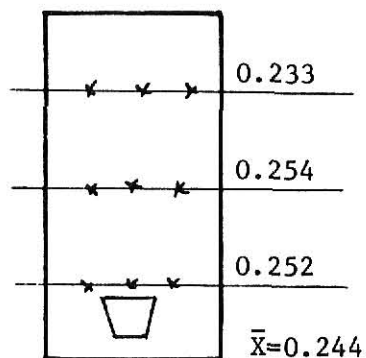


Plate #8, Opening at B.
s=0.0 in.

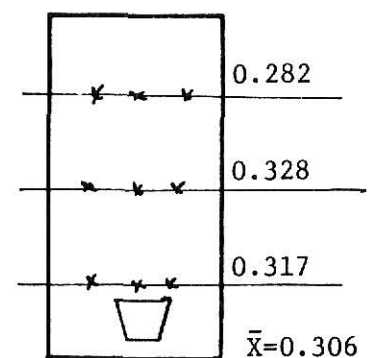


Plate #9, Opening at B.
s=1/2 in.

All dimensions in inch, 1 in.=25.4 mm

* ~~Average~~ Thickness used in the evaluation
of the calculated buckling load, P_{crC} .

\bar{X} = Average Thickness Fabrication of 21 readings.

** All plates tested at that particular position
when Opening Impact at Top or Bottom.

T = Top, B = Bottom.

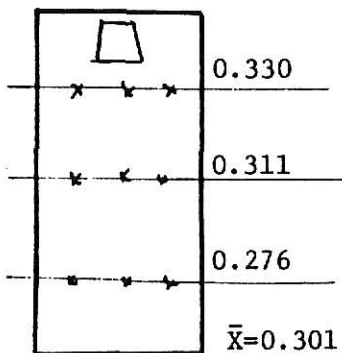


Plate #10, Opening at T.
s=1/2 in.

Figure 4.10b Plate Average Thicknesses

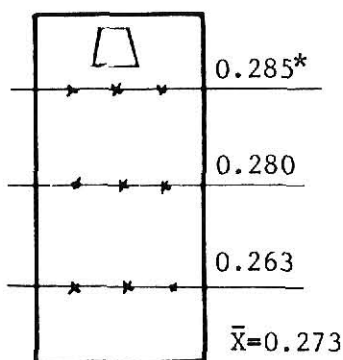


Plate #11, Opening at T.
s=0.0 in.

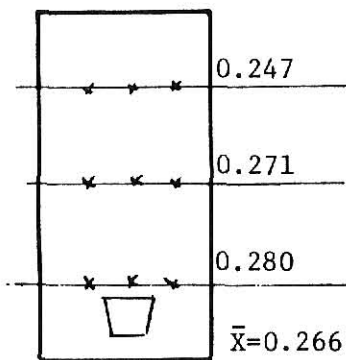


Plate #12, Opening at B.
s=1/2 in.

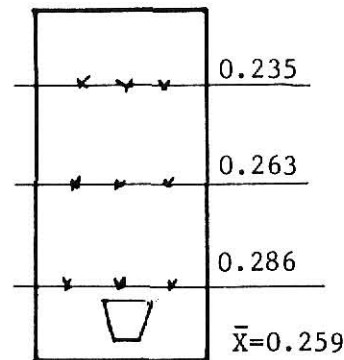


Plate #13, Opening at B.
s=2.0 in.

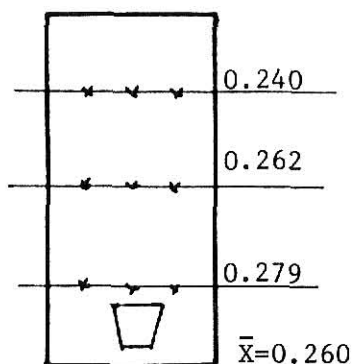


Plate #14, Opening at B.
s=2.0 in.

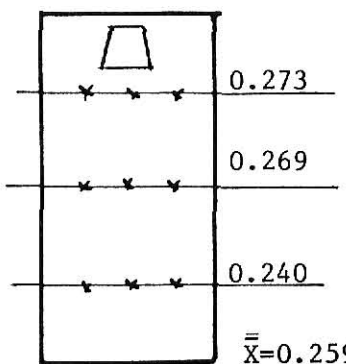


Plate #15, Opening at T.
s=2.0 in.

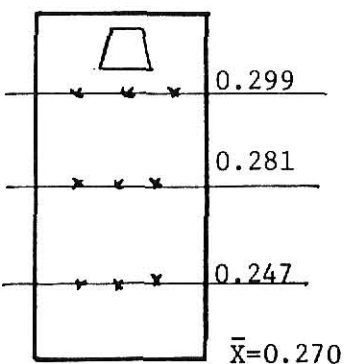


Plate #16, Opening at T.
s=1/2 in.

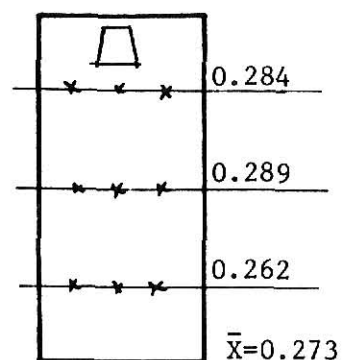


Plate #17, Opening at T.
s=1.0 in.

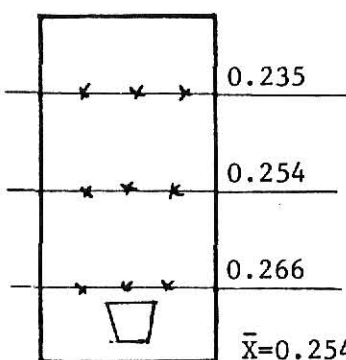


Plate #18, Opening at B.
s=2.0 in.

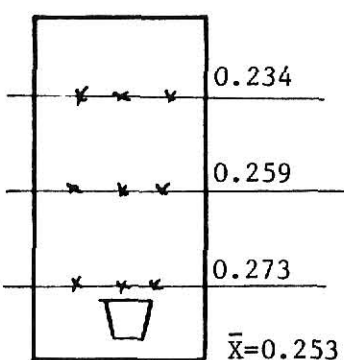


Plate #19, Opening at B.
s=2.0 in.

All dimensions in inch, 1 in.=25.4 mm

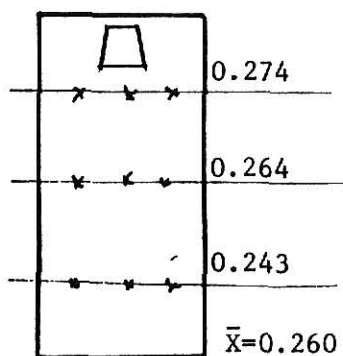


Plate #20, Opening at T.
s=2.0 in.

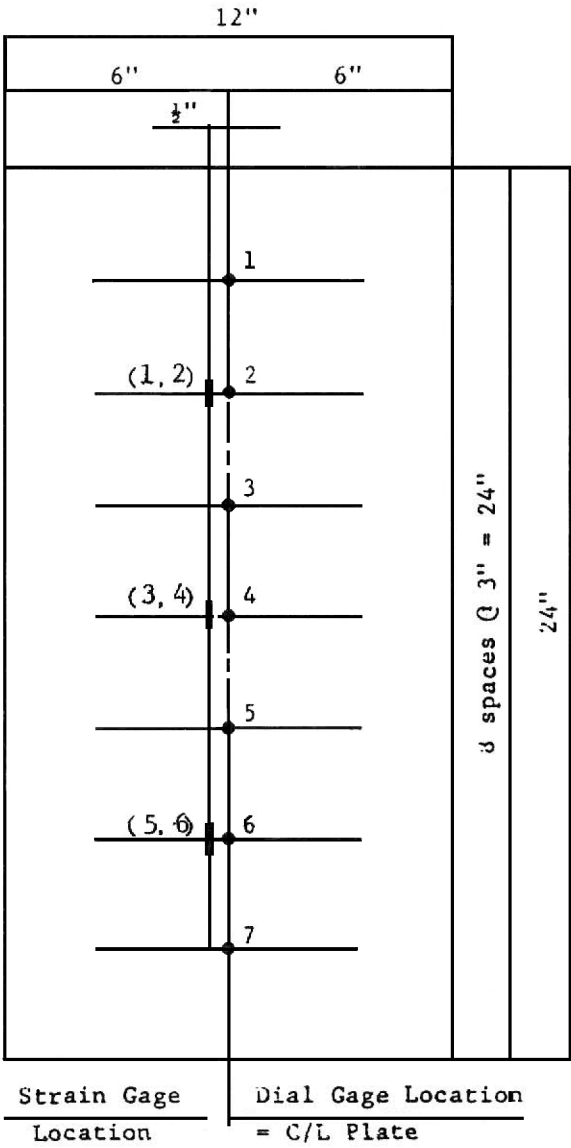
* Average Thickness used in the evaluation
of the calculated buckling load, P_{crC} .

\bar{X} = Average Thickness Fabrication of 21 readings.

** All plates tested at that particular position
when Opening Impact at Top or Bottom.

T = Top, B = Bottom.

Figure 4.10a Plate Average Thicknesses



1 in. = 2.54 cm.

Figure 4.12 Gage Locations on Test Plate

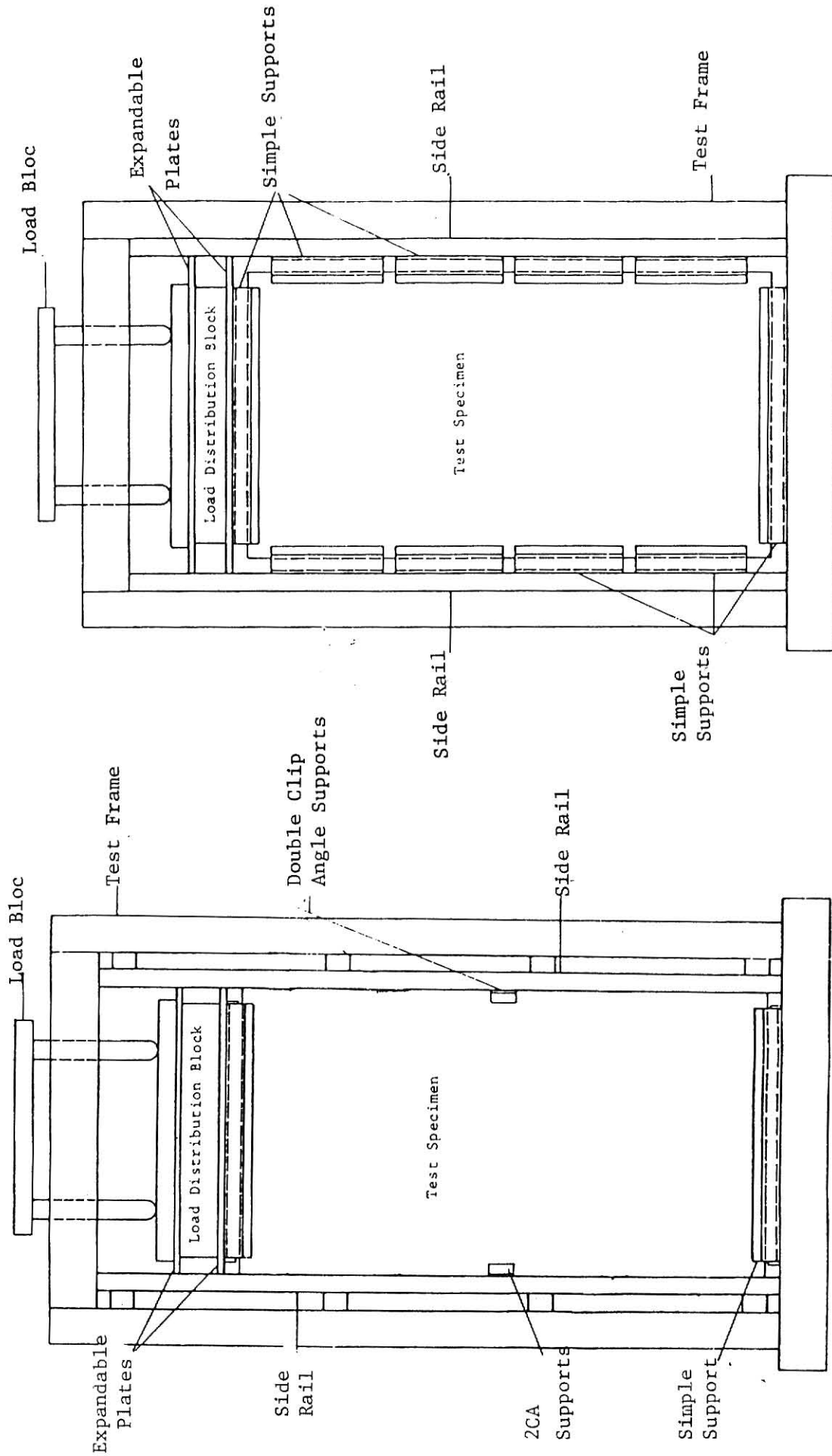


Figure 4.13 Simply-Supported Test Plate

Figure 4.14 Test Plate with Two Double Clip Angles

Table 4.5 Strain Gage Properties

Strain Gage	Series EA PRECISION Strain Gages
Gage Type	EA-06-250 BB-120
Resistance in ohms	120.0 \pm 0.15 %
Gage Factor at 75 F	2.03 \pm 0.5 % \pm 0.4 % kt

Table 4.6 Panel Support Conditions

Top and Bottom of the Plates Always Simply-Supported

Panel Number	Long Side (Vertical) Support Conditions	Spacing (in)	Pouring Date	Testing Date	# of Strains Gages/Plate	Age At Test Days
1	SS	1	07/21/82	11/04/82	6	106
2	SS	1	07/21/82	11/19/82	6	121
3	2CA	1	07/21/82	12/02/82	6	135
4	2CA	1	07/21/82	12/03/82	6	136
5	Free	$\frac{1}{2}$	09/01/82	12/08/82	6	99
6	2CA	$\frac{1}{2}$	09/01/82	12/10/82	6	101
7	(damaged) Free	1	09/01/82	12/14/82	0	105
17	Free	1	09/01/82	02/15/83	6	168
9	SS	$\frac{1}{2}$	10/06/82	01/26/83	0	112
10	2CA	$\frac{1}{2}$	10/06/82	01/27/83	6	231
11	2CA	0	10/06/82	02/04/83	0	239
8	SS	0	10/06/82	01/25/83	0	260
12	Free	$\frac{1}{2}$	10/25/82	02/03/83	0	101
16	SS	$\frac{1}{2}$	10/25/82	02/11/83	6	109
13*	(broken)	2	10/28/82	--	--	--
14	SS	2	10/28/82	02/04/83	6	99
15	SS	2	11/01/82	02/11/83	6	102
20**	(broken)	2	11/01/82	--	--	--
18	Free	2	11/04/82	02/15/83	0	103
19	2CA	2	11/04/82	02/19/83	6	107

*(Broken) When Fixing Strain Gages

**(Broken) When Measuring Deflection Due To 10# Load

previous testing procedure over one cylinder per batch from five batches out of seven. A total of four strain gages were used per cylinder. They were oriented in horizontal, vertical, horizontal and vertical pattern over the circumference of the mid-height line of the cylinder. They were also located on opposite tangents and equidistant. A special and tedious technique was required to fix the strain gages on the cylinders as well as the plates. They were glued using an adhesive bond and protected by M-COAT A after being checked for good. Then, the leads were connected to the Vishay/Ellis-20 A (V/E-20 A) Strain Indicator for testing. The Southwark Compression Testing Machine was used for the purpose. The stress-strain curves of the cylinders are shown in Figures 4.4 to 4.8 as indicated earlier in this report.

CHAPTER 5

REVIEW AND DISCUSSION OF TEST RESULTS

5.1 General Comments

This chapter deals with the analytical prediction, the graphical interpretation, and the comparison of different results obtained in the determination of the buckling load. The analytical prediction was based on certain equations or proposed design formulas that were derived for the purpose, while the graphical interpretation was based on the load-strain or load-deflection responses of a concrete structure. These two methods of evaluation of the critical load are compared in this report.

5.2 Analytical Method

Three methods of analysis were utilized to determine the

predicted buckling load as previously discussed in Chapter 3. The ACI Journal reduced formula, the column type-buckling formula and the plate type-formula were used for this intent.

Tables 5.1, and 5.2 show respectively the values of the critical load using the theoretical and the actual panel thickness in the ACI Journal reduced formula. The values of the average cylinder strength and the strain at ultimate stress are summarized in Table 5.3.

Tables 5.4 and 5.5 contained the values of the calculated critical load of all tested plates using the theoretical and the actual plate thickness, respectively. The column type-buckling formula was used for the plates that behaved as a column showing one or two sine waves, while the plate type was required for those that behaved as a plate by showing a biaxial curvature.

These methods of calculation were based on the evaluation of the average cylinder compressive strength and strain at ultimate stress obtained from Figures 4.4 thru 4.8 and recorded in Table 5.3. In all calculations, the actual plate thickness considered for each specimen was the average value obtained from three readings accross the width of the thinner section of the plate as indicated in Figures 4.10a and 4.10b. It was felt that buckling occured first at this region. Also, the mean out of twenty one

readings of each plate which was the average thickness of the entire plate was mentioned in Figures 4.10a and 4.10b.

5.3 Experimental Method

As stated in Chapter 3, three different approaches were used in the evaluation of the experimental buckling load. The observed buckling load were recorded in Table 5.6 along with the failure load and the buckling location. Those experimental buckling loads described earlier were defined as follow:

P_{crE1} = critical buckling load using Miknail and Guralnick Method;

P_{crE2} = critical load estimated from the Vertical Deflection Profiles;

P_{crE3} = critical load obtained from the Averaged Strain Method.

P_{crE1} and P_{crE3} were evaluated from the data collected by plotting the different load-strain relationship curves.

P_{crE2} was read from the vertical deflection profile diagrams as the last load recorded before the plate failure stage. Figures 5.1a, b, c, d thru 5.19a, b, c, d contained different graphes that were used to identify the experimental critical loads P_{crE1} , P_{crE2} , and P_{crE3} .

5.4 Comparison and Discussion of Results

The observed experimental value was taken to be P_{crE1} when strain readings were available, and P_{crE2} otherwise. The method used to find P_{crE1} is considered to be the most accurate for material, such as concrete, showing inelastic behavior when subjected to higher stresses. This experimental buckling load along with the failure load, the theoretical buckling load, and the calculated buckling load using the actual panel thickness at the bulged face of the plate are presented in Table 5.7. All tested specimens were load until failure occurred.

The plates simply-supported on the long edges showed a plate type-buckling behavior characterized by a biaxial curvature as indicated in Figure 5.1(i) and (ii). The average ratio of experimental to predicted buckling loads was 0.729. The difference between the experimental and calculated buckling loads is perhaps due to certain imperfections such as the dimensions of the plates or the initial excentricity when testing the specimens. Failure occurred shortly after the buckling load, showing a square panel mechanism in the weak section of the plate.

The buckling loads for plates with clip angles in Table 5.7, showed a very good agreement between the experimental and

calculated buckling loads where the average ratio of P_{crE} to P_{crC} as 1.364. In this case, the plates with two double clip angles at the long edges were characterized by a column type-buckling behavior displaying two sine waves as shown in Figure 5.1 (iii). The final load carrying-capacity was greater than the initial buckling load.

The plates with a free support at the vertical edges were also characterized by a column type-buckling behavior showing one sine wave and having an average ratio of P_{crE} to P_{crC} of 1.004. Satisfactory agreement was especially reached in that case between the experimental buckling load and the observed buckling with the deletion of Plate 12.

In all cases, the location where the initial buckling load occurred was the section of the test specimen that had a smaller thickness as previously mentioned in Figures 4.10a and 4.10b. These figures also show the average thickness of each plate for twenty one readings and the average thickness out of three readings accross the bulged face.

In addition to this analysis, Table 5.9 shows the values of the modulus of elasticity of a few plates calculated according to the following:

- 1) The Tangent Modulus Formula from column type-buckling: $E_T = \frac{2f'_c}{\epsilon_o} \left(1 - \frac{\epsilon_{cr}}{\epsilon_o}\right)$
- 2) The ACI's Formula: $E_c = 33w^{1.5}\sqrt{f'_c}$
- 3) The classical method of determining the deflection of a simply-supported beam loaded at midlength: $\Delta = \frac{Pl^3}{48EI}$, Hence $E = \frac{Pl^3}{48\Delta I}$

The last represents a value of the modulus of elasticity not valid in the domain of plate buckling, but evaluated to see whether it could be used to approximate the specimen Modulus of Elasticity.

CHAPTER 6

SUMMARY, CONCLUSIONS, AND RECOMMENDATIONS

6.1 Summary

The experimental study of this report consisted of making and testing twenty reinforced concrete plate structure models. Three of the plates were damaged with two unusable. The remaining plates were tested in uniaxial compression with three types of support conditions along the vertical edges. In addition, three different ratios of galvanized steel wire reinforcement were used.

A Moyno Open Throat Pump was used to place microconcrete with an maximum aggregate size of 0.3 in. (8mm), into the set of forms on different dates of pouring. Each plate was separately prepared for testing to collect data.

The analytical study to determine the theoretical and predicted buckling loads was performed using the plate or column type-buckling design formulas described earlier in Chapter 3 of

this report.

The experimental buckling load was obtained by using the Miknail and Guralnick Method of evaluating the load-strain curves of the strain gages located nearest the center of the bulged face of each plate. When such strain readings were not available, the Load Deflection Profiles curves were used to find experimental buckling loads. Six Electric strain gages were mounted per plate onto twelve of the plates and seven deflection measuring dial gages were used on all test specimens.

The predicted and the observed buckling loads and their ratio are presented in Table 5.8 for comparison.

6.2 Conclusions

The principal objective of this report was to build and test in uniaxial compression, microconcrete plate models to see whether or not the load-strain or load-deflection responses could be used to determine their buckling load in comparison with the proposed design formulas. A pumped mix was used to make the specimens. A few difficulties such as maintaining a constant plate thickness were encountered during the fabrication procedure. Indeed, it was felt that when pouring the plate in the vertical position, a flow of pumped concrete thru the funnel

inserted into the mold opening, exerted a pressure that had the tendency to bow out the top plexiglass form plate. As a result of this phenomena, all the specimens were thicker at the location of the opening. That imperfection could lead to the early initial buckling of the plate at the surface with thinner section, especially for plate type-buckling.

Another serious problem was to prevent excentricity during testing. It was extremely difficult to center the test frame on the testing machine and therefore, to apply a perfectly axial load.

The plates tested with the vertical edge free showed an initial excentricity at the midheight due to the weight of the compressive block (13) on the test panel. Although this set of plates showed good agreement between the analytical and experimental analysis, they buckled at stress level considerably lower than the plates simply-supported along the long edges. The latter exhibited a biaxial curvature due to the buckling in two dimensions as expected in the prototype. Good agreement was observed between the yield line orientations and the predicted direction of expansion of the cracks in spite of occuring at the location of the smaller thickness as indicated in Figure 5.1(i). These plates were subjected to compressive stresses of relative large amplitude when compared to plates with two double clip

angles at the midheight along the long support. However, good agreement was reached between the experimental and predicted buckling loads (P_{crE}/P_{crC}) of the plates with two double clip angles at the long edges where the average ratio was 1.364. The ratio of the observed to the predicted buckling loads of the plates simply-supported along all edges was 0.729. More experimental investigations are needed to verify the proposed plate design formula although it appears that this ratio shows a relative good agreement.

In addition to the reinforced microconcrete plates, two plates without reinforcement were tested. They explosively failed at load level that confirmed the good response of a plain concrete under compressive stresses.

Although, it is somewhat inconclusive, it does appear that an increase in the steel ratio does increase the critical load.

Finally, a computer program was developed in Appendix 1 to evaluate some of the values in different Tables.

6.3 Recommendations

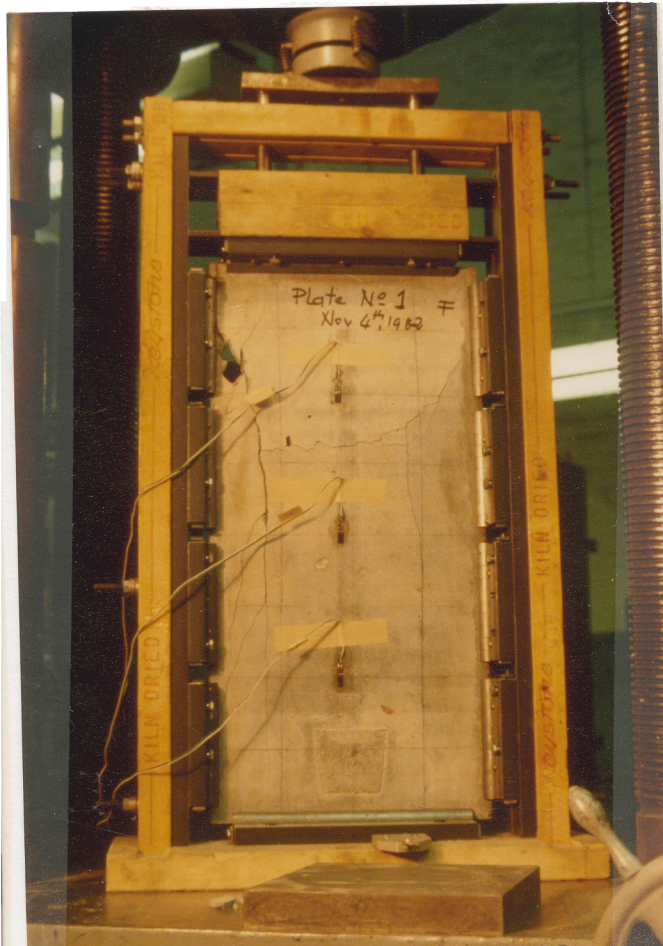
As a result of this study , the following steps are recommended for future reseach:

- 1)If the plates are to be pumped, stiffeners should be added to the top plates at the location of the opening where the pumped microconcrete exerted enough pressure to cause variable thickness accross each plate. Alternate methods forming plates should be attempted. Perhaps placing the concrete on a horizontal vibrating table would produced plates of more uniform thickness and density.
- 2)Transporting freshly pumped form on the cart should be avoided. It could result in lowering the concrete level at the upper edge of the mold which was designed to permit excess concrete to escape during pumping (13).
- 3)Particular care should be taken to center the uniaxial load during testing.
- 4)The presence of steel reinforcement is important with regard to the load carrying-capacity, but it also prevents the flow of the microconcrete between the two plexiglass plates at the time of pumping. The plates reinforced with

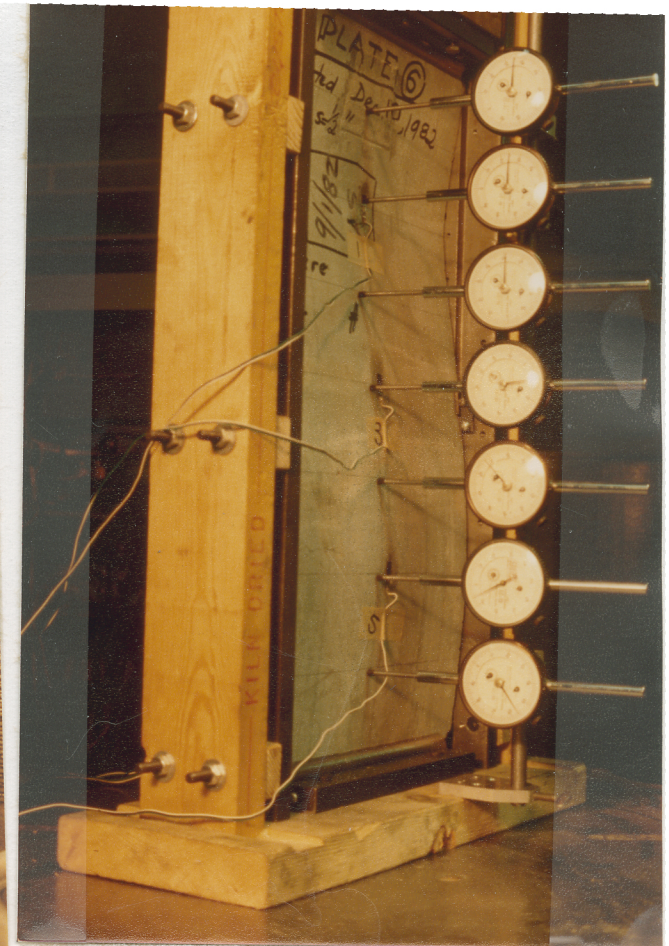
wires at one-half inch spacing were the hardest to pump. Perhaps a one inch spacing is the minimum that can be used when pumping. To better simulate deformed concrete reinforcement steel, a deformed wire should be tried for the experiment. A procedure using knurling wheels was worked out, but not implemented in this research because of the time involved in getting the device built.



i) Plate Type Buckling Case



ii) Plate Type Buckling Case



iii) Column Type Buckling Case

Figure 5.1 Typical Behavior of Plate when Subjected to Plate or Column Type Buckling Load

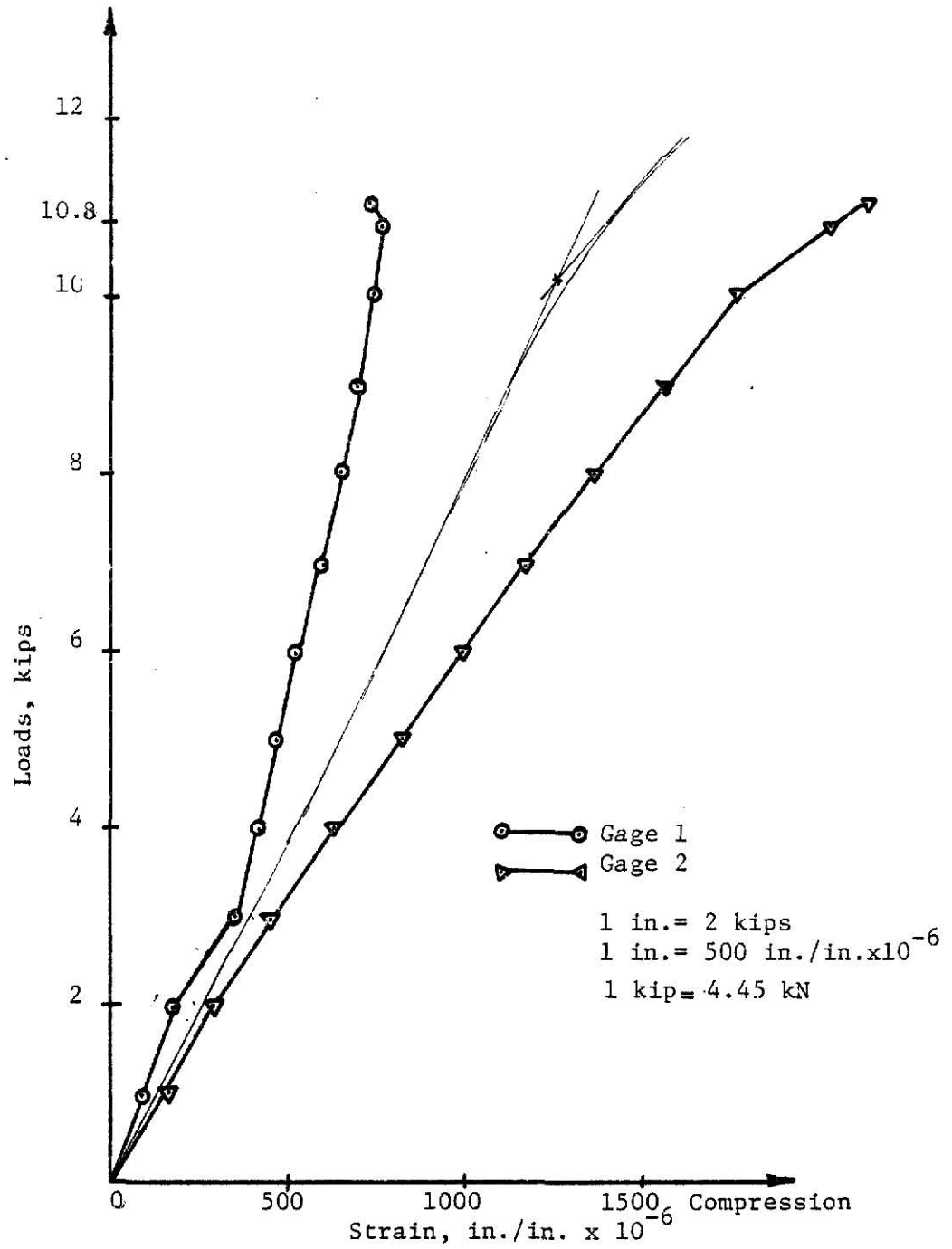


Figure 5.1a Load vs. Strain, Plate 1, Gage 1 & Gage 2
(SS - Opening at Bottom - $s = 1.0$ in.)

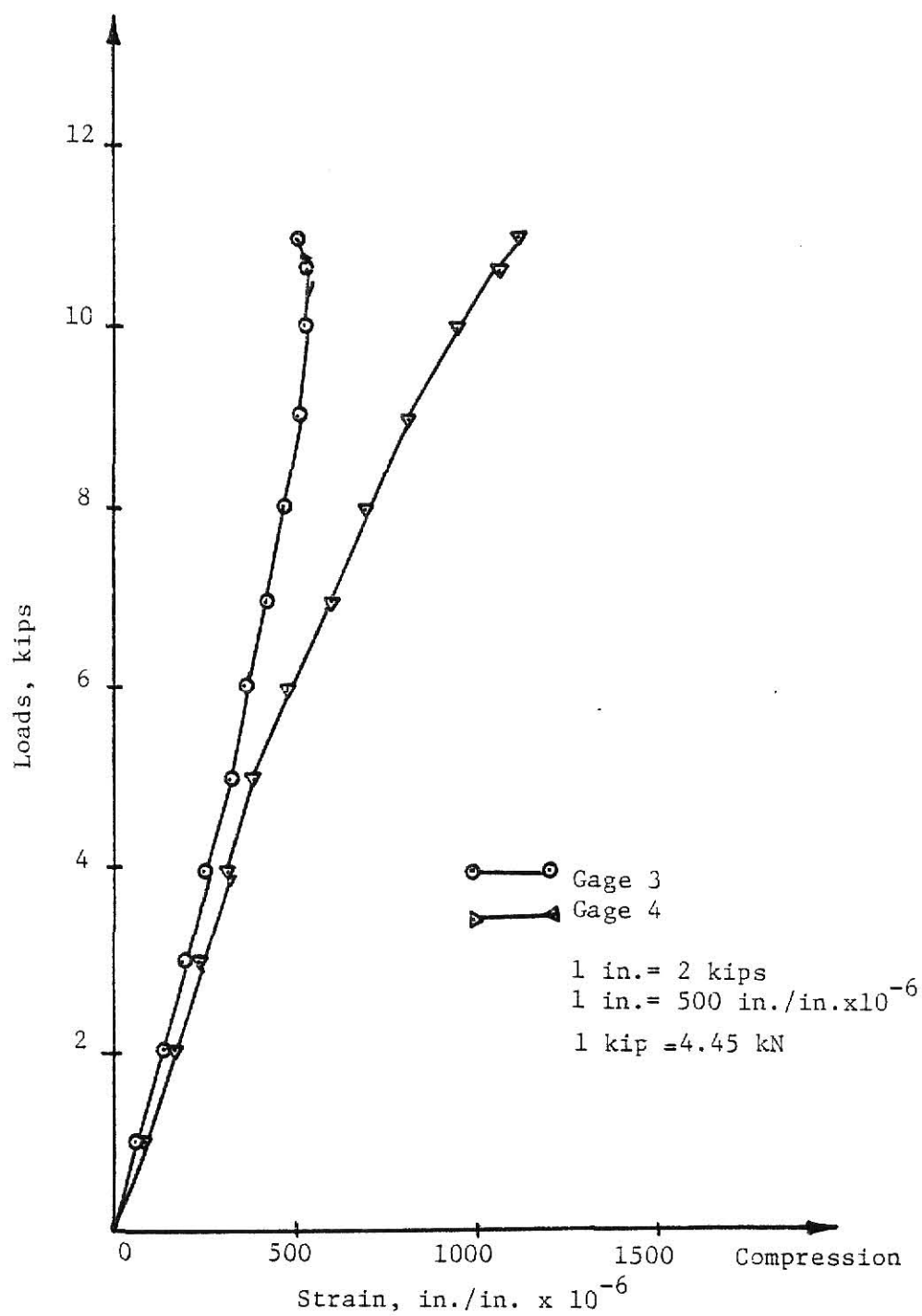


Figure 5.1b Load vs. Strain, Plate 1, Gage 3 & 4
(SS - Opening at Bottom - $s = 1.0$ in.)

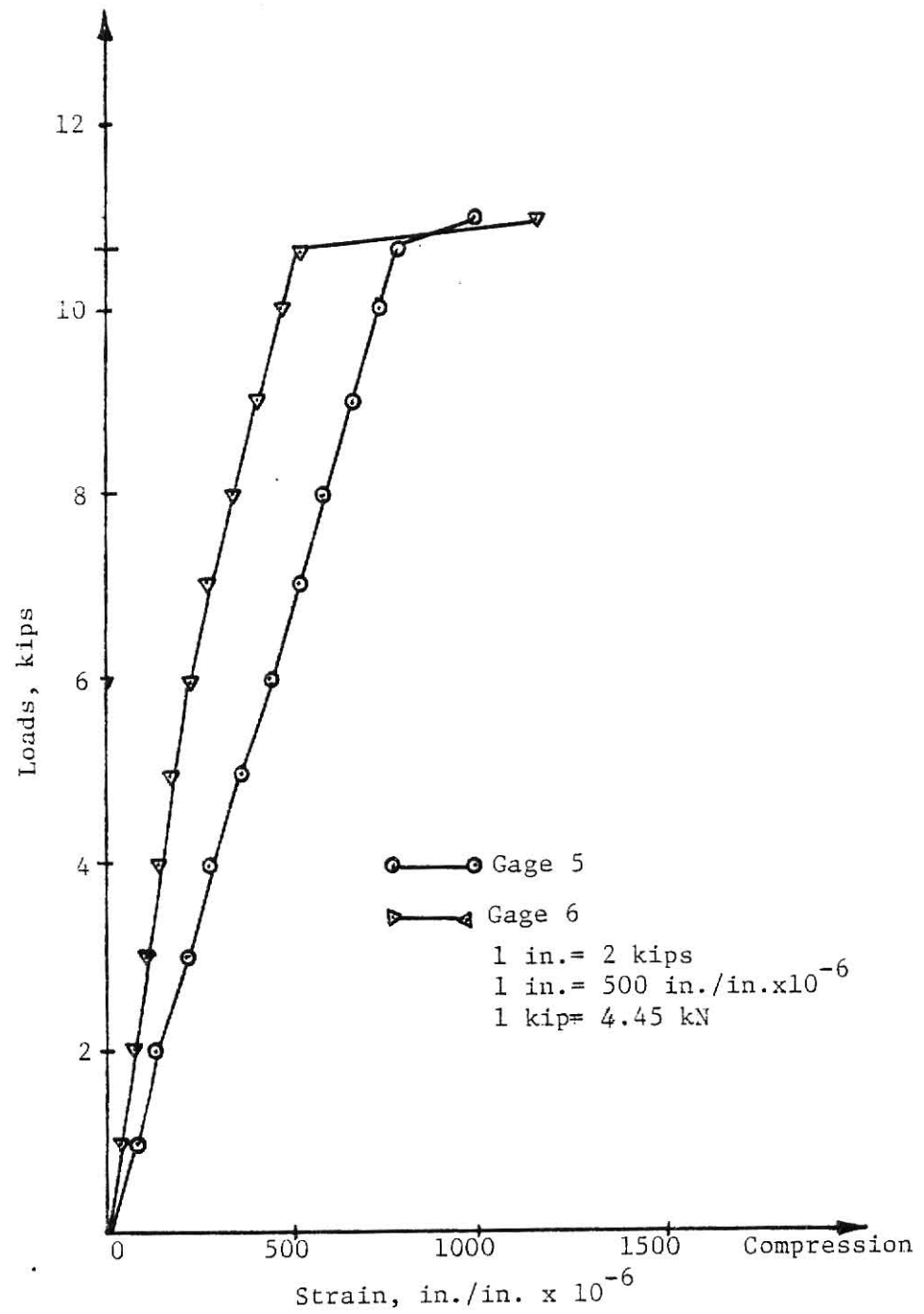


Figure 5.1c Load vs. Strain, Plate 1, Gage 5 & 6
(SS - Opening at Bottom - $s = 1.0$ in.)

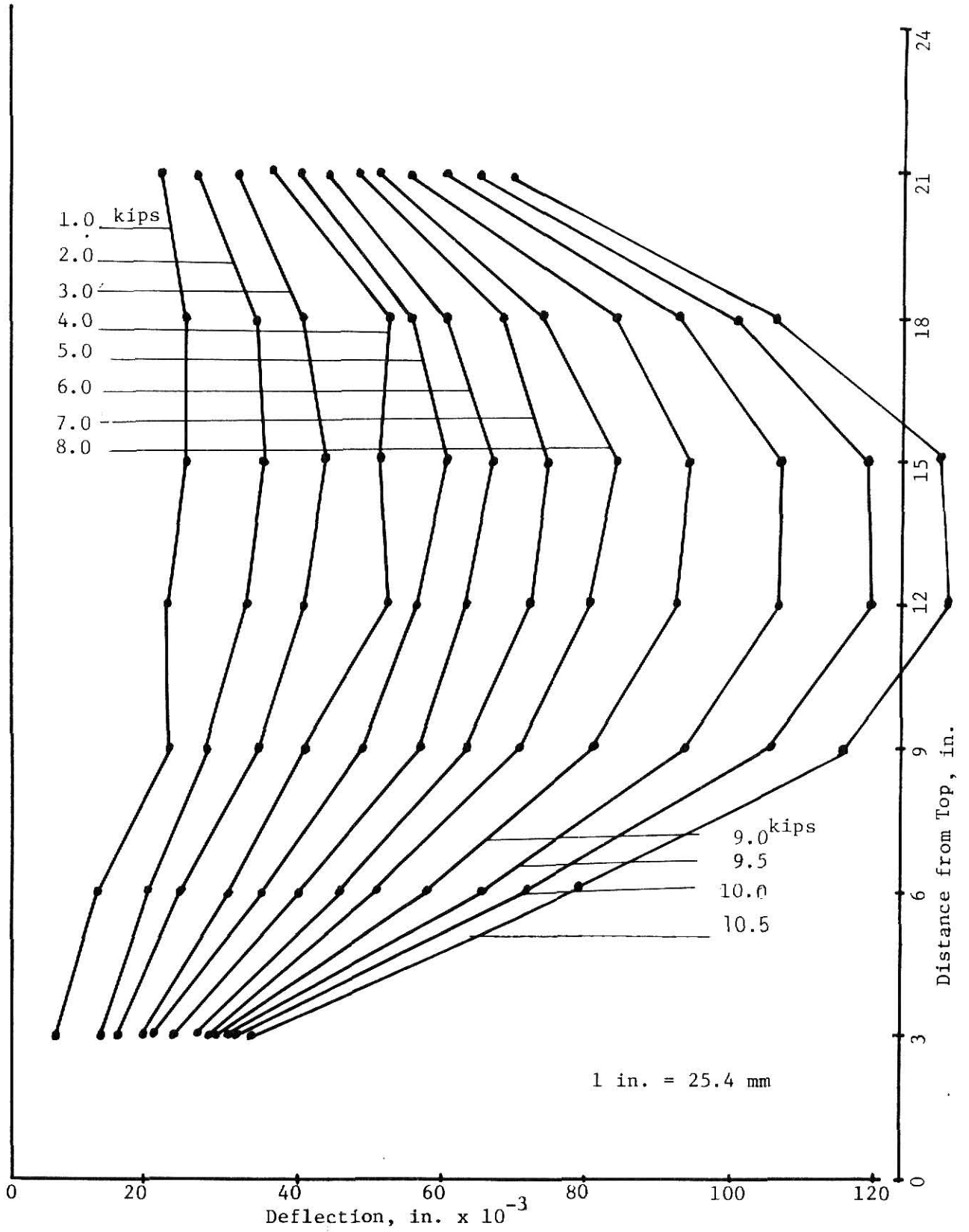


Figure 5.1d Deflection Profiles for Panel 1
(SS - Opening at Bottom - s=1.0 in.)

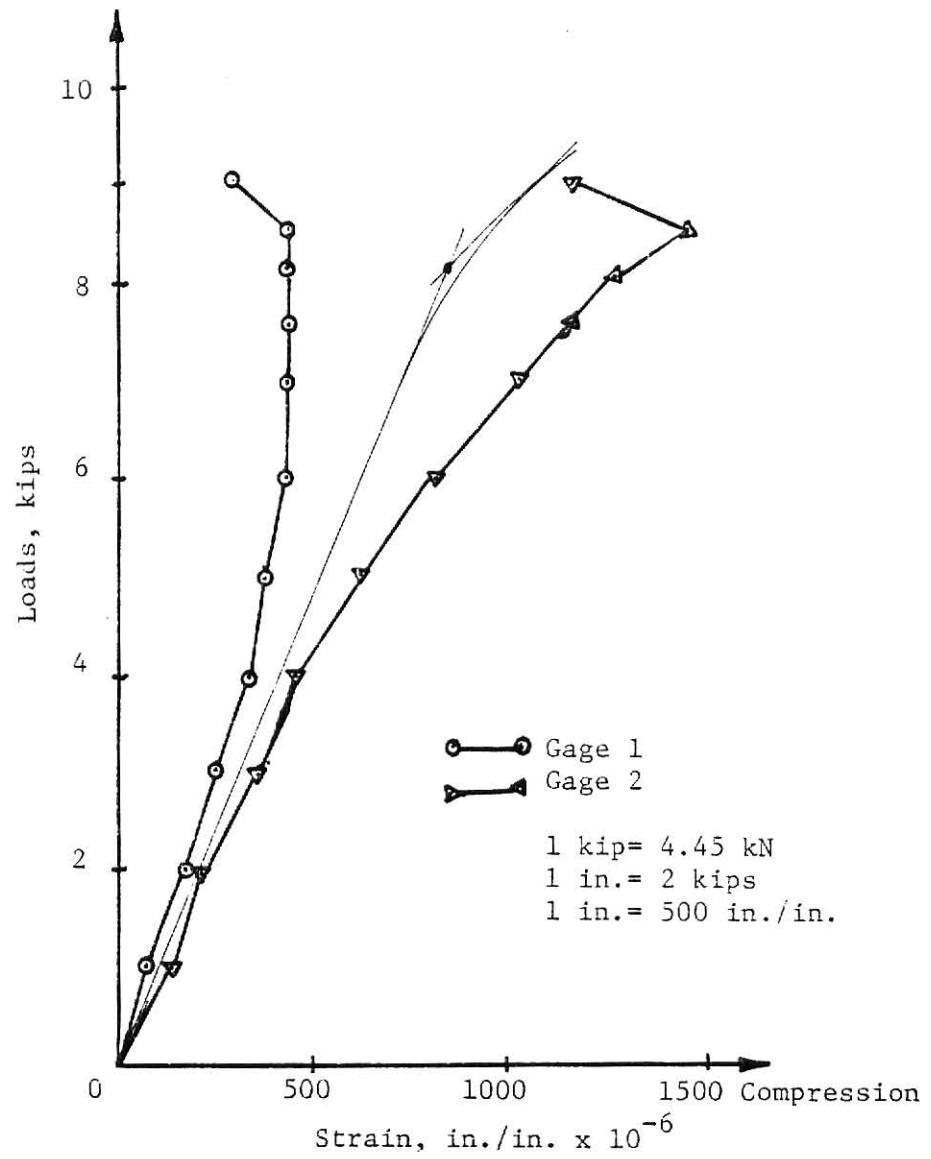


Figure 5.2a Load vs. Strain, Plate 2, Gage 1 & Gage 2
 (SS - Opening at Bottom - $s = 1.0$ in.)

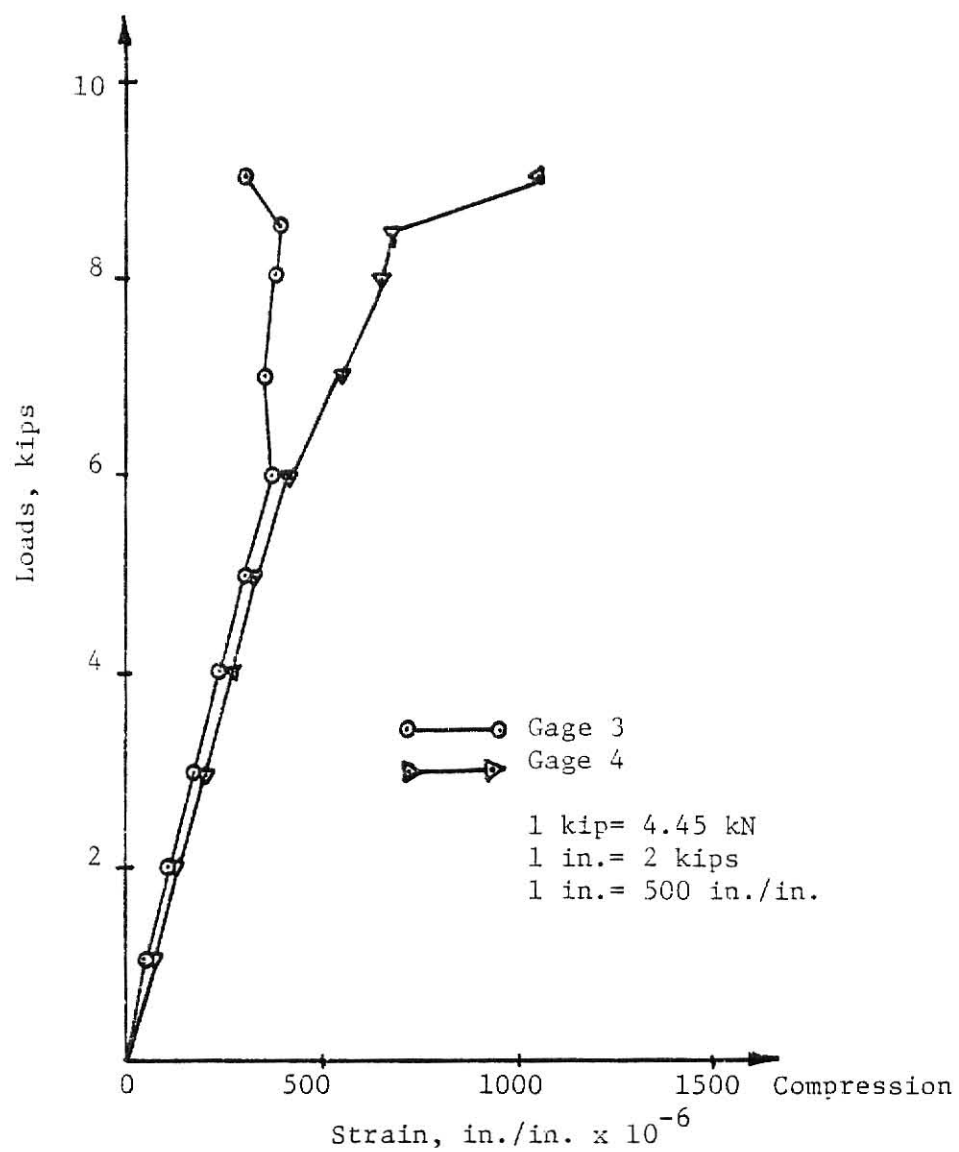


Figure 5.2b Load vs. Strain, Plate 2, Gage 3 & Gage 4
(SS - Opening at Bottom - $s = 1.0$ in.)

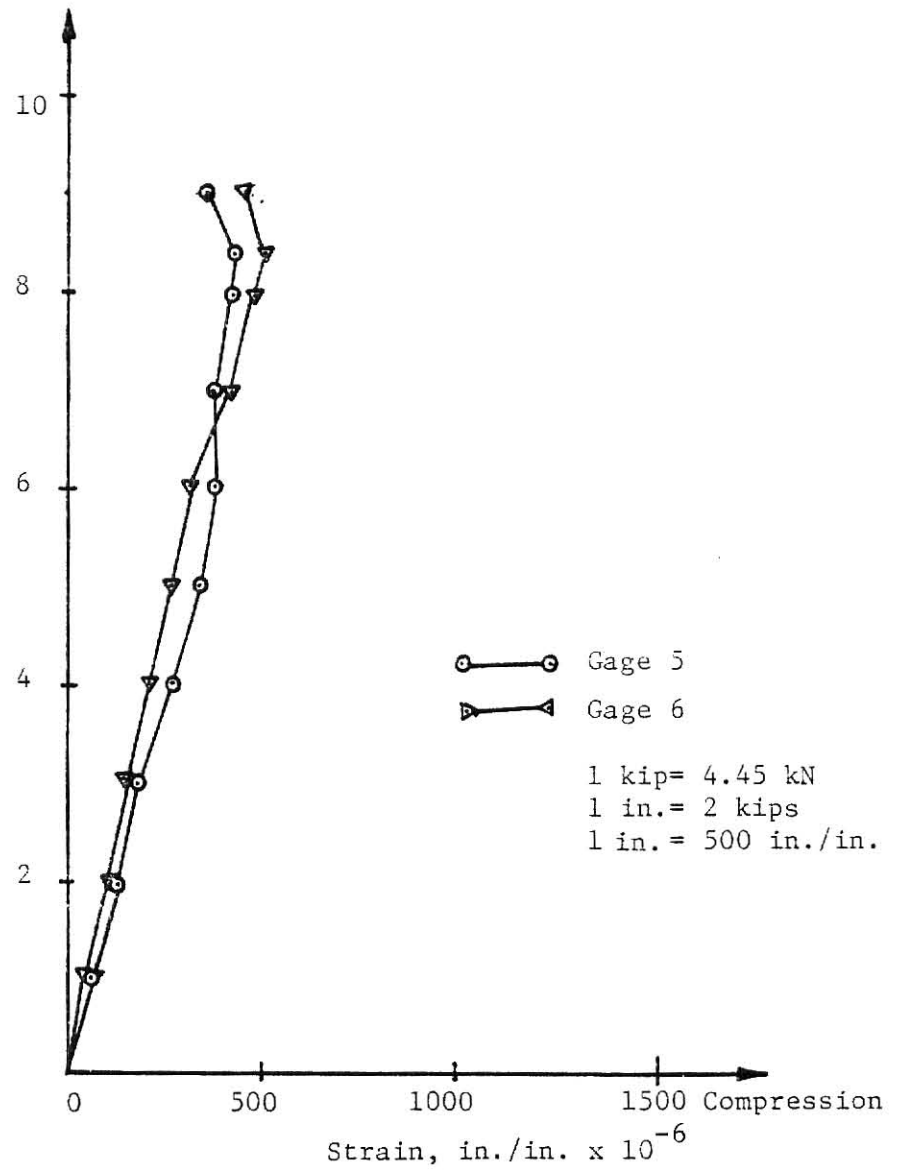


Figure 5.2c Load vs. Strain, Plate 2, Gage 5 & Gage 6
(SS - Opening at Bottom - S = 1.0 in.)

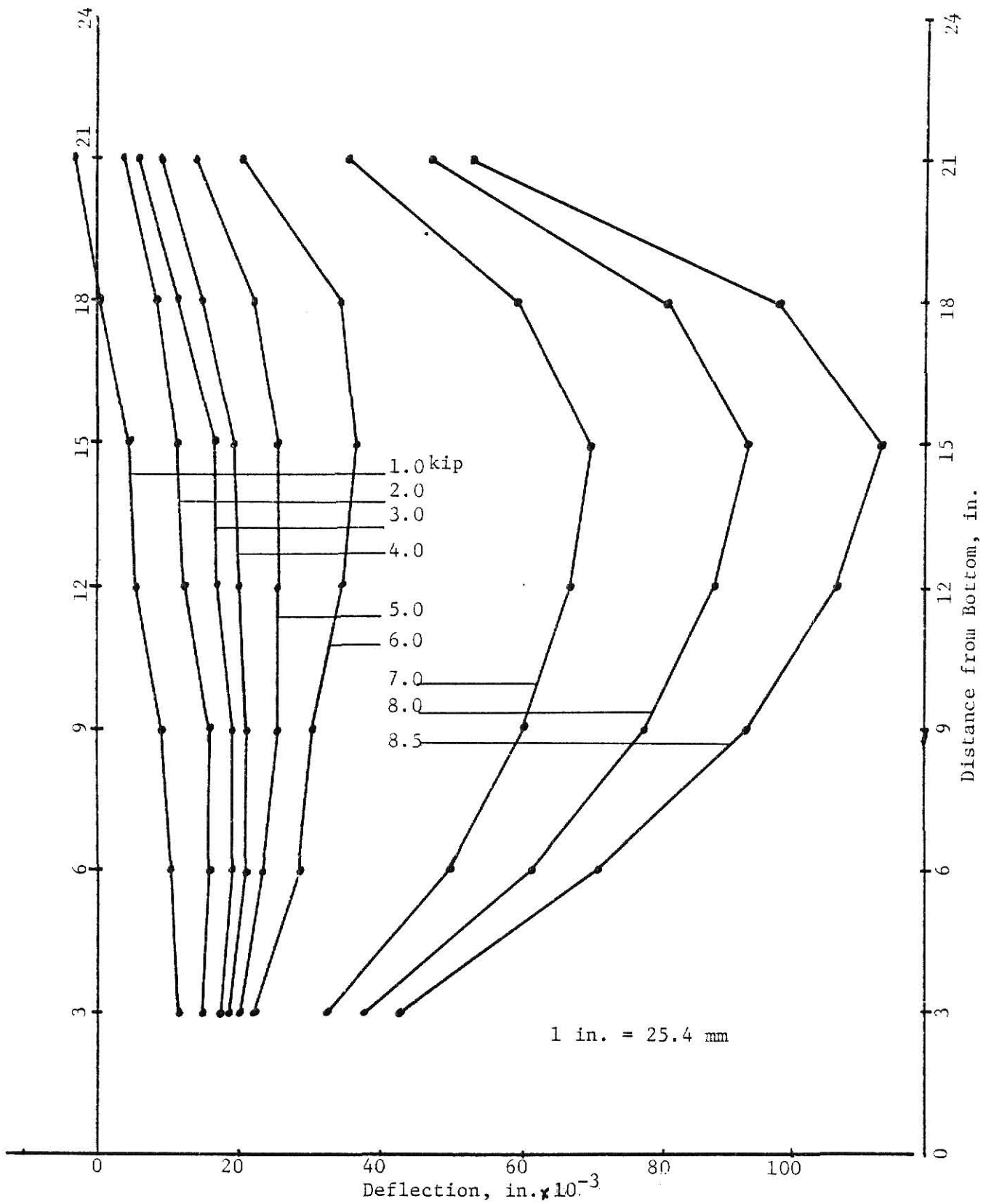
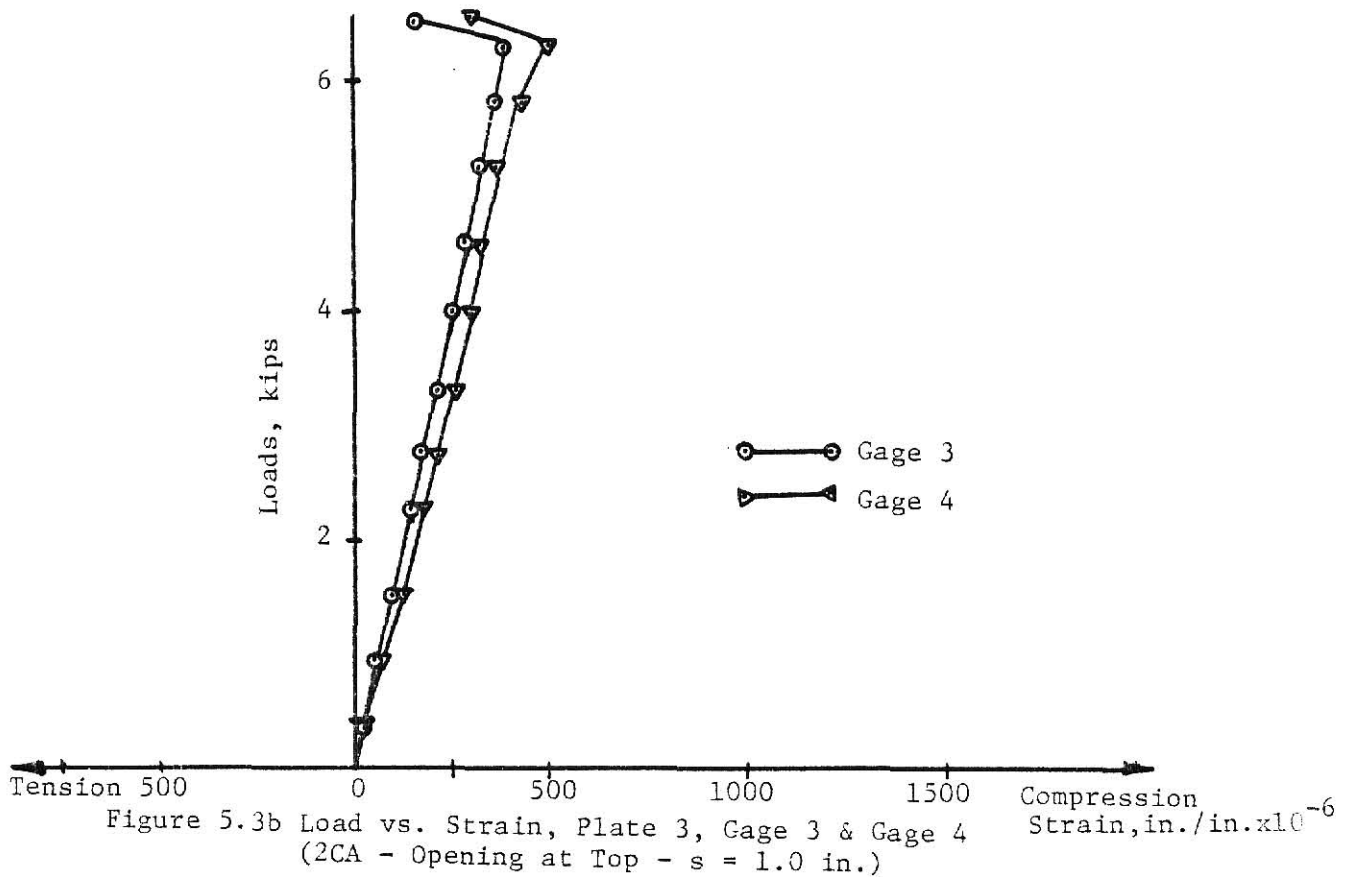
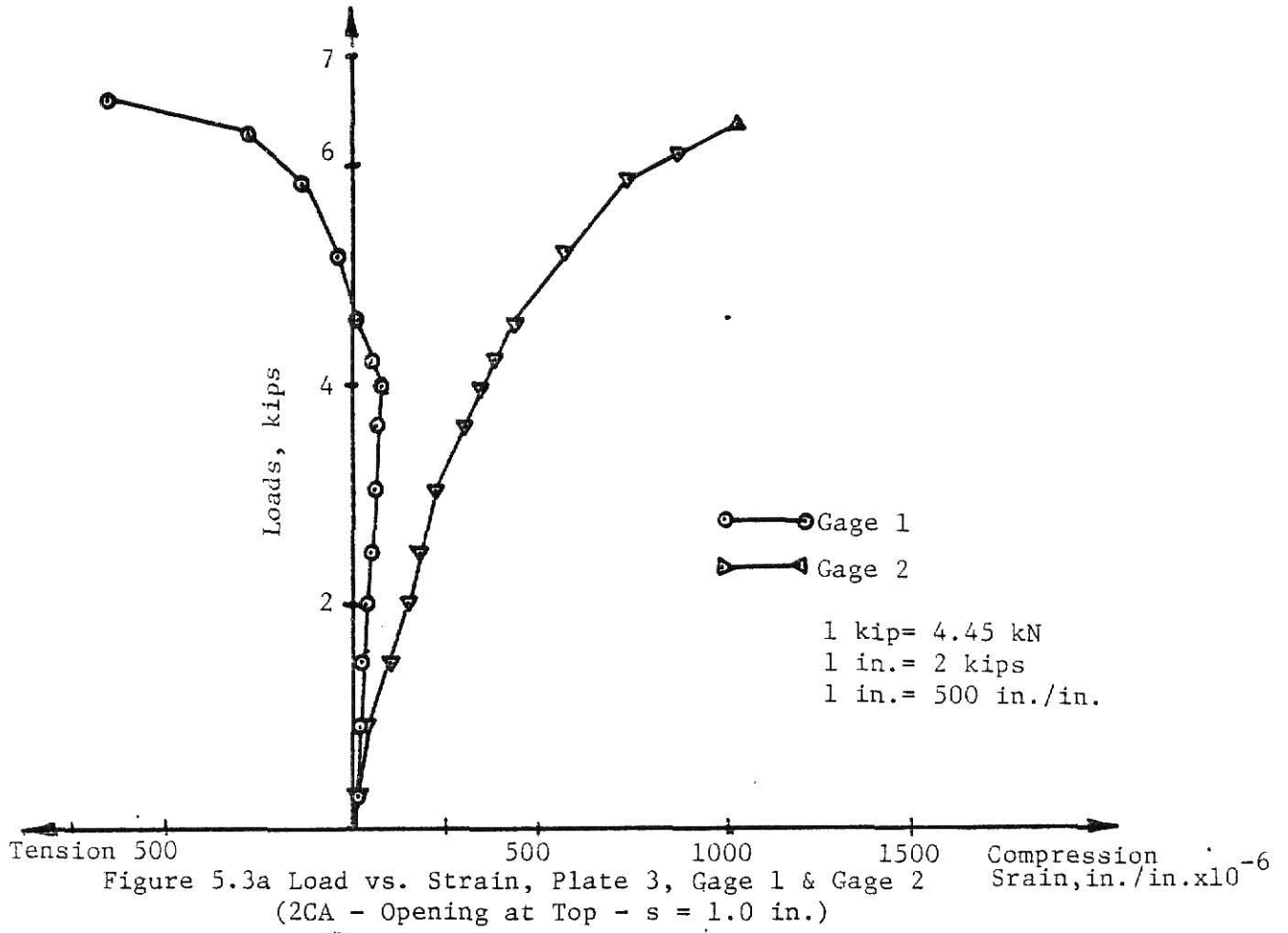


Figure 5.2d Deflection Profiles for Panel 2
(SS - Opening at Bottom - $s = 1.0$ in.)



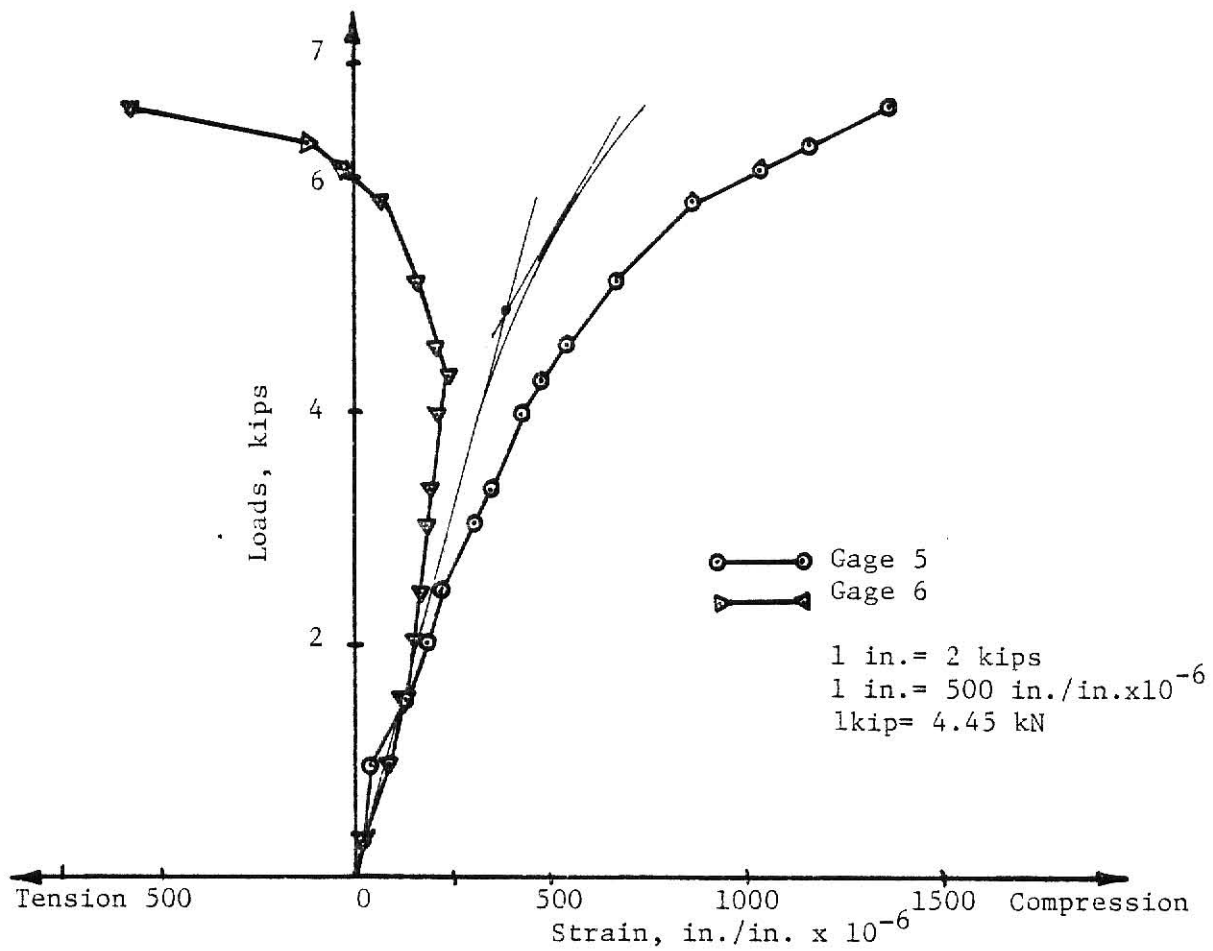


Figure 5.3c Load vs. Strain, Plate 3, Gage 5 & Gage 6
 (2CA - Opening at Top - $s = 1.0$ in.)

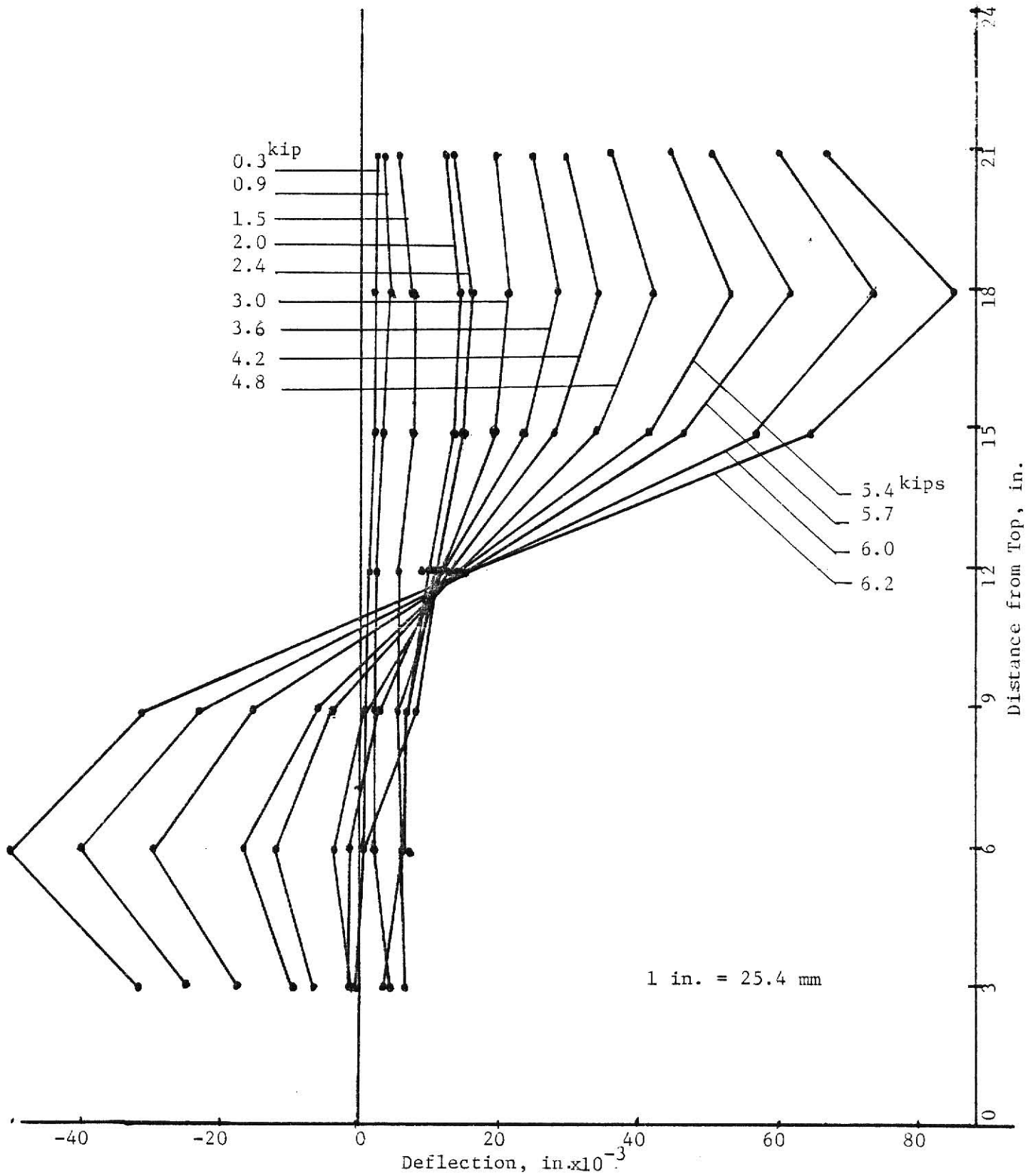


Figure 5.3d Deflection Profiles for Panel 3
(2CA - Opening at Top- $s = 1.0$ in.)

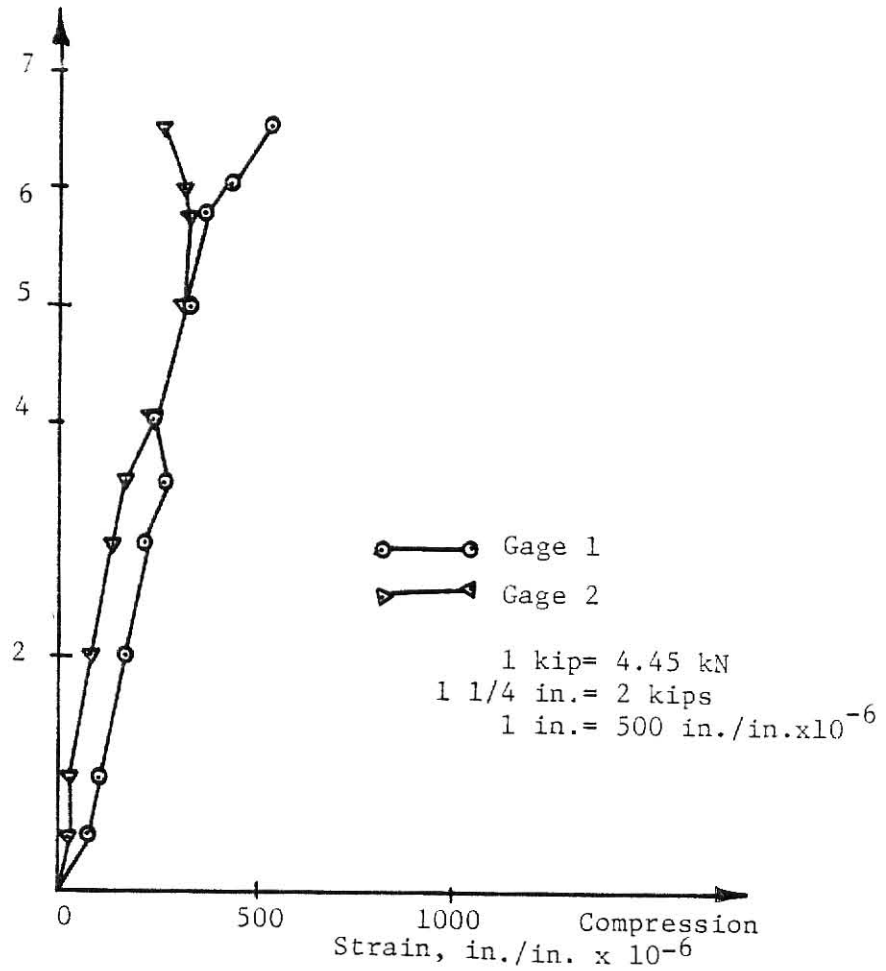


Figure 5.4a Load vs. Strain, Plate 4, Gages 1 & 2
(2CA - Opening at Top - $s = 1$ in.)

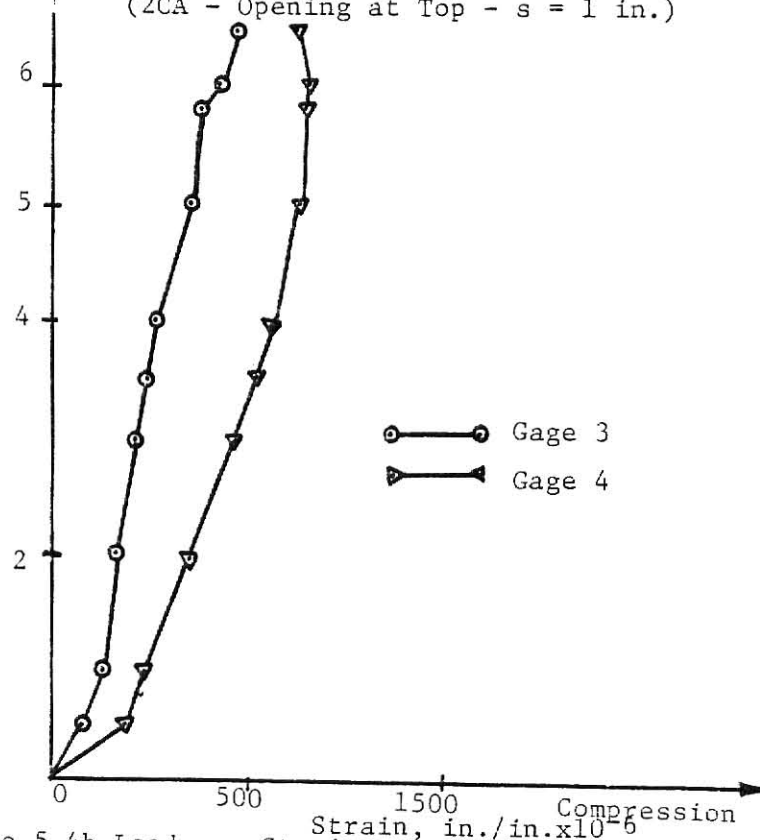


Figure 5.4b Load vs. Strain, Plate 4, Gages 3 & 4

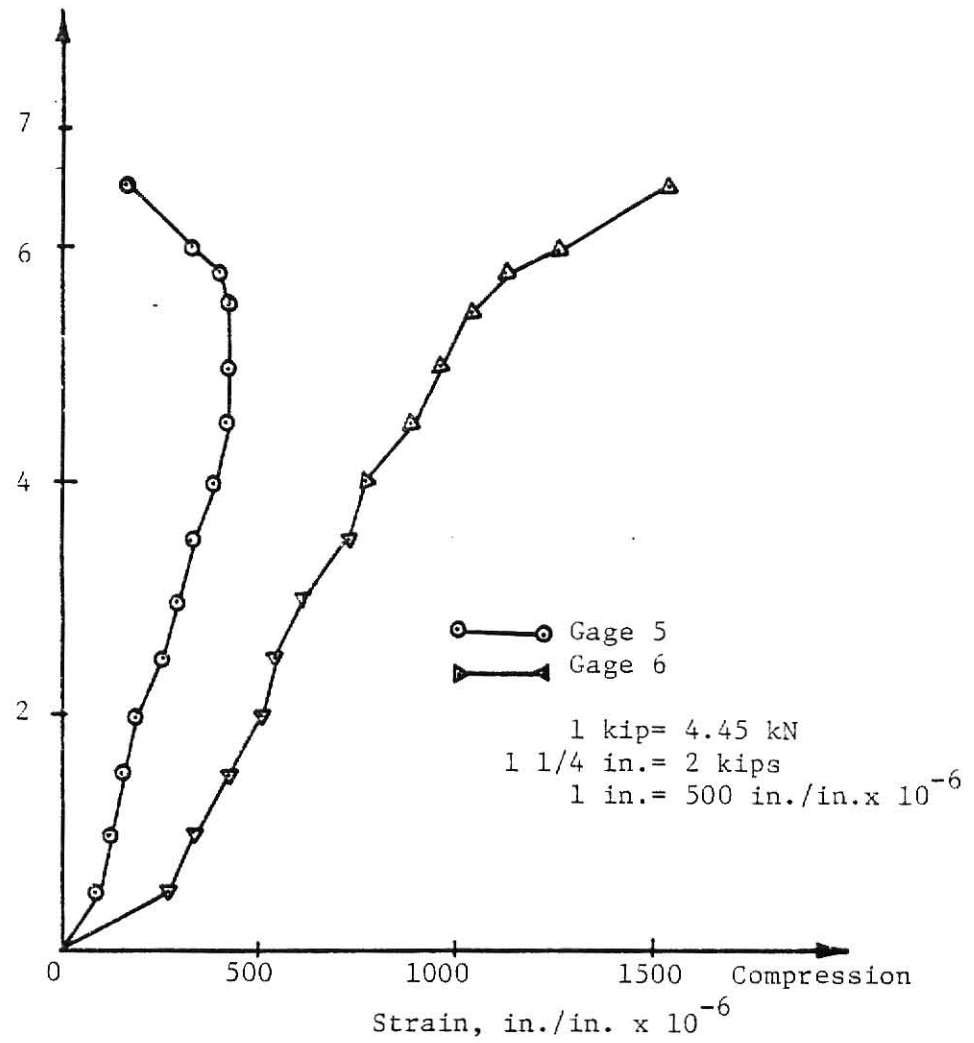


Figure 5.4c Load vs. Strain, Plate 4, Gages 5 & 6
 (2CA - Opening at Top - $s = 1$ in.)

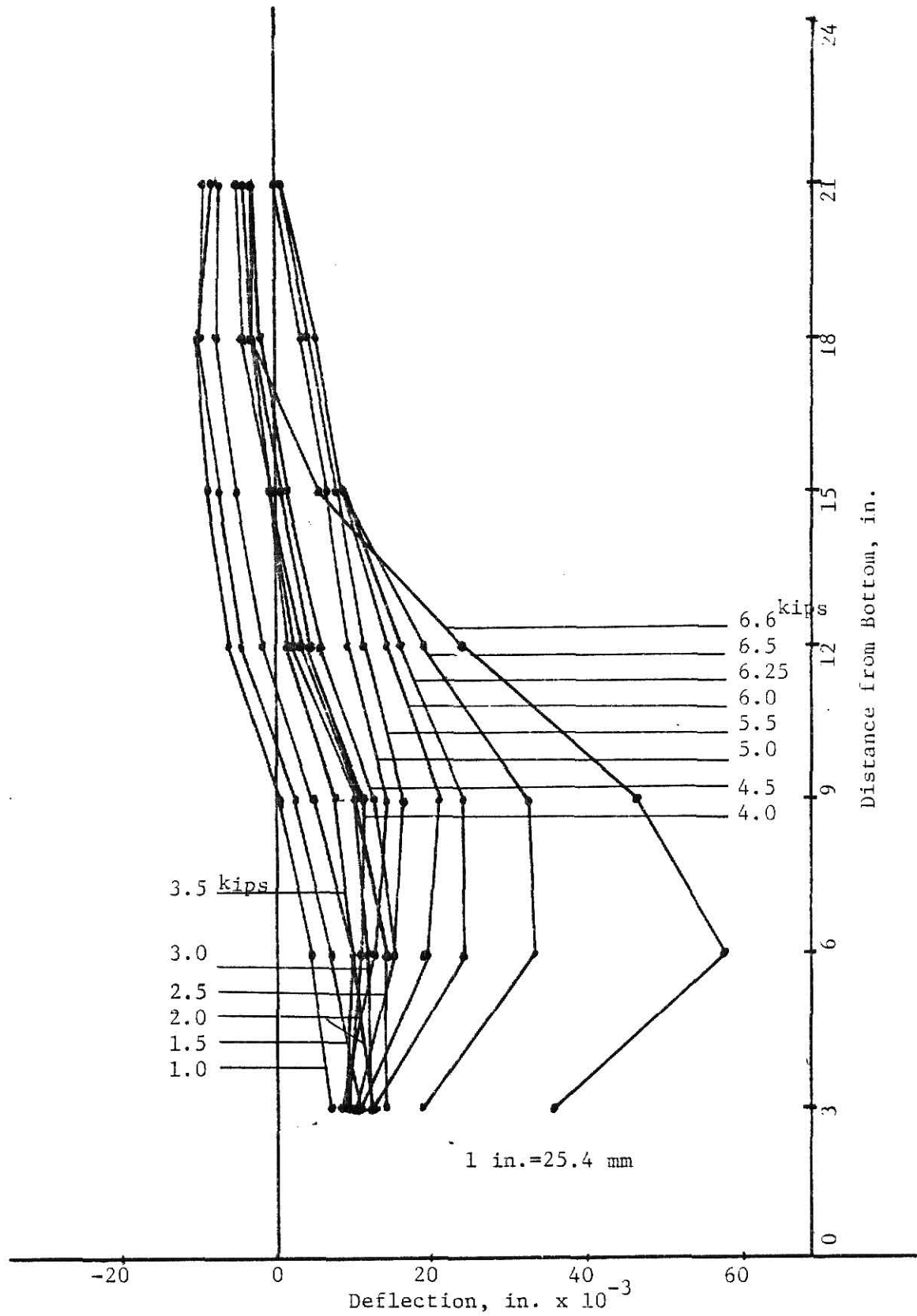


Figure 5.4d Deflection Profiles for Panel 4
(2CA - Opening at Top - $s = 1.0$ in.)

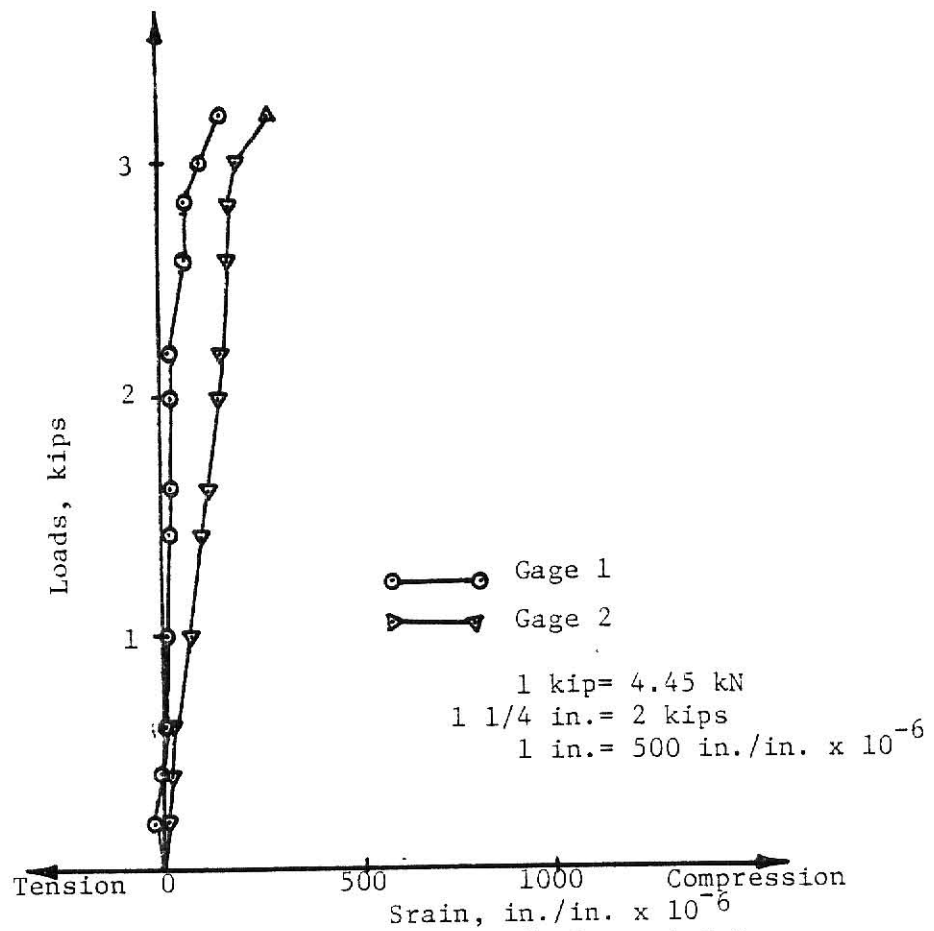


Figure 5.5a Load vs. Strain, Plate 5, Gages 1 & 2
(Free - Opening at Top - $s = 1/2$ in.)

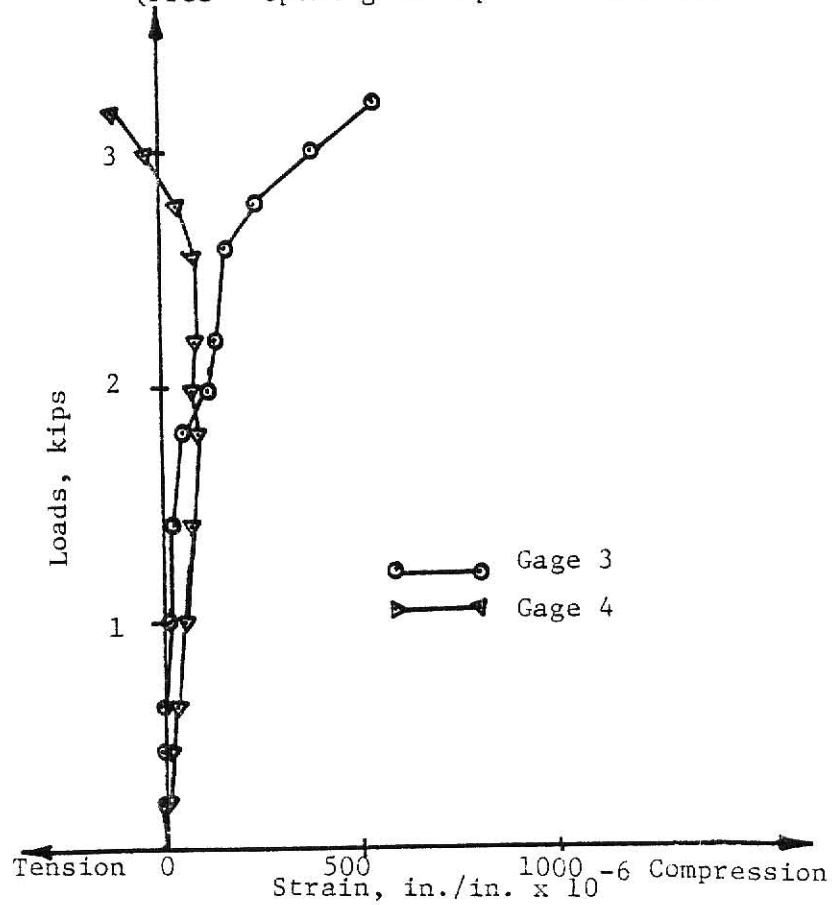


Figure 5.5b Load vs. Strain, Plate 5, Gages 3 & 4

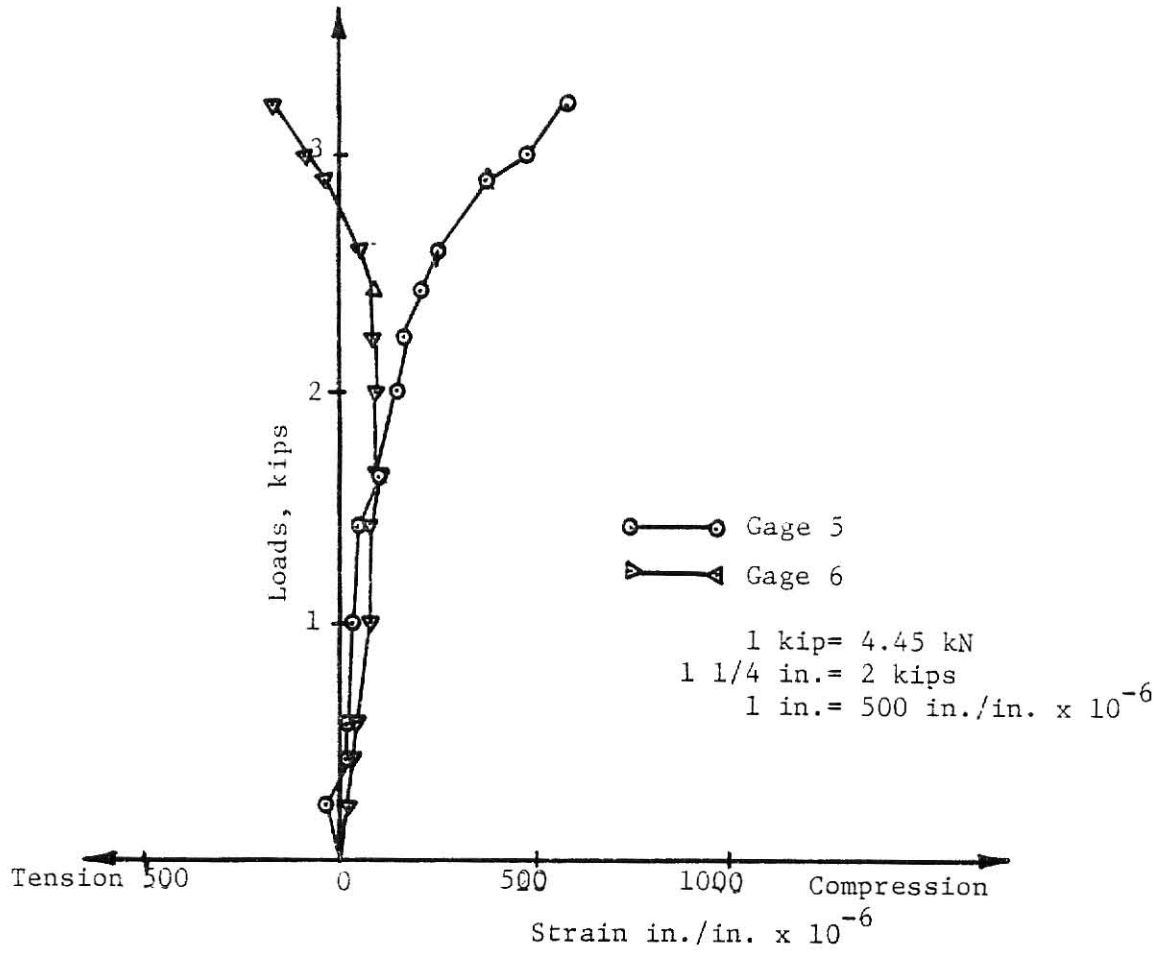


Figure 5.5c Load vs. Strain, Plate 5, Gages 5 & 6
 (Free - Opening at Top - $s = 1/2$ in.)

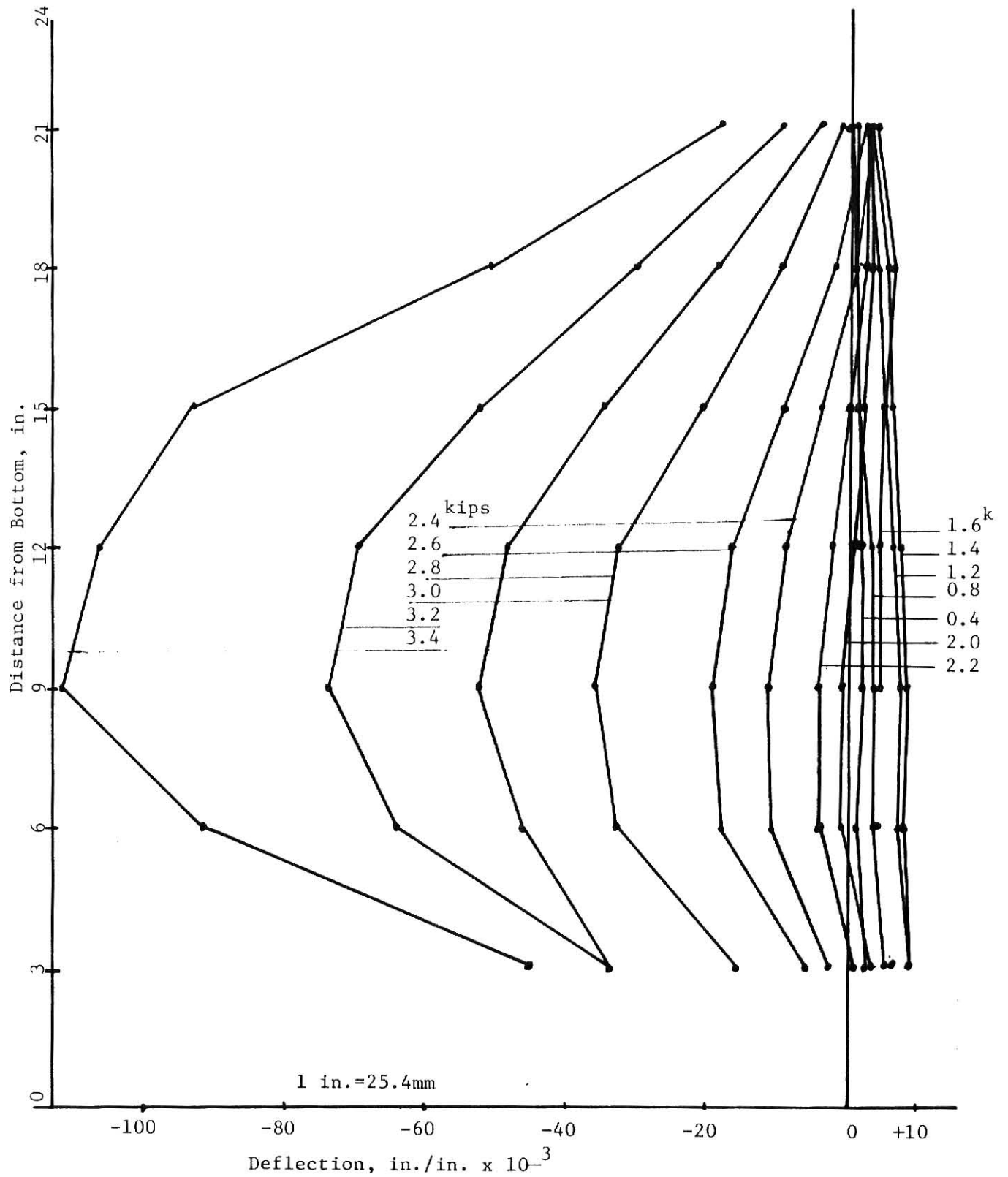


Figure 5.5d Deflection Profiles for Panel 5
(Free - Opening at Top - $s = 1/2$ in.)

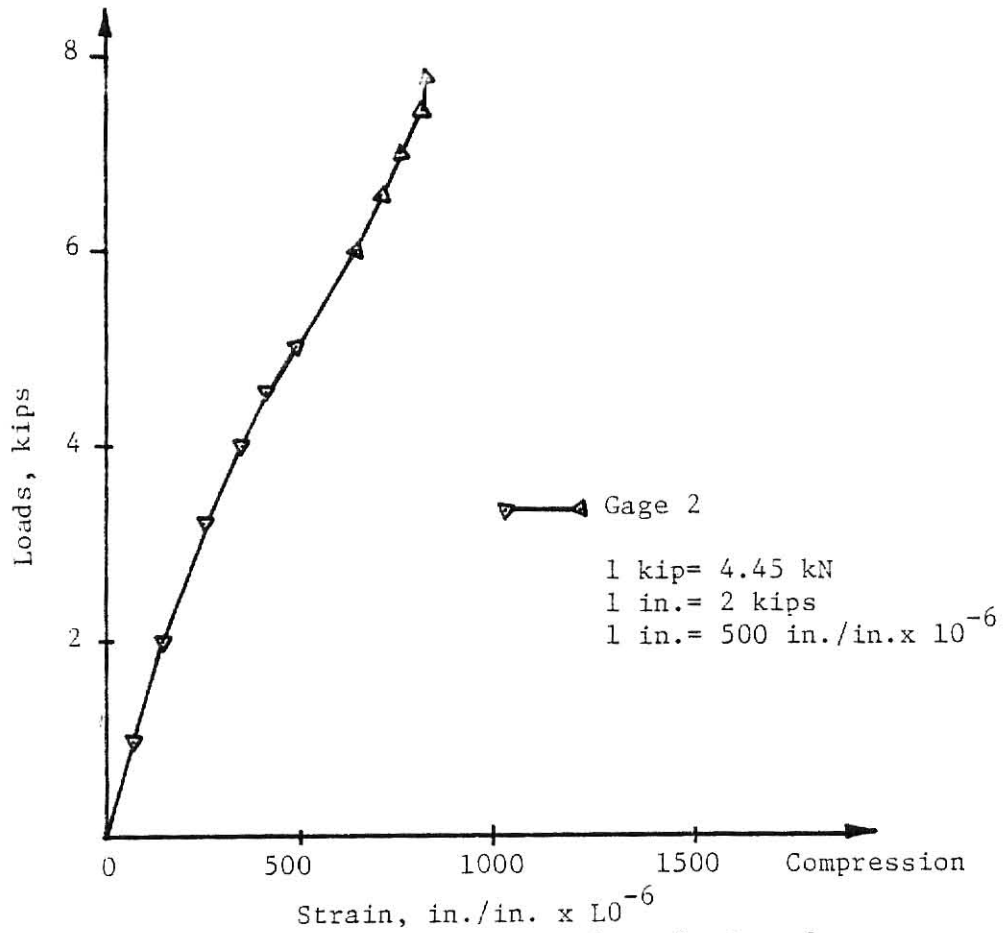


Figure 5.6a Load vs. Strain, Plate 6, Gage 2
(2CA - Opening at Top - $s = 1/2$ in.)

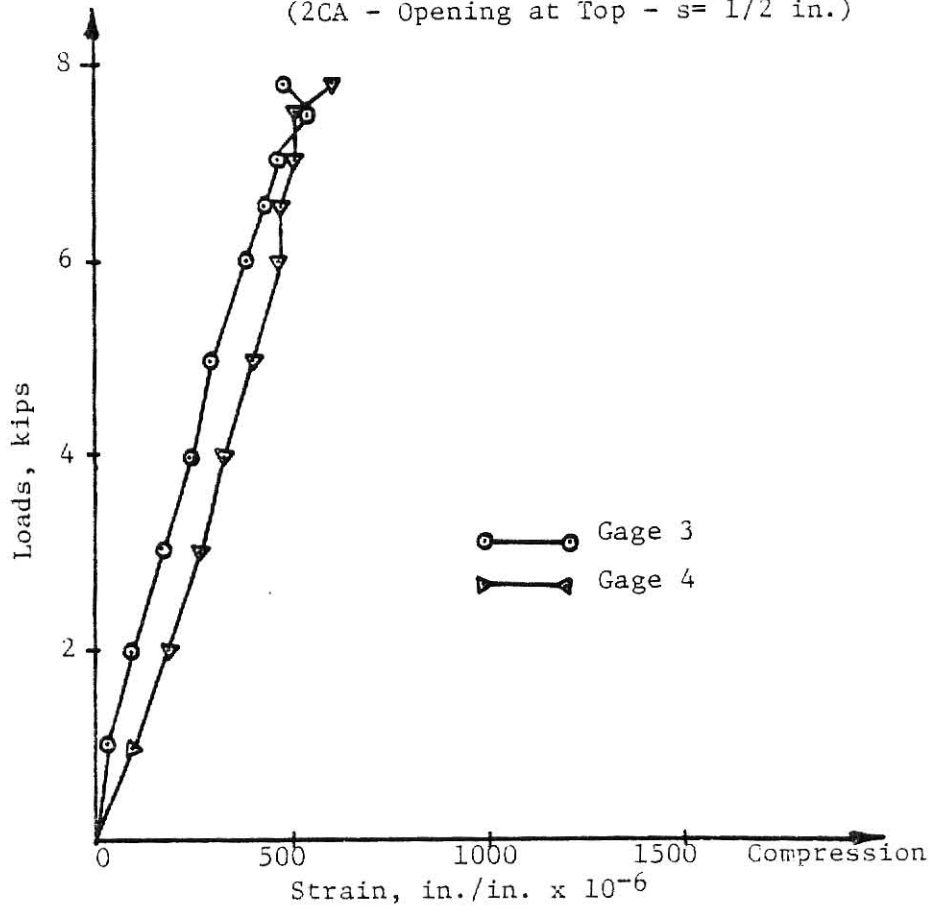


Figure 5.6b Load vs. Strain, Plate 6, Gages 3 & 4

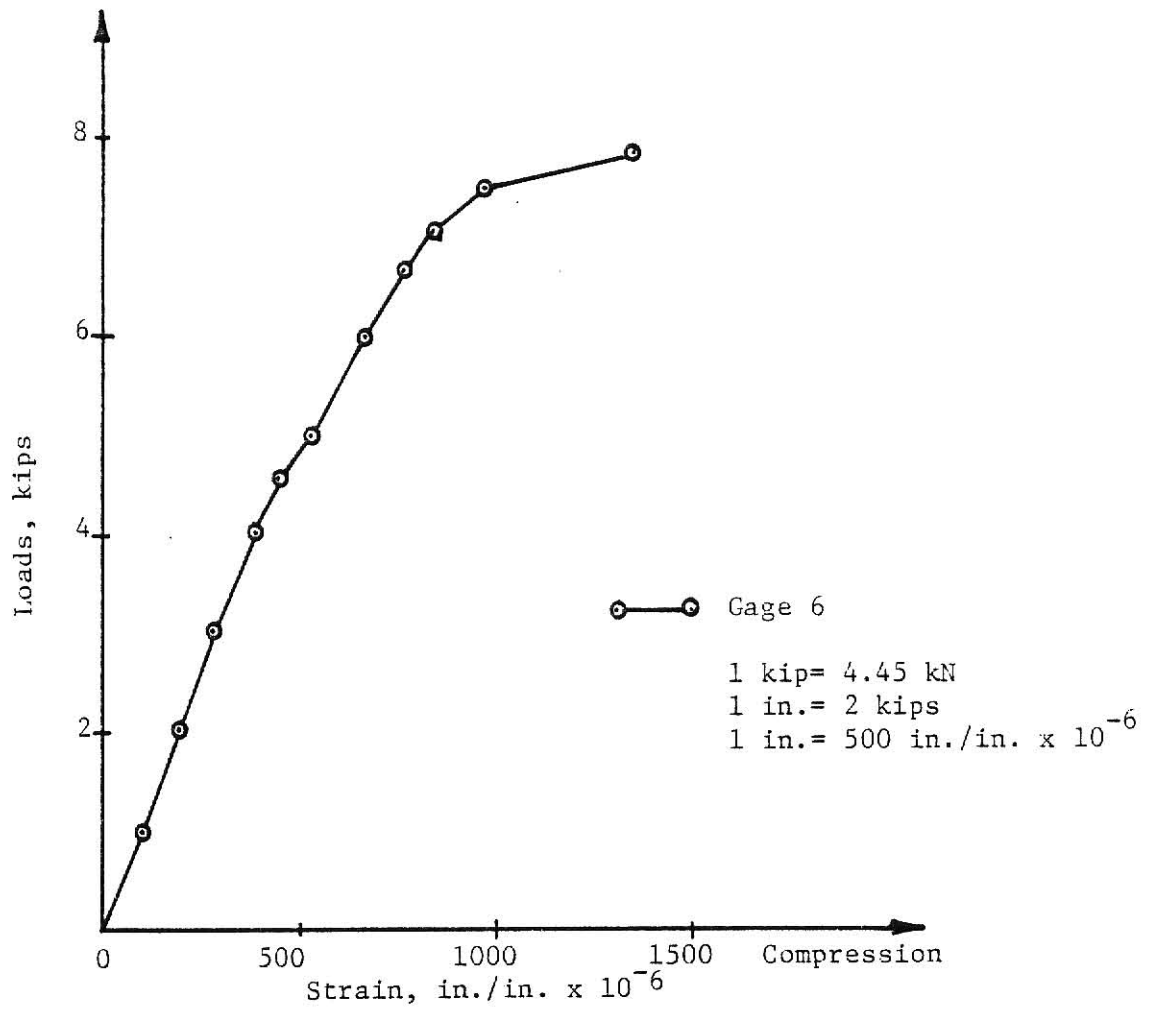


Figure 5.6e Load vs. Strain, Plate 6, Gage 6
(2CA - Opening at Top - $s = 1/2$ in.)

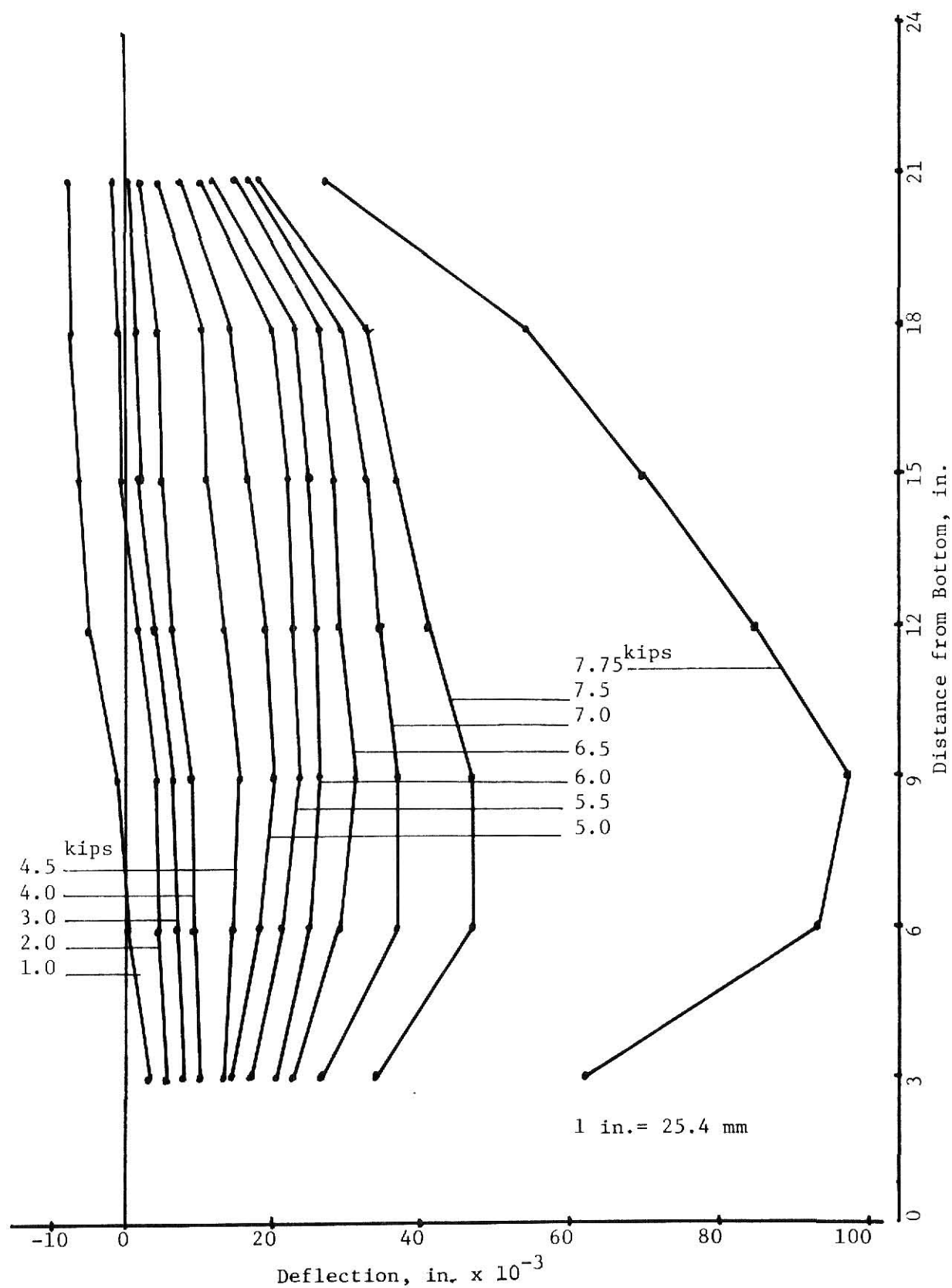


Figure 5.6d Deflection Profiles for Panel 6
(2CA - Opening at Top - $s=1/2$ in.)

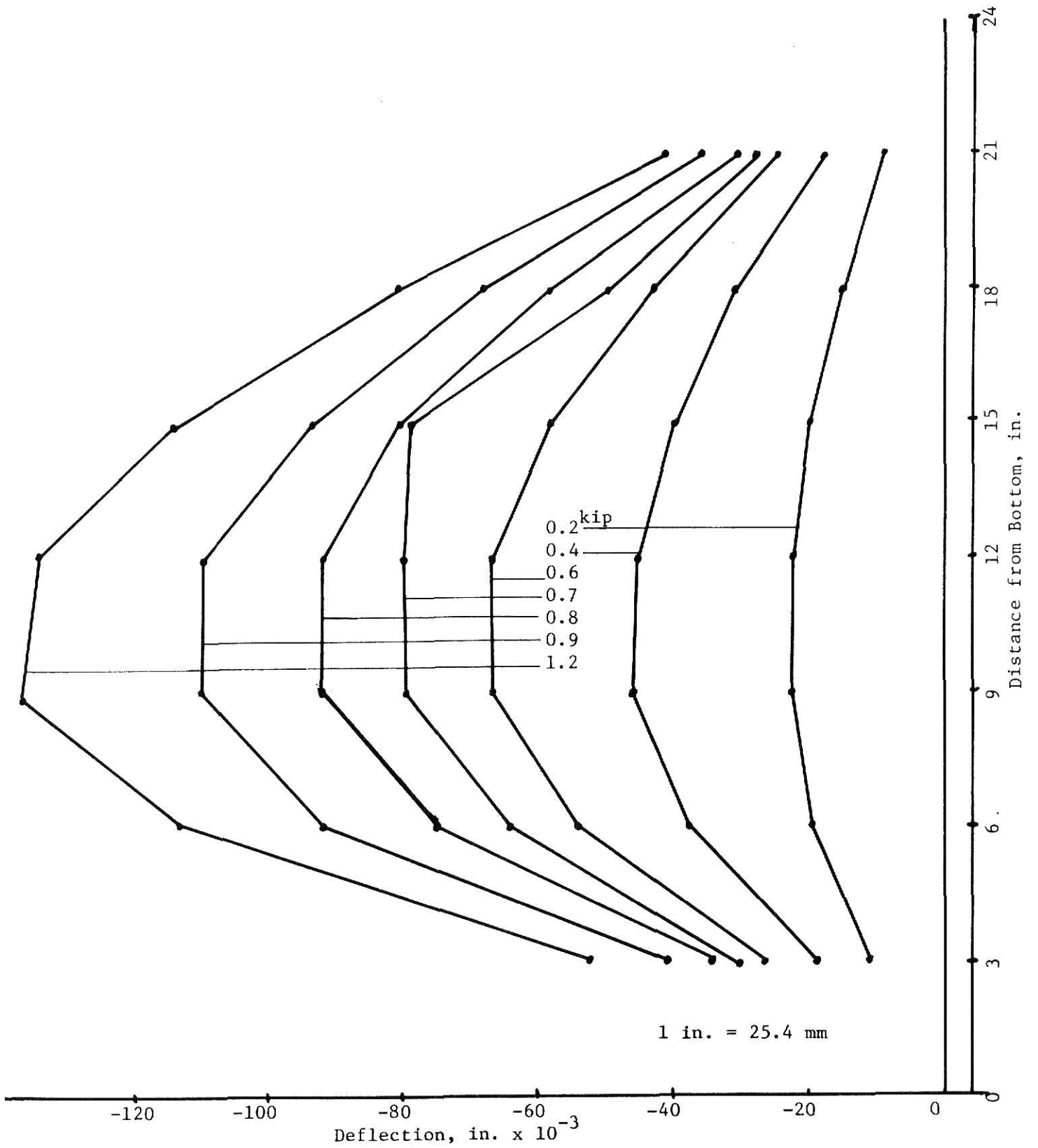


Figure 5.7d Deflection Profiles for Plate 7
(Free Opening at Top- $s=1.0$ in.)

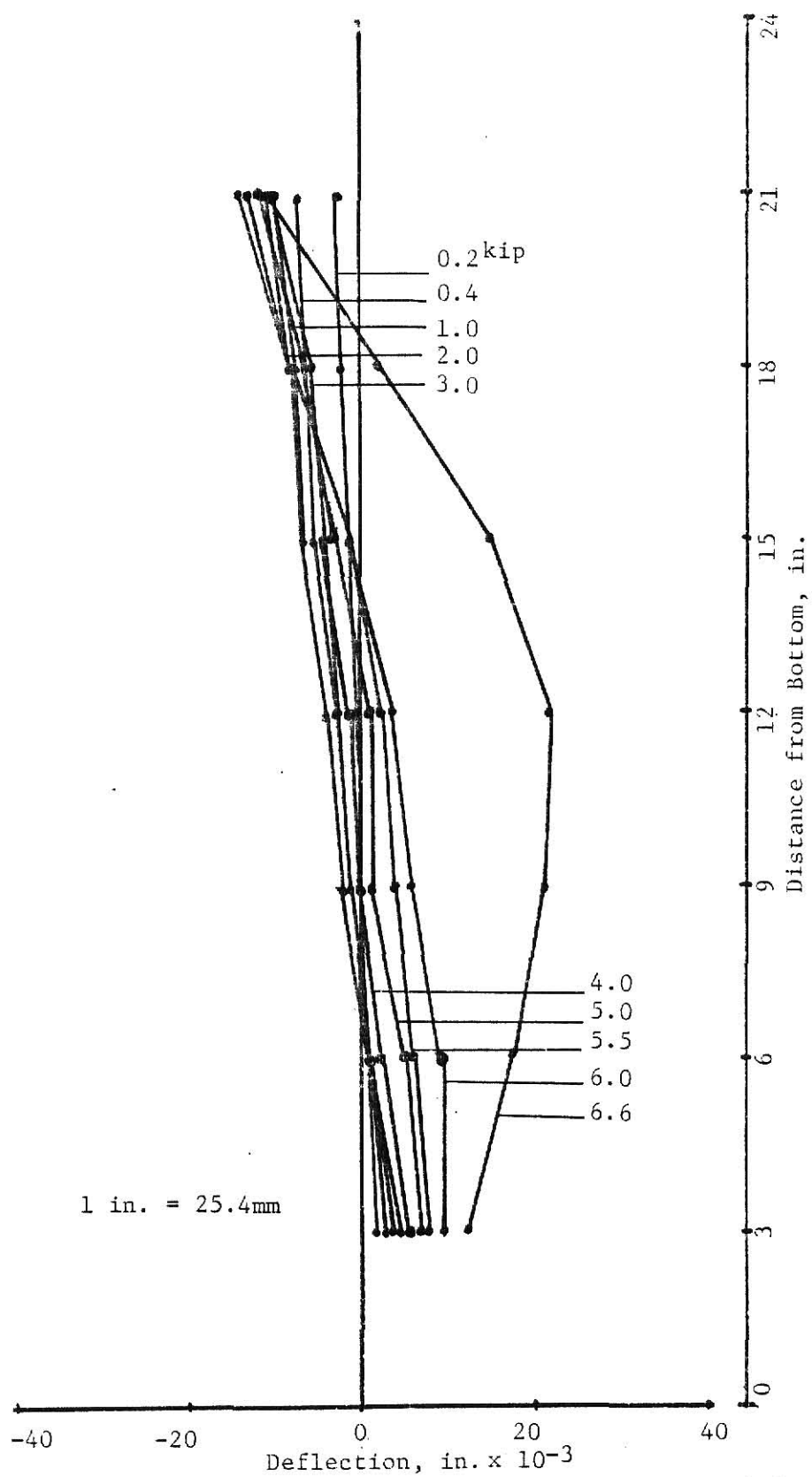


Figure 5.8d Deflection Profiles for Panel 8
(SS - Opening at Bottom $s=0.0$ in.)

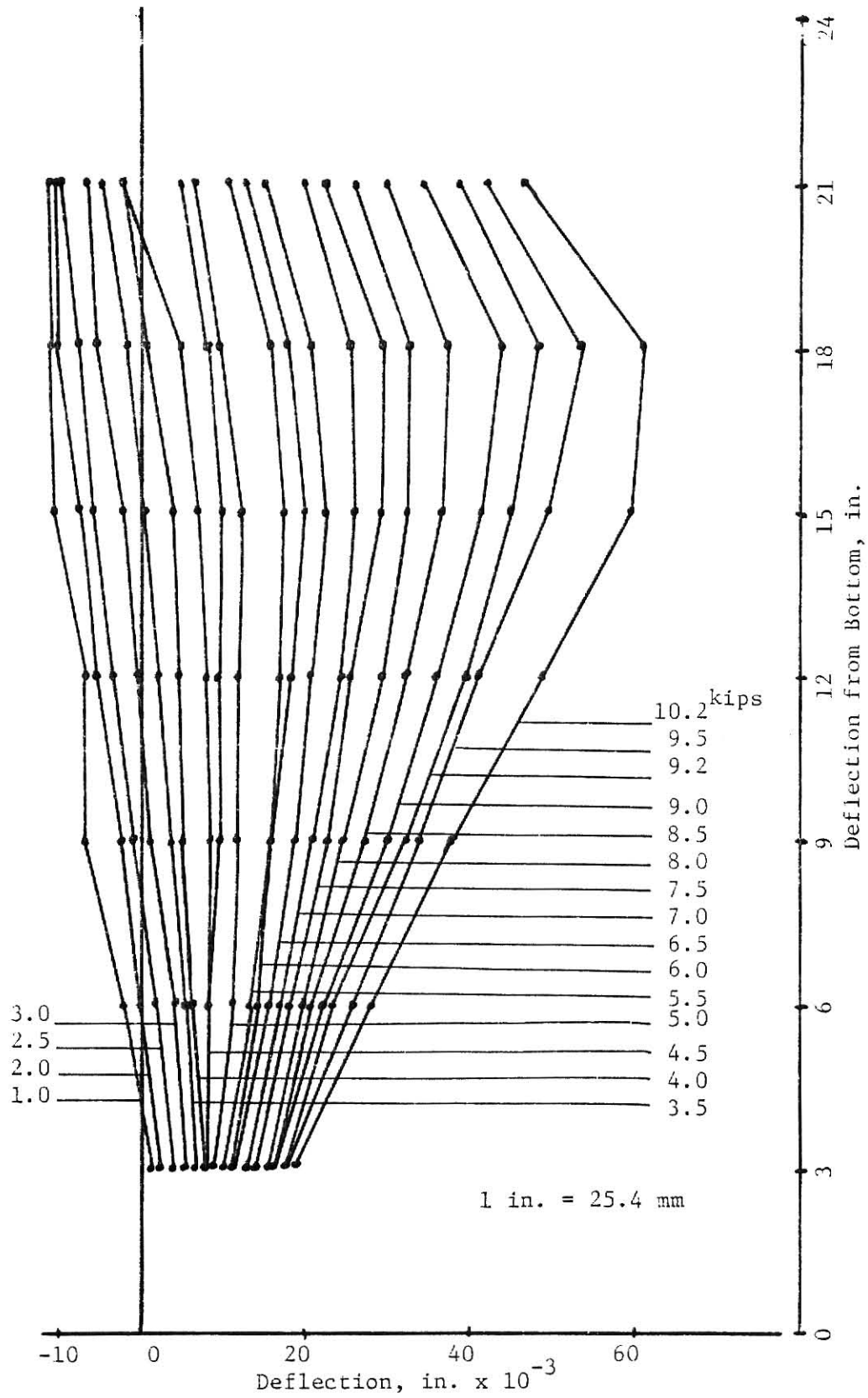


Figure 5.9d Deflection Profiles for Panel 9
(SS - Opening at Bottom, $s=1/2$ in.)

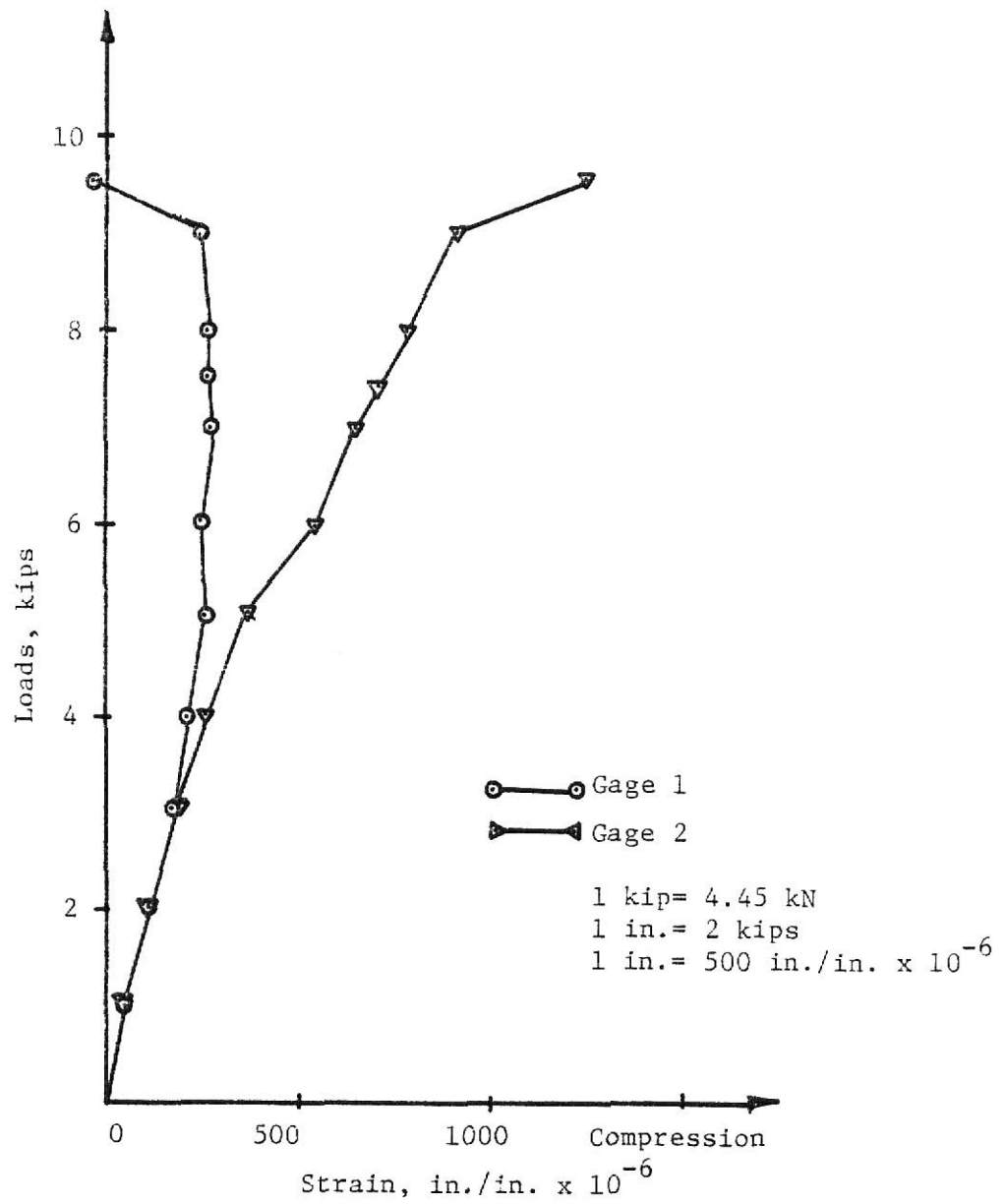


Figure 5.10a Load vs. Strain, Plate 10, Gages 1 & 2
(2CA - Opening at Top - $s=1/2$ in.)

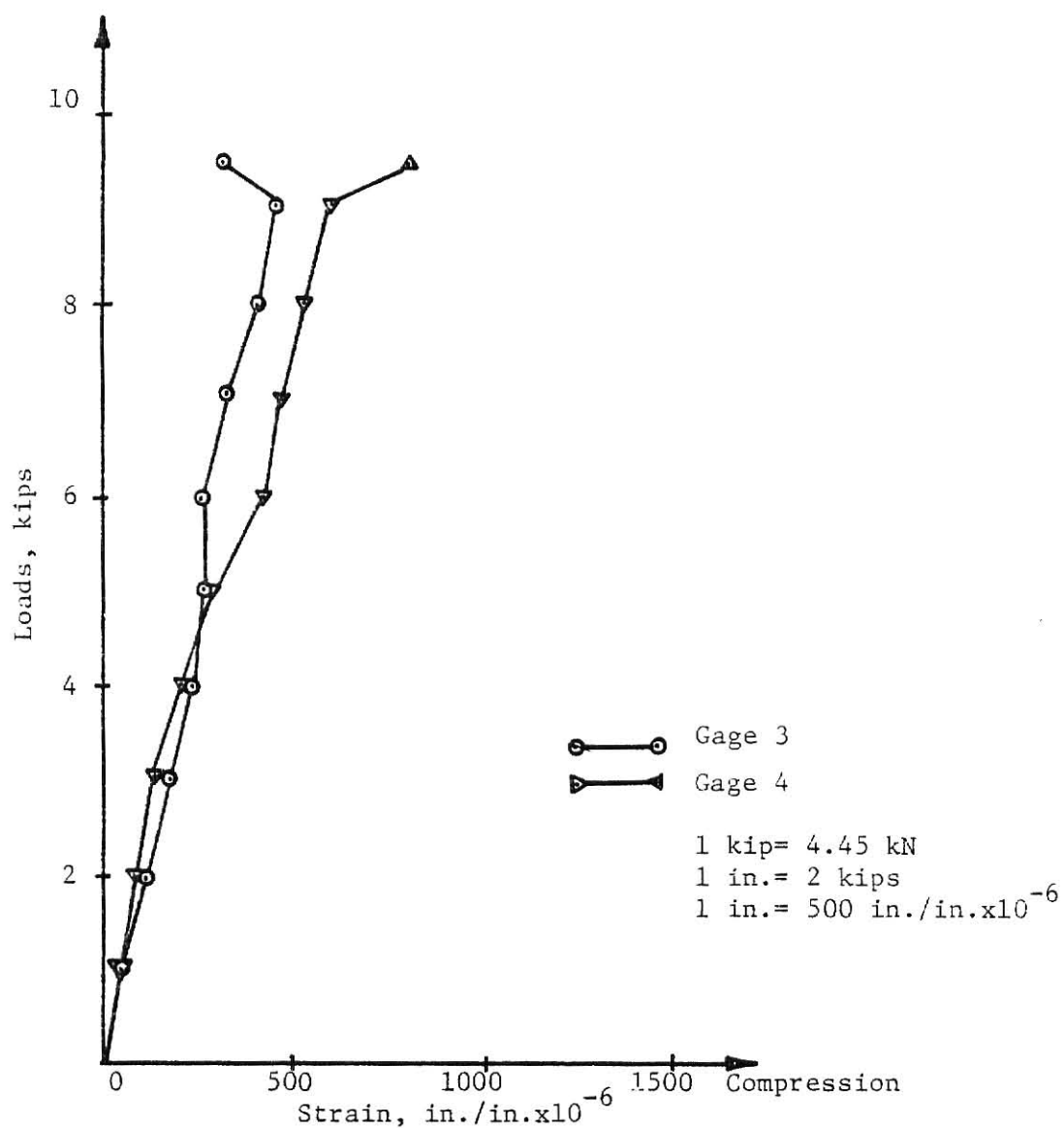


Figure 5.10b Load vs. Strain, Plate 10, Gages 3 & 4
(2CA - Opening at Top - $s = 1/2$ in.)

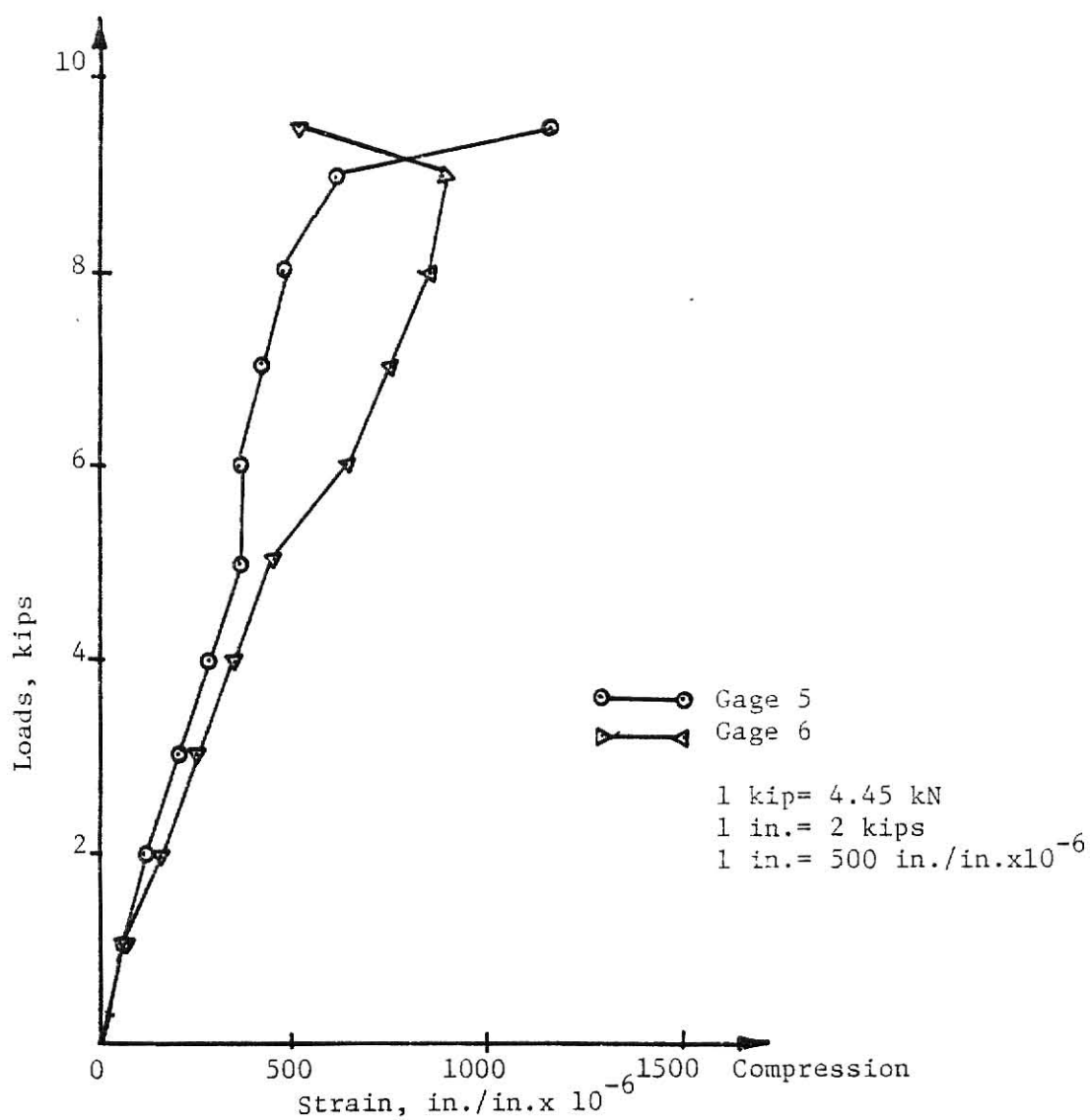


Figure 5.10c Load vs. Strain, Plate 10, Gages 5 & 6
(2CA) - Opening at Top - $s = 1/2$ in.)

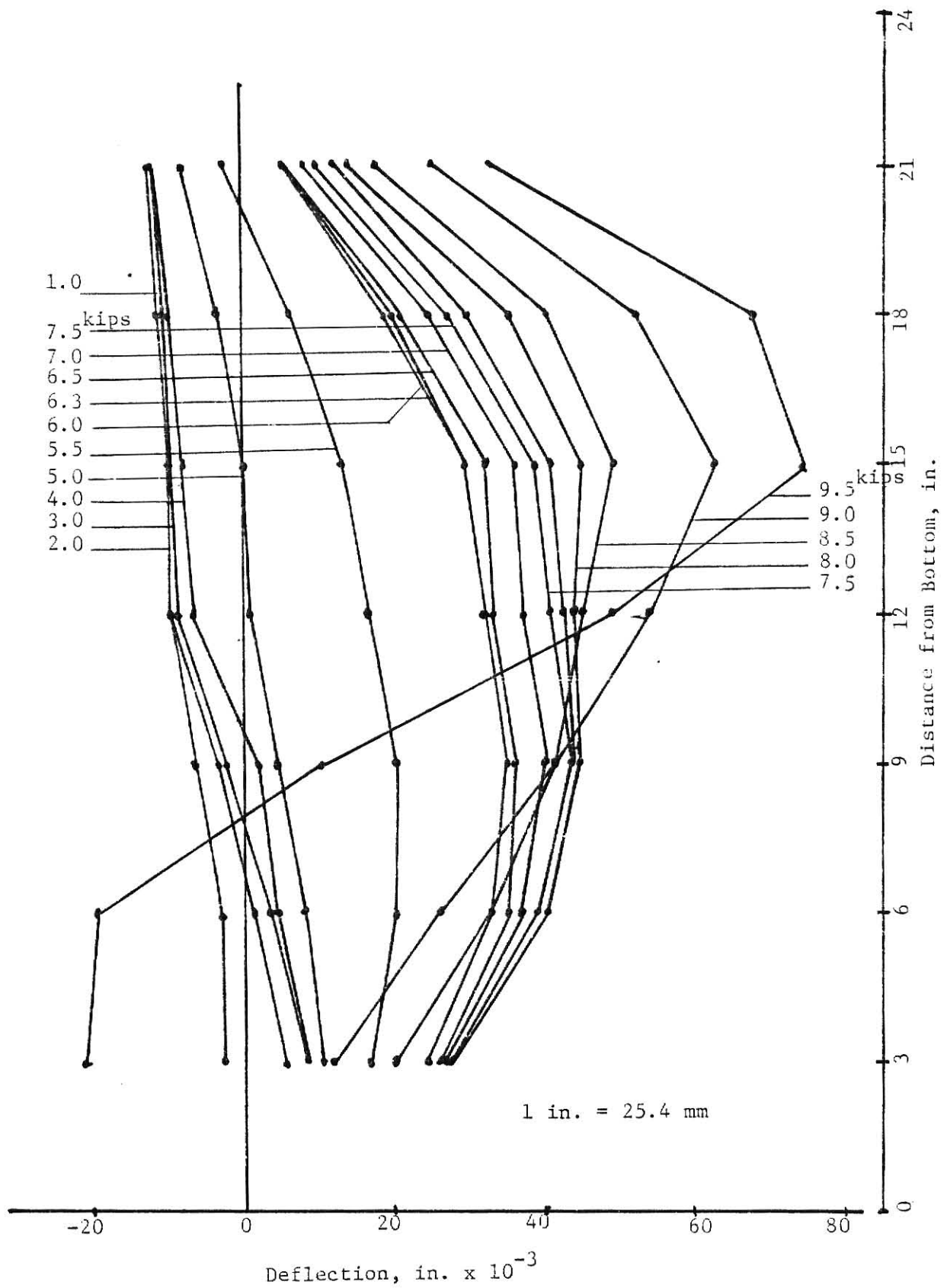


Figure 5.10d Deflection Profiles for Plate 10
(2CA - Opening at Top - $s=1/2$ in.)

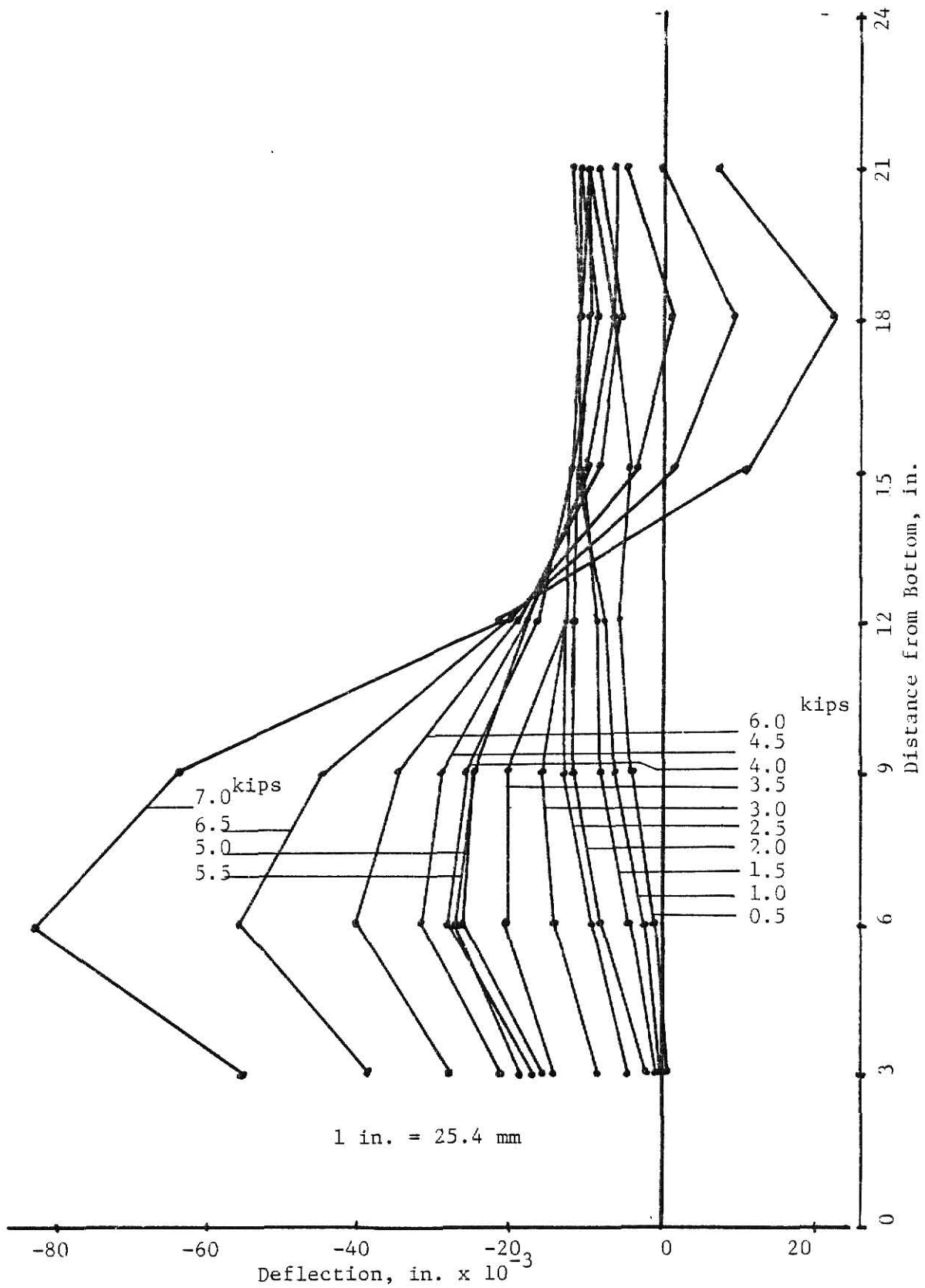


Figure 5.11d Deflection Profiles for Plate 11
(2CA - Opening at Top- $s = 0.0$ in.)

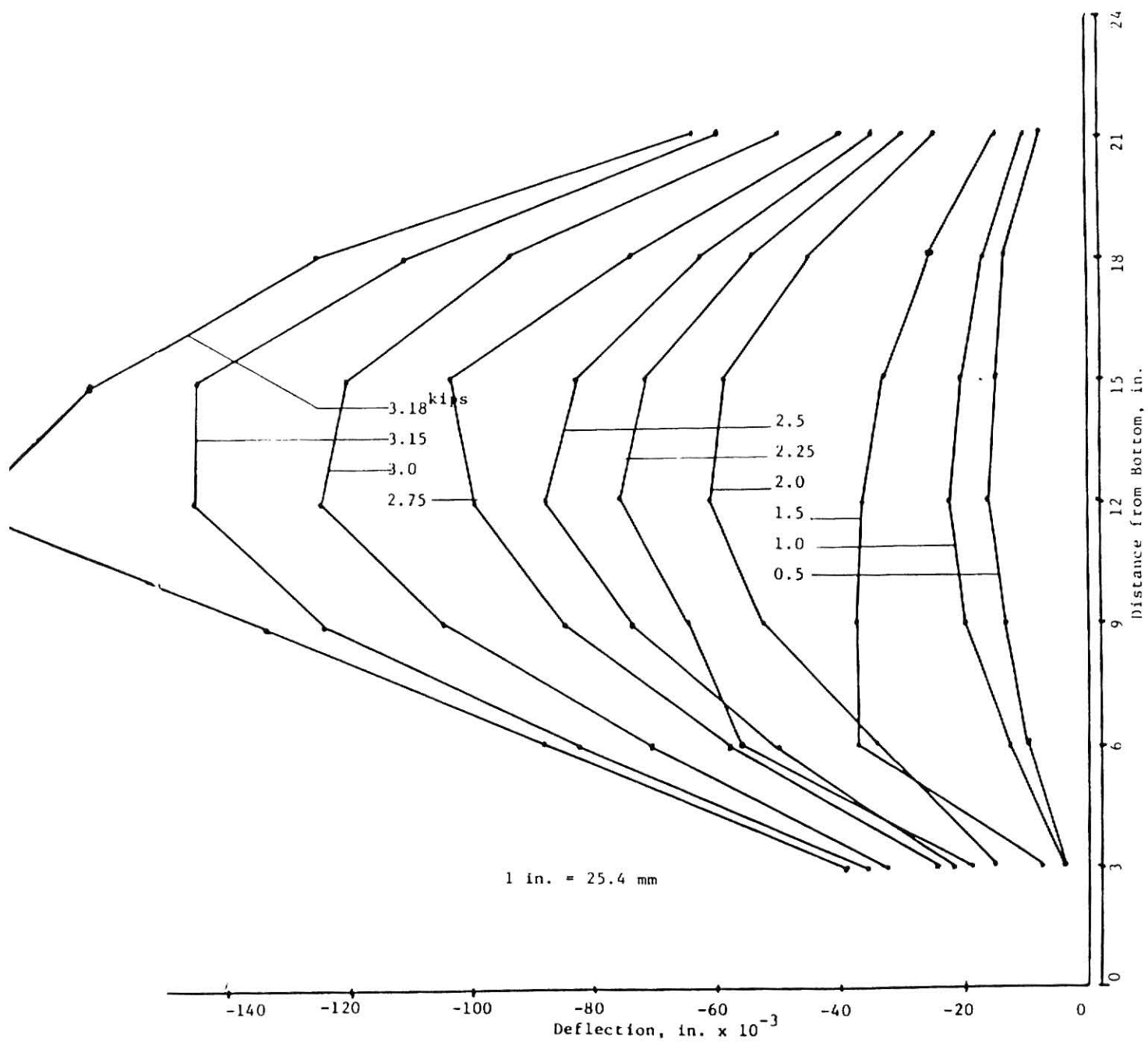


Figure 5.12d Deflection Profiles for Plate 12
(Free edges - Opening at Bottom $-s=0.5$ in.)

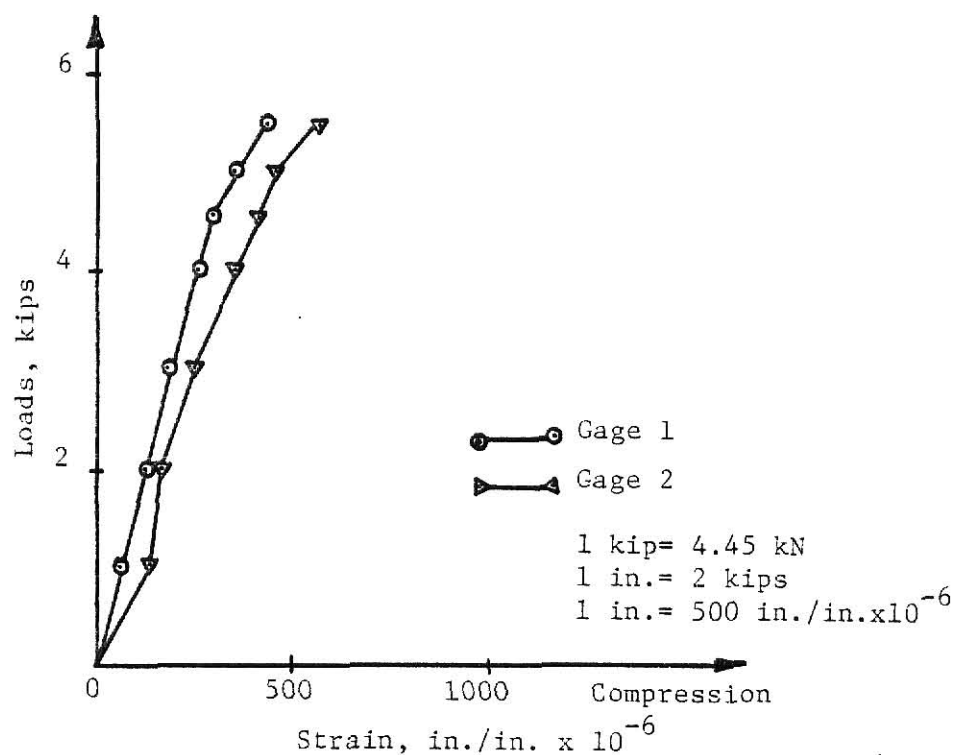


Figure 5.14a Load vs. Strain, Plate 14, Gages 1 & 2
(SS - Opening at Top - $s=2.0$ in.)

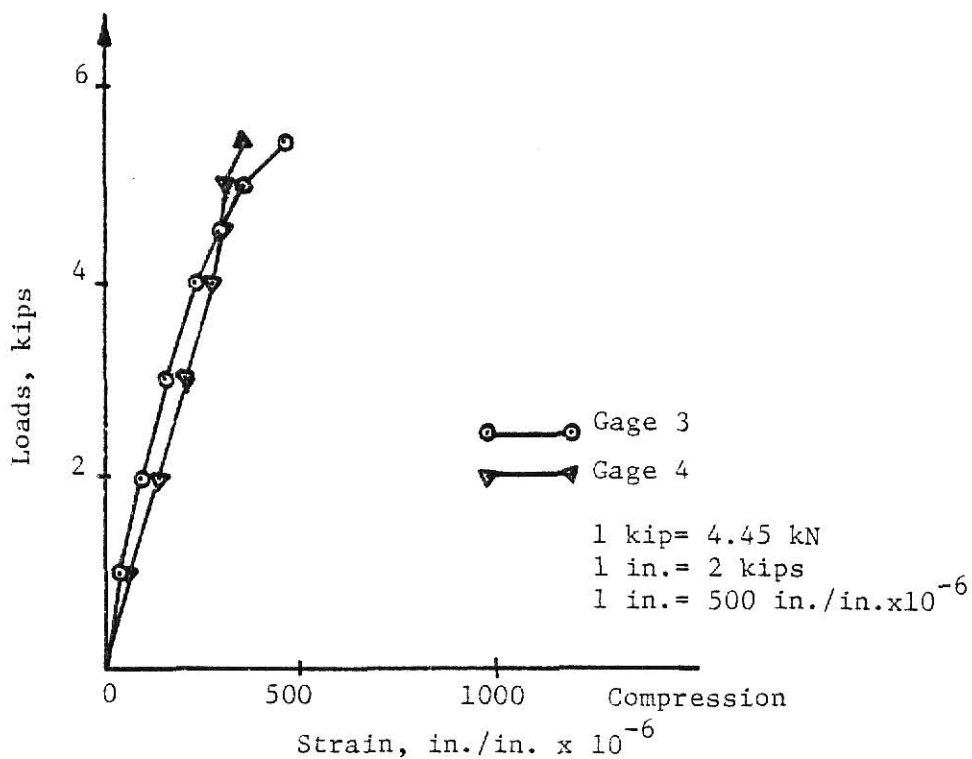


Figure 5.14b Load vs. Strain, Plate 14, Gages 3 & 4
(SS - Opening at Top - $s=2.0$ in.)

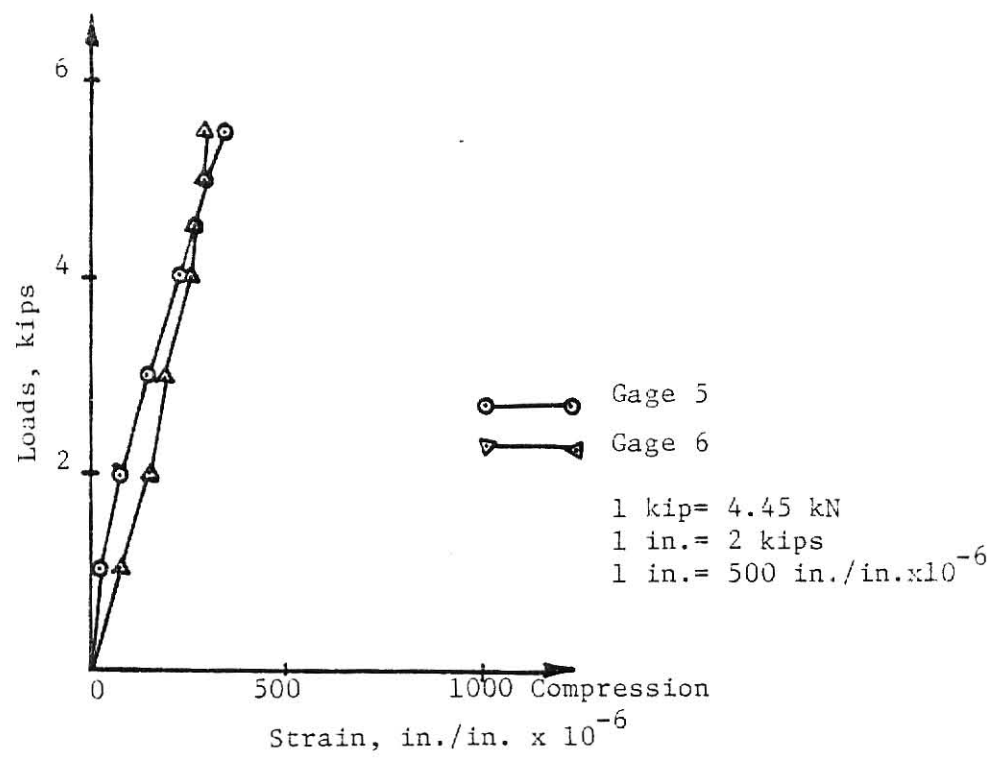


Figure 5.14c Load vs. Strain, Plate 14, Gages 5 & 6
(SS - Opening at Top - $s = 2.0$ in.)

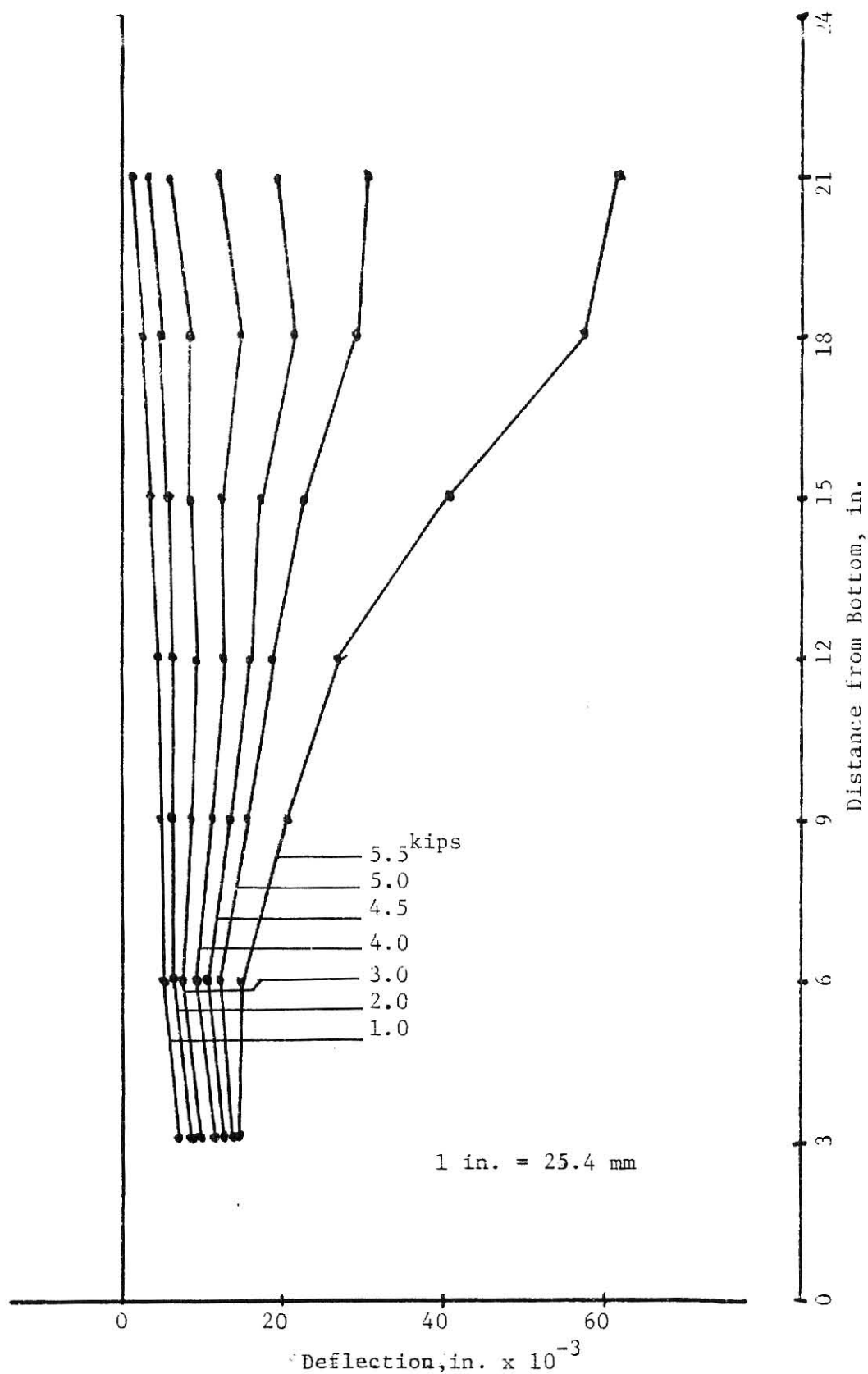


Figure 5.14d Deflection Profiles for Plate 14
(SS - Opening at Bottom - $s=2.0$ in.)

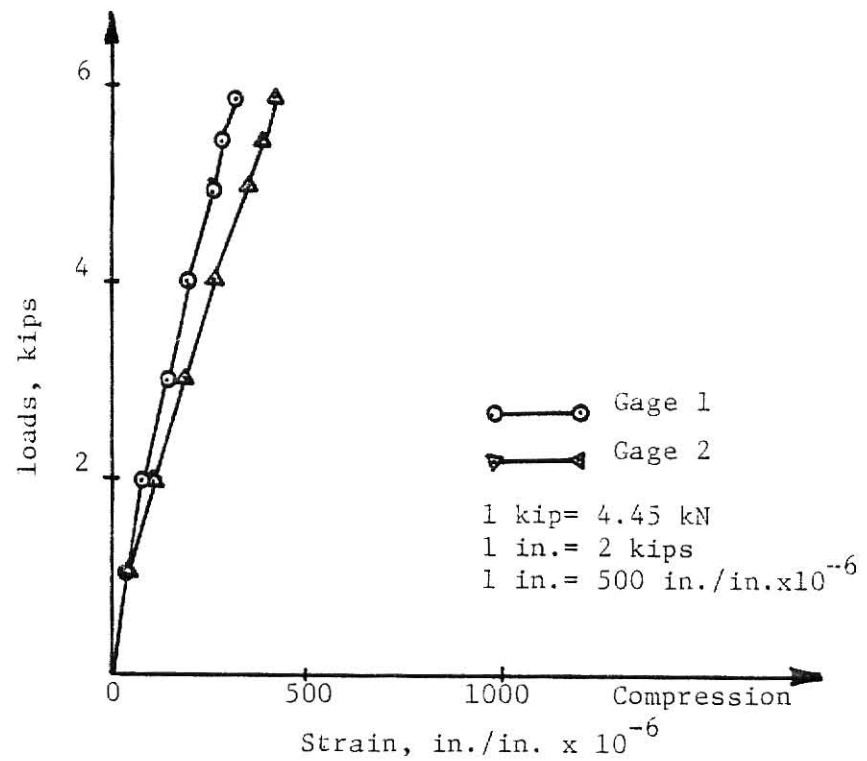


Figure 5.15a Load vs. Strain, Plate 15, Gages 1 & 2
(SS - Opening at Top - $s = 2.0$ in.)

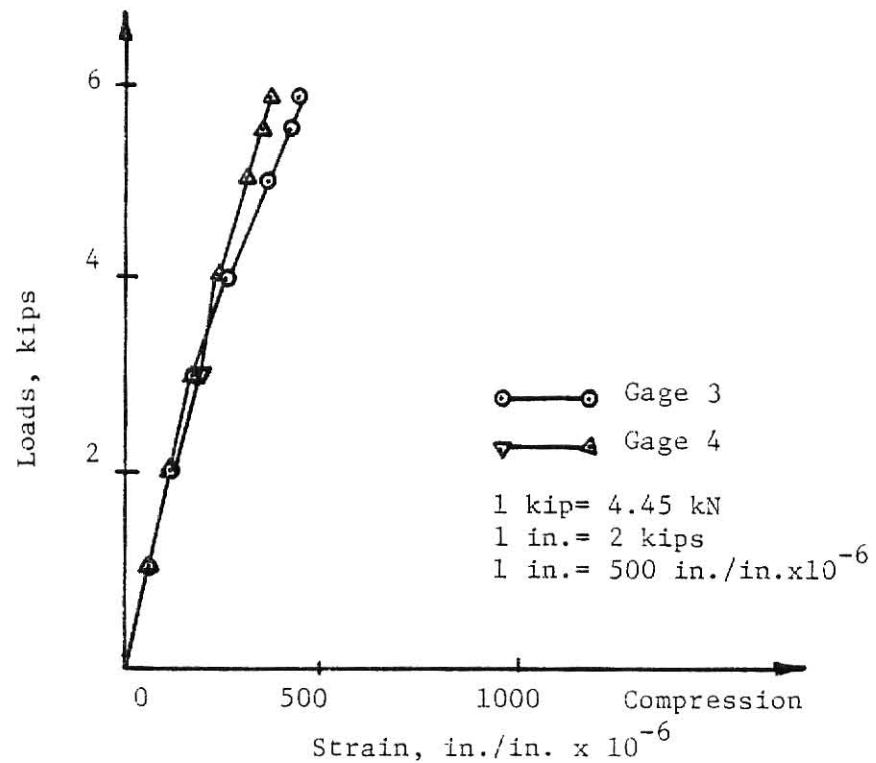


Figure 5.15b Load vs. Strain, Plate 15, Gages 3 & 4
(SS - Opening at Top - $s = 2.0$ in.)

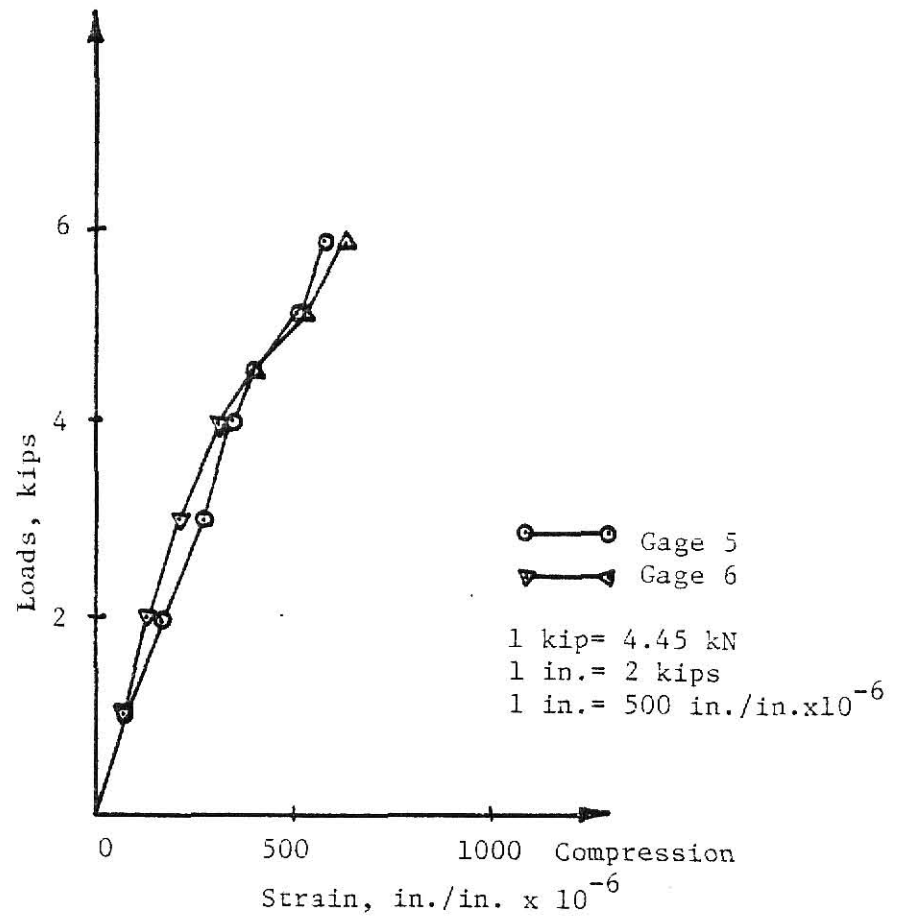


Figure 5.15c Load vs. Strain, Gages 5 & 6, Plate 15
(SS - Opening at Top - $s=2.0$ in.)

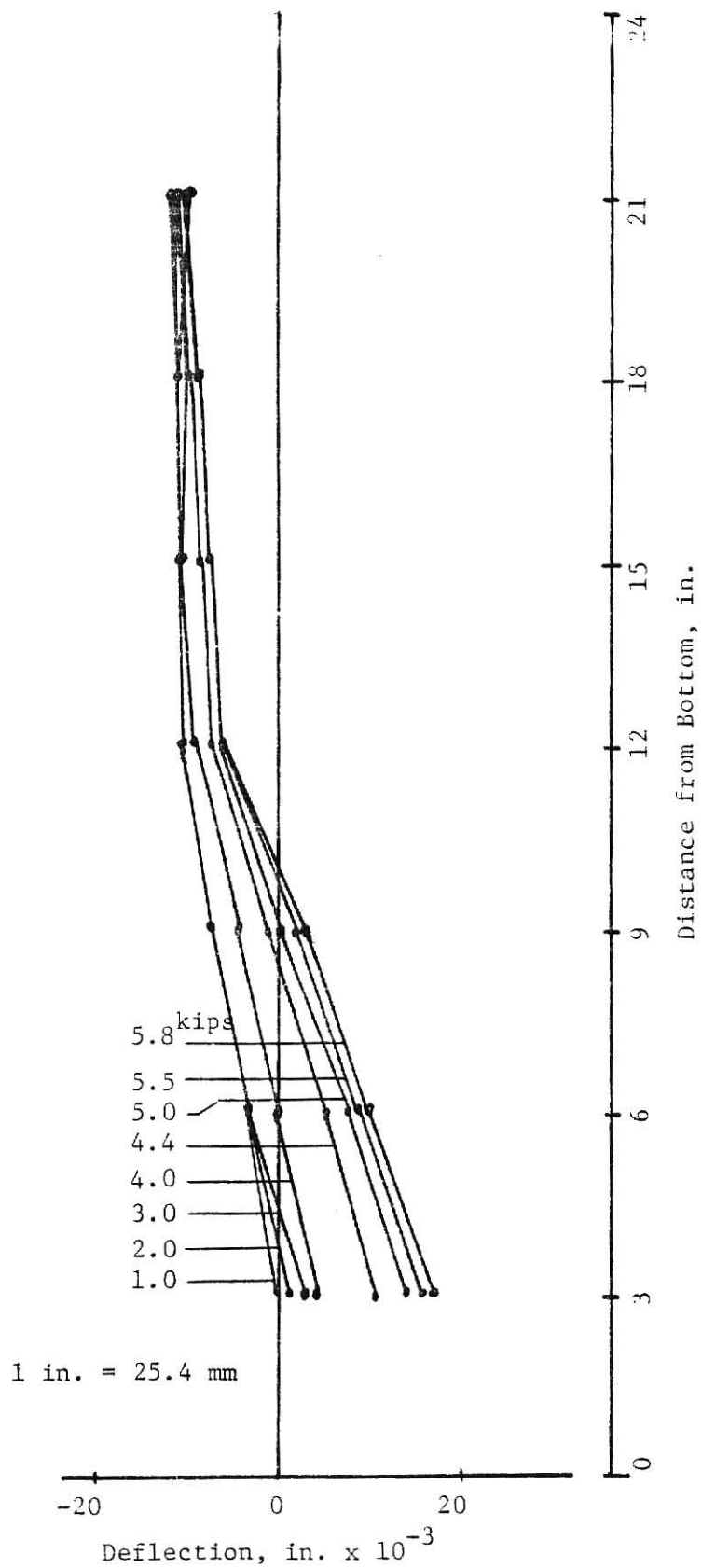


Figure 5.15d Deflection Profiles for Plate 15
(SS - Opening at Top - $s = 2.0$ in.)

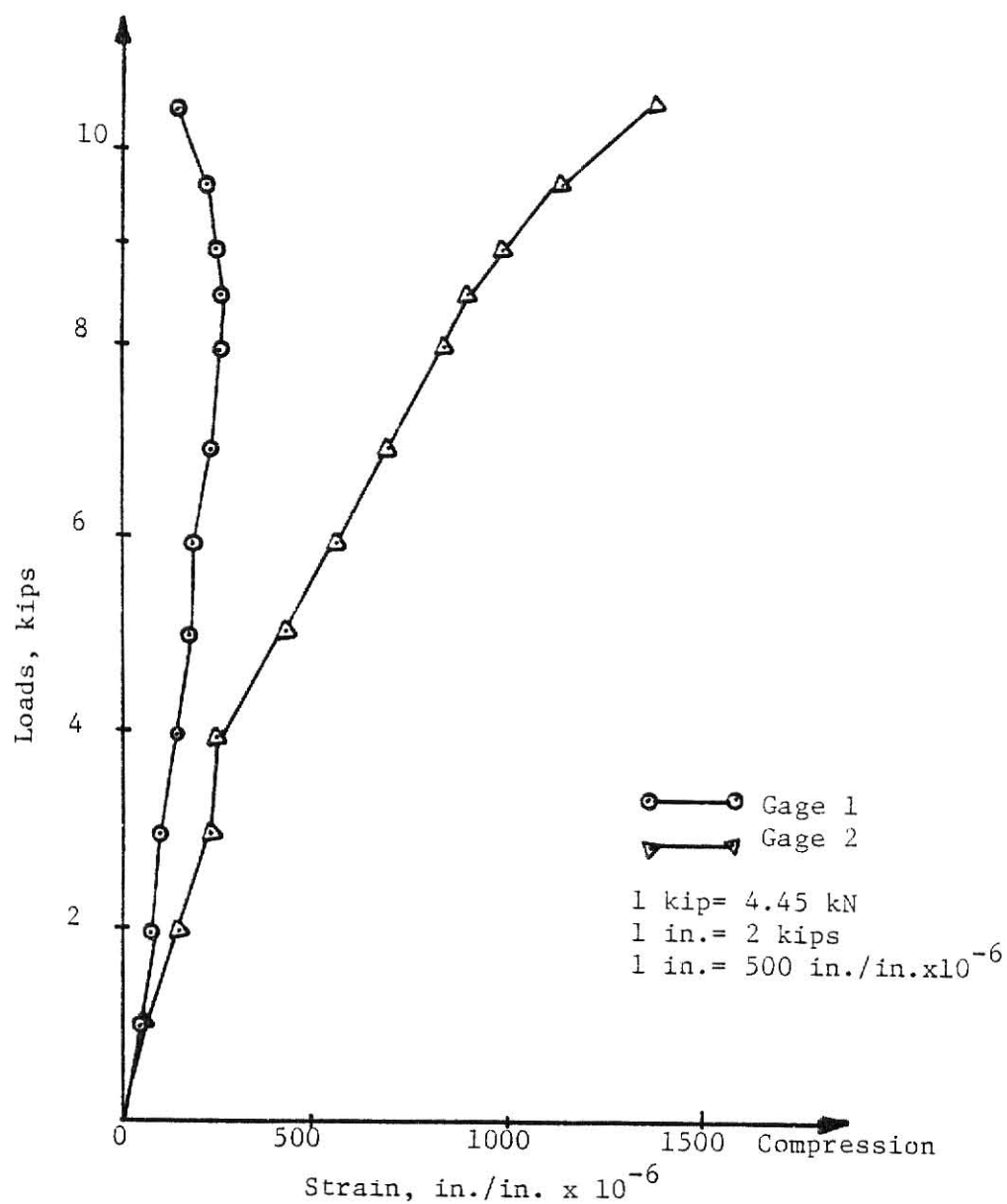


Figure 5.16a Load vs. Strain, Plate 16, Gages 1 & 2
 (SS - Opening at Top, $s = 1/2$ in.)

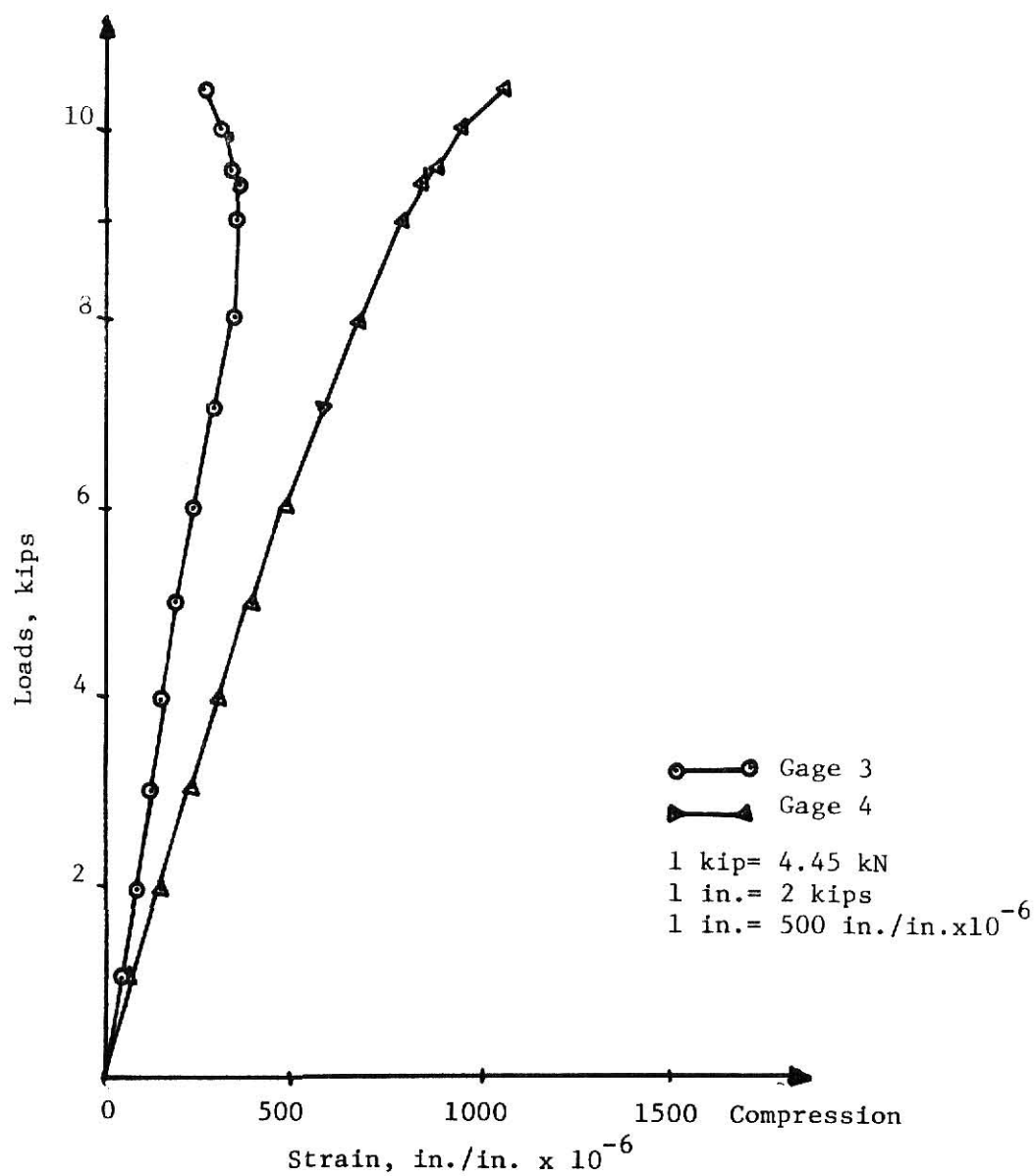


Figure 5.16b Load vs. Strain, Plate 16, Gages 3 & 4
(SS - Opening at Top - $s=1/2$ in.)

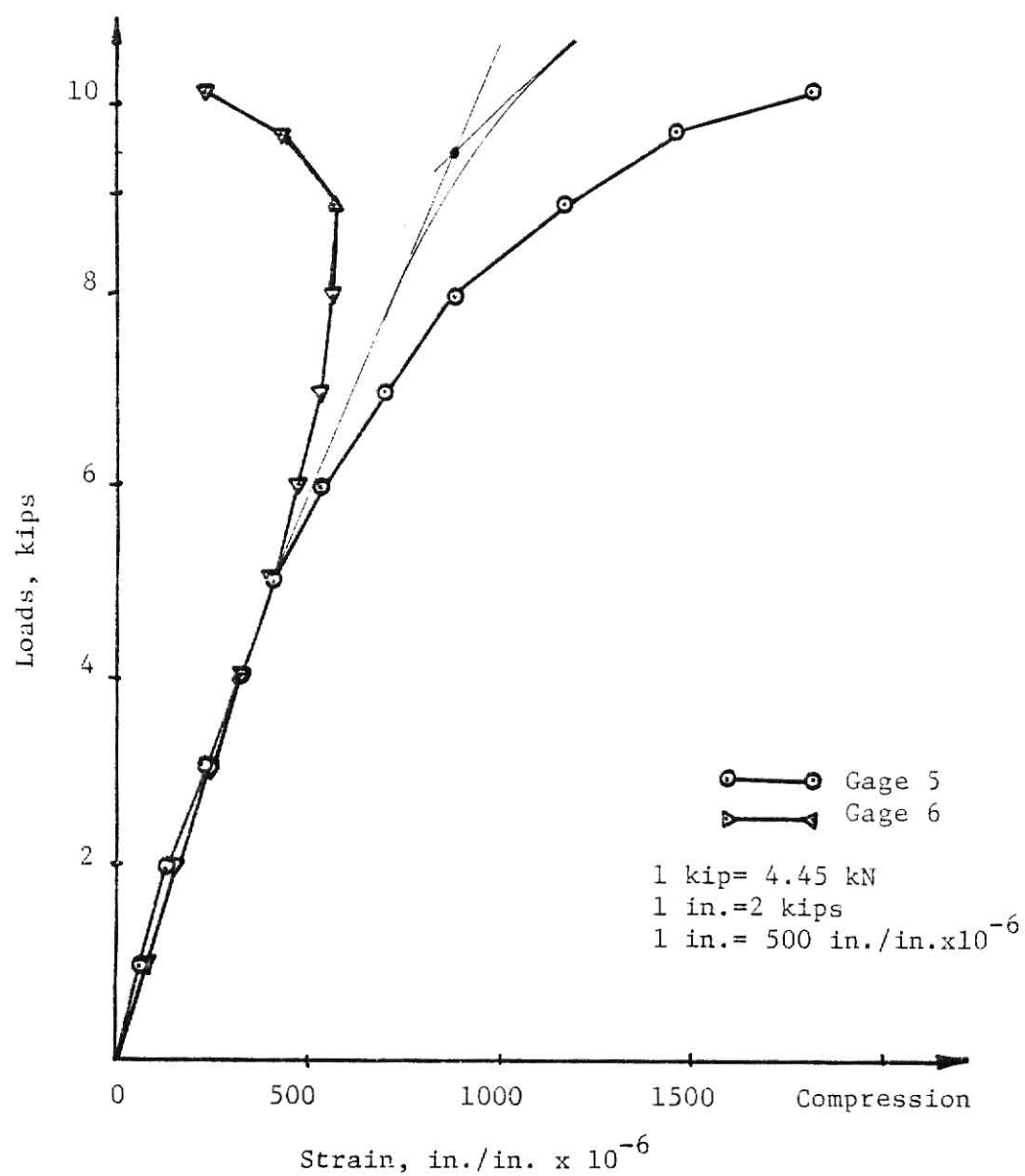


Figure 5.16c Load vs. Strain, Plate 16, Gages 5 & 6
(SS - Opening at Top - $s = 1/2$ in.)

**THE FOLLOWING
PAGE WAS BOUND
WITH THE PRINTING
EXTENDING INTO THE
BINDING, AND IS
ILLEGIBLE DUE TO
BEING CUT OFF AND
BEING A POOR
QUALITY COPY.**

**THIS IS AS RECEIVED
FROM THE
CUSTOMER.**

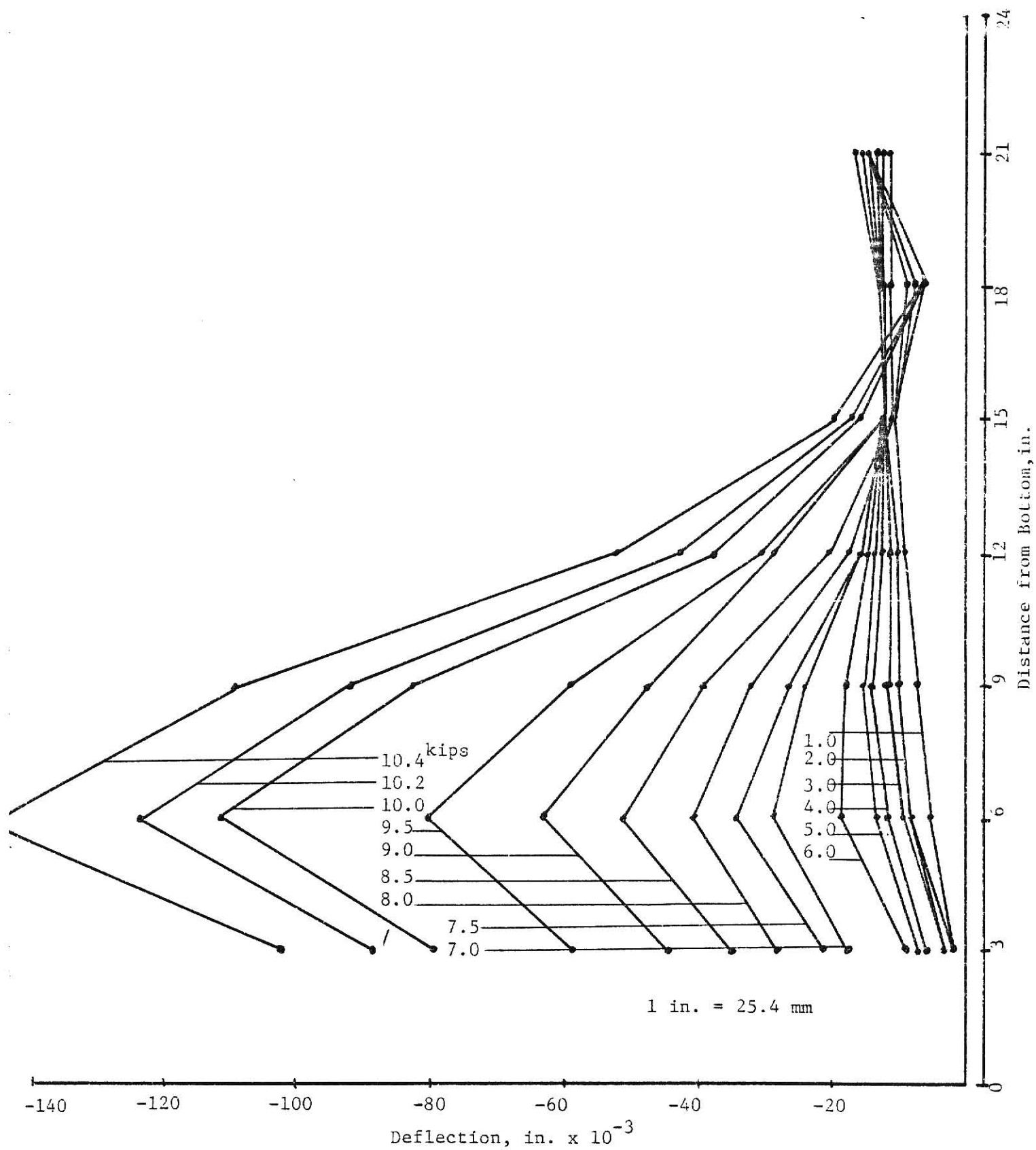


Figure 5.16d Deflection Profiles for Plate 16
(SS - Opening at Top - $\bar{s} = 1/2$ in.)

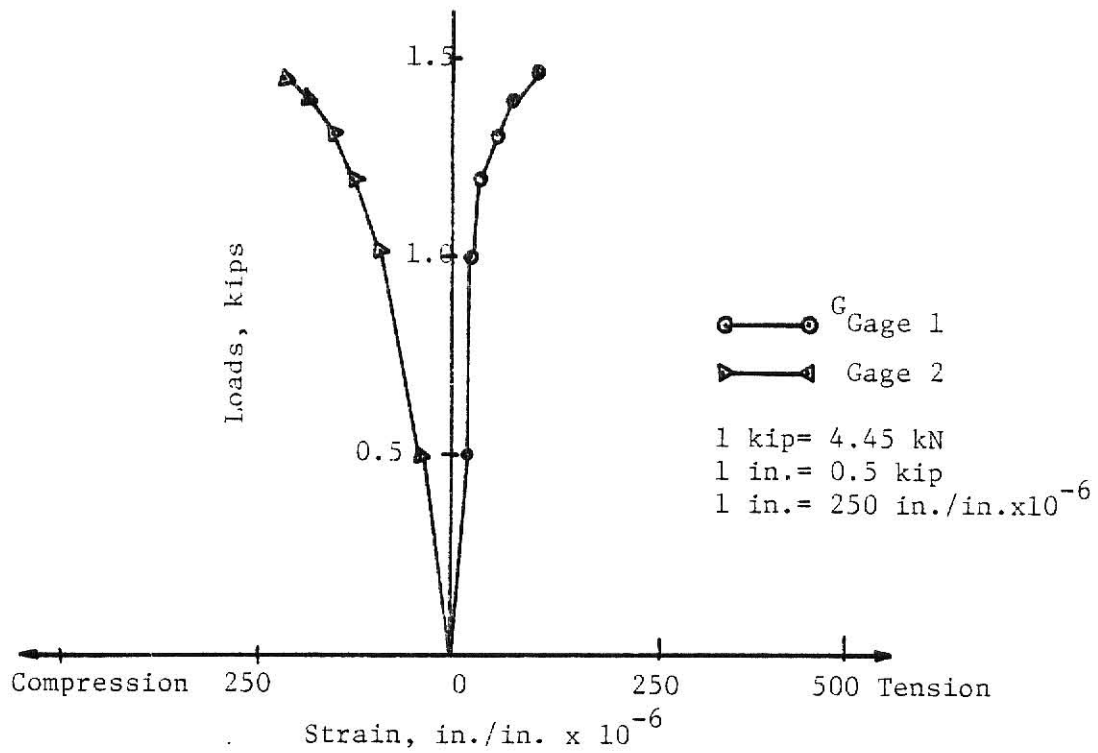


Figure 5.17a Load vs. Strain, Plate 17, Gages 1 & 2
(Free - Opening at Top - $s = 1.0$ in.)

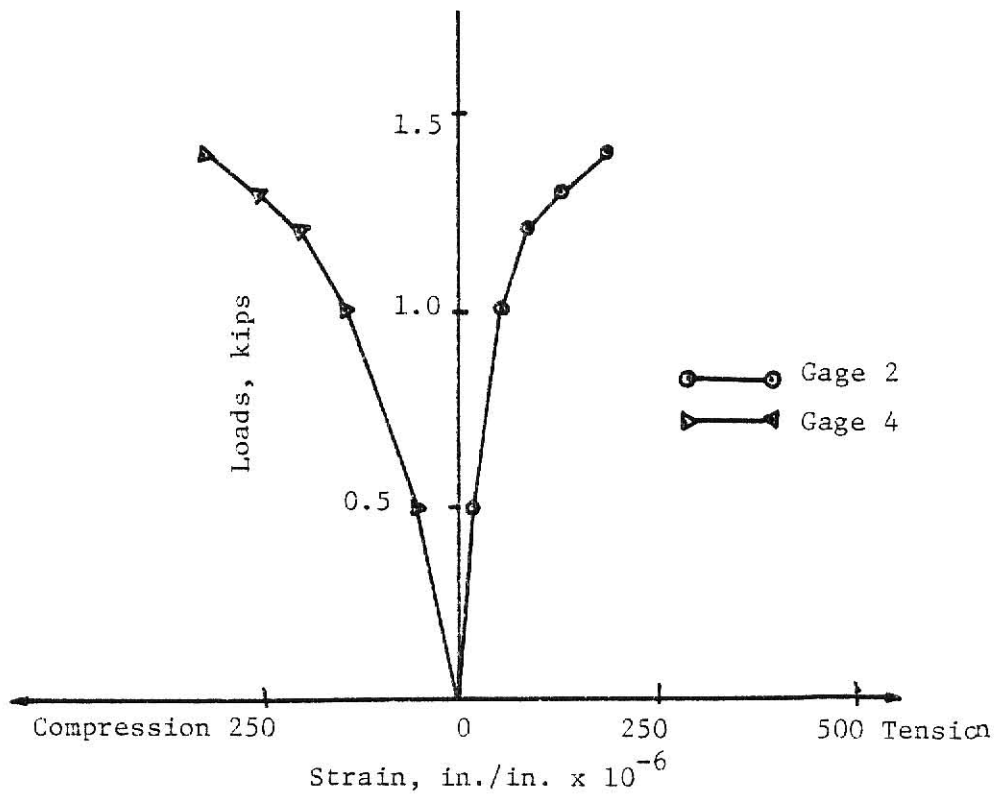


Figure 5.17b Load vs. Strain, Plate 17, Gages 3 & 4
(Free - Opening AT Top - $s = 1.0$ in.)

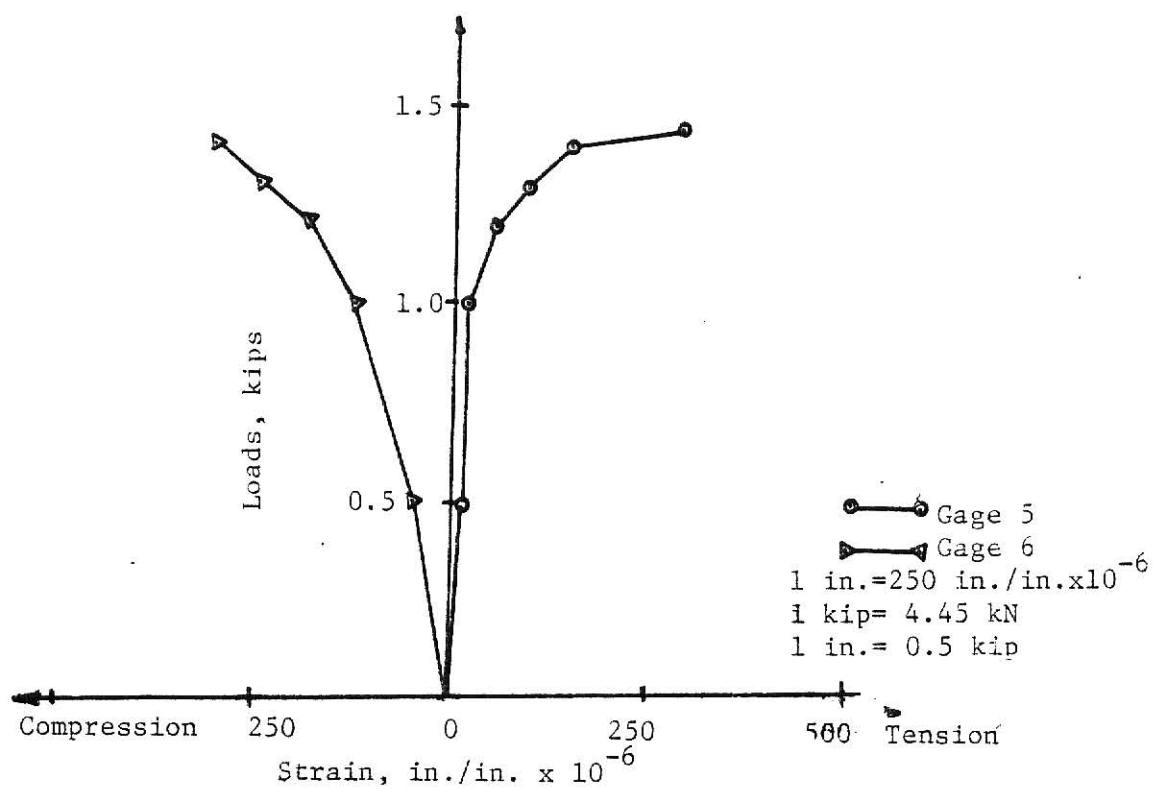


Figure 5.17c Load vs. Strain, Plate 17, Gages 5 & 6
 (Free - Opening at Top - $s=1.0$ in.)

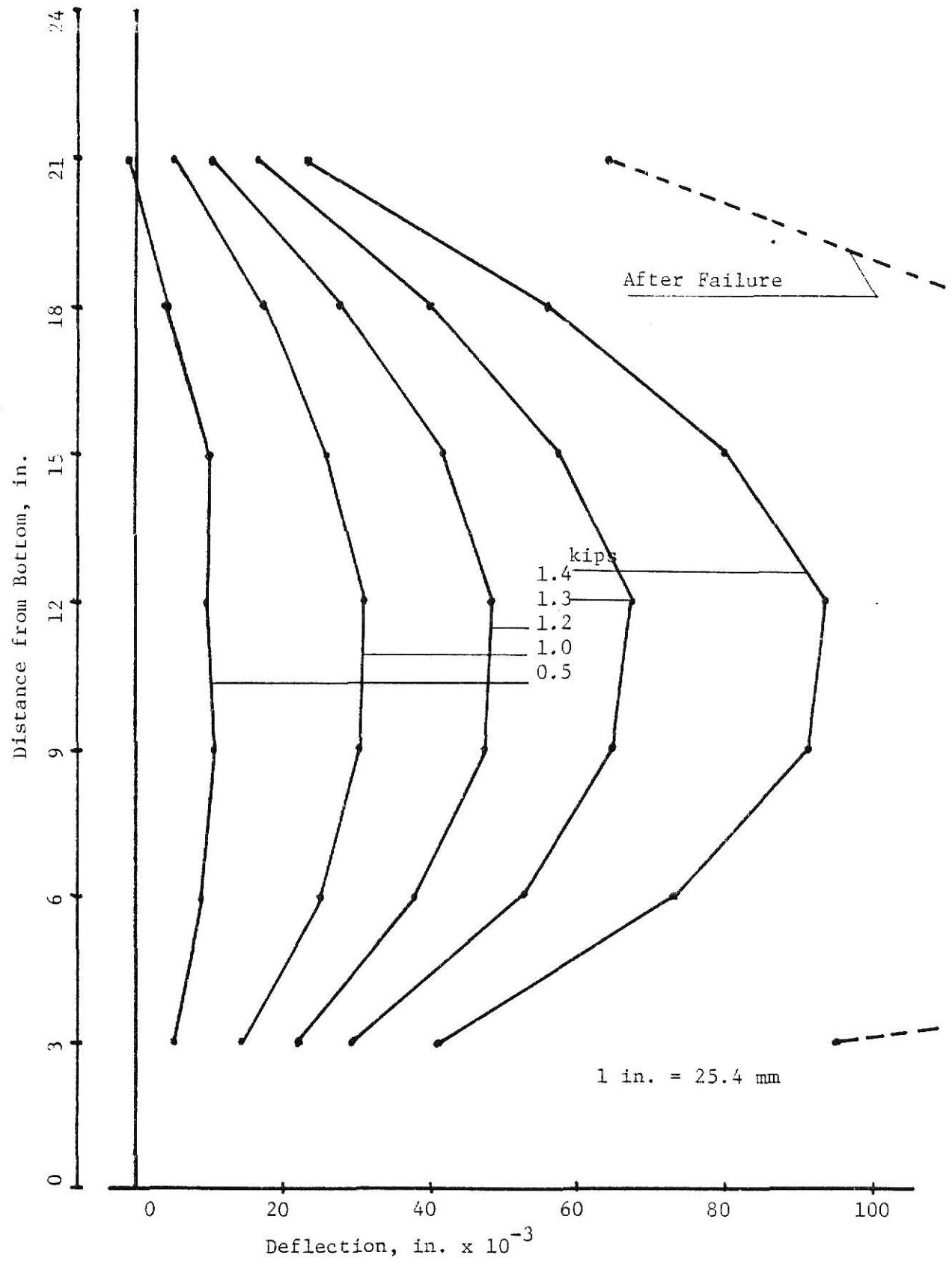


Figure 5.17d Deflection Profiles for Plate 17
(Free - Opening at Top - $s=1.0$ in.)

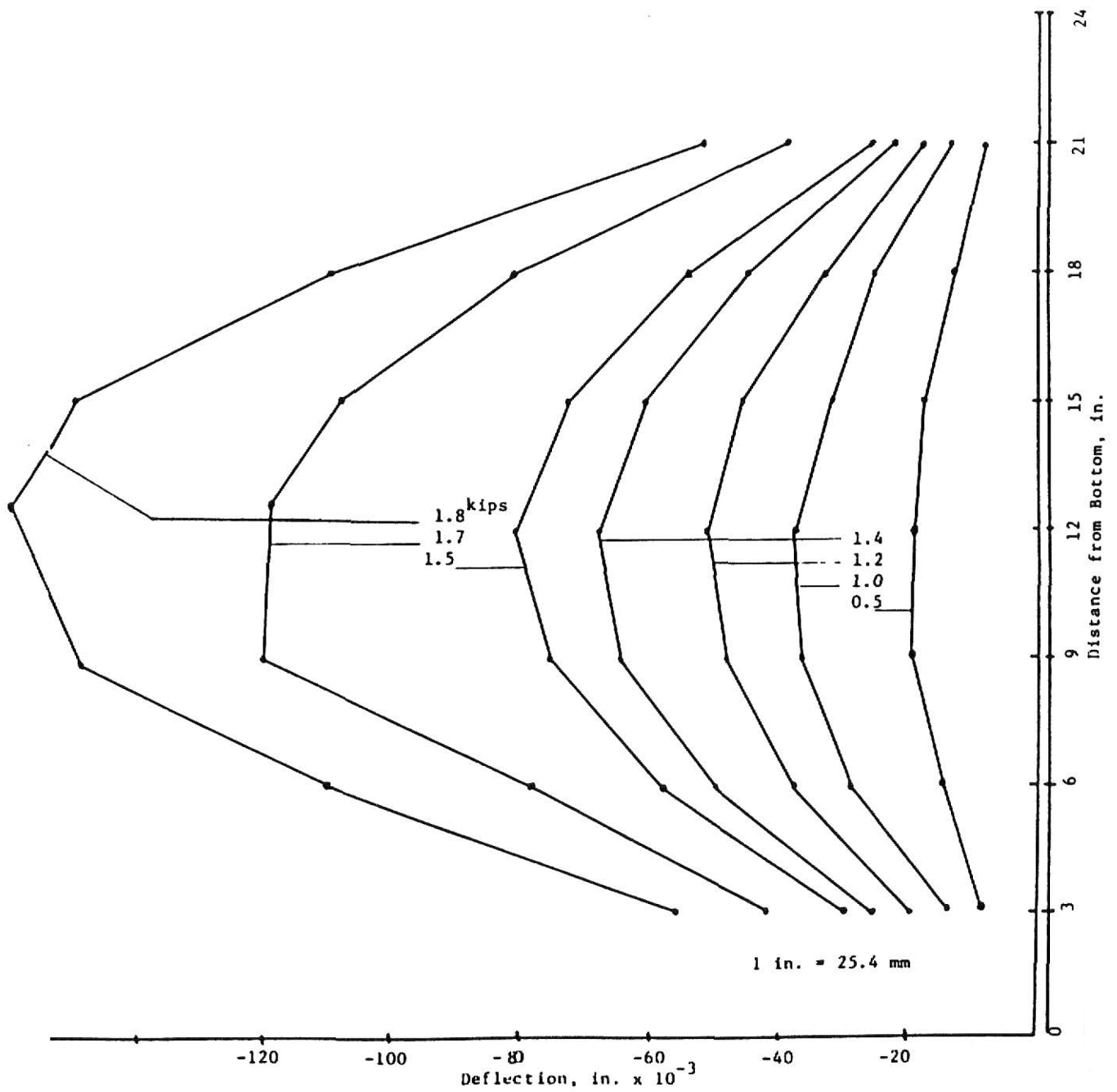


Figure 5.18d Deflection Profiles for Plate 18
(2CA - Opening at Bottom - $s=2.0$ in.)

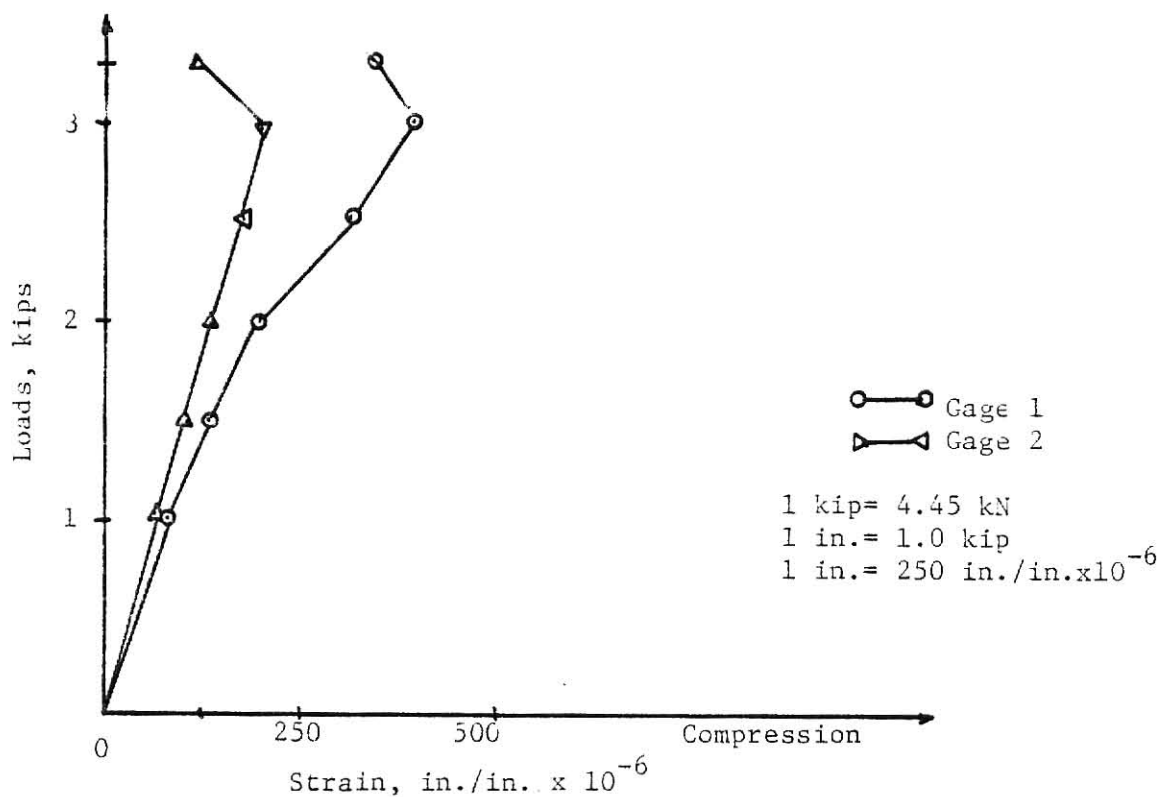


Figure 5.19a Load vs. Strain, Plate 19, Gages 1 & 2
 (2CA - Opening at Bottom, $s = 2.0$ in.)

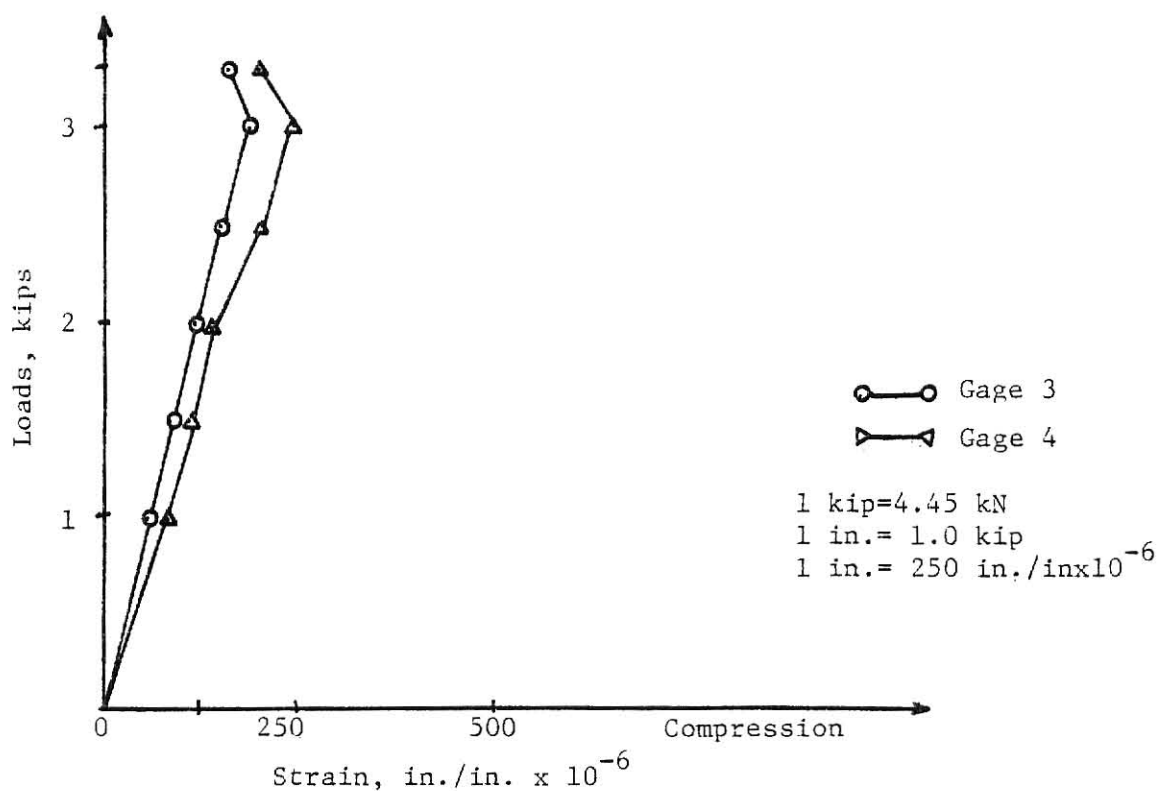


Figure 5.19b Load vs. Strain, Plate 19, Gages 3 & 4
 (2CA - Opening at Bottom - $s = 2.0$ in.)

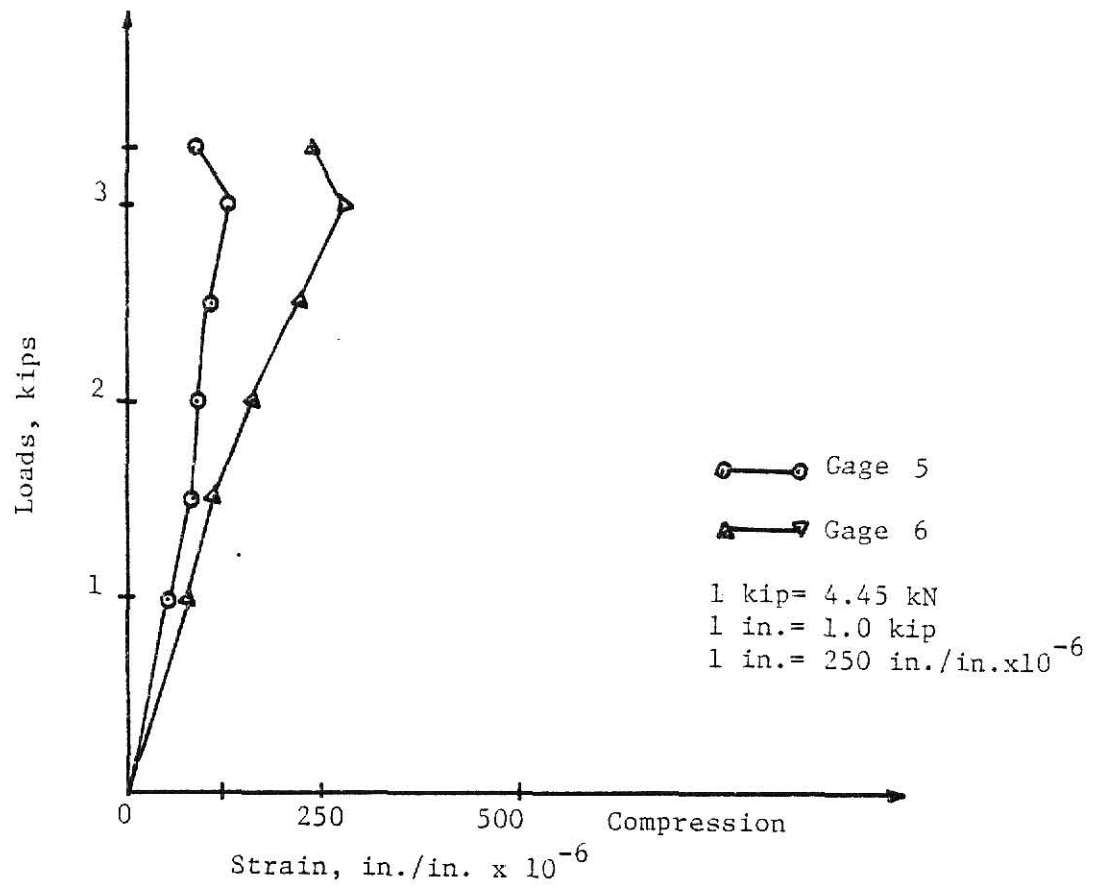


Figure 5.19c Load vs. Strain, Plate 19, Gages 5 & 6
(2CA - Opening at Bottom - $s=2.0$ in.)

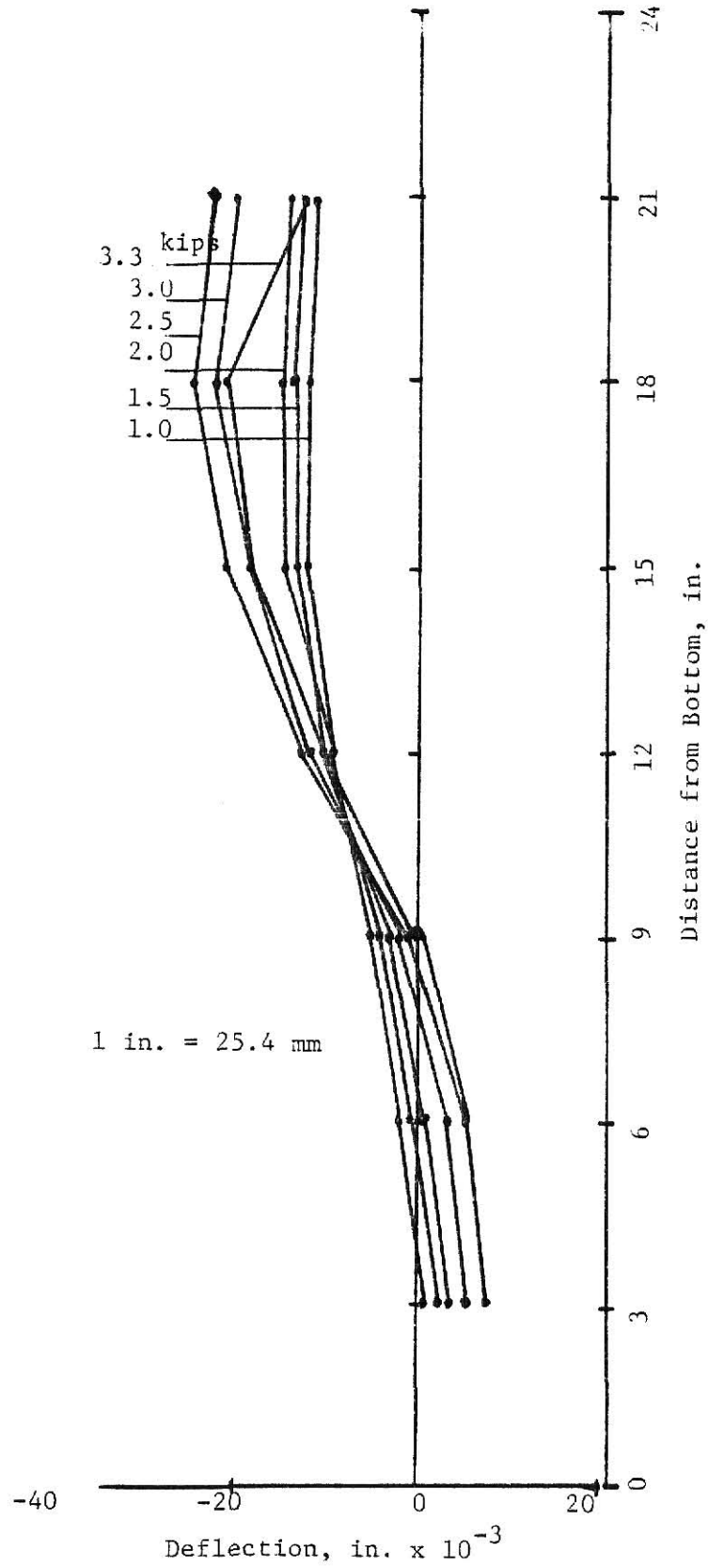


Figure 5.19d Deflection Profiles for Plate 19
(2CA - Opening at Bottom - $s=2.0$ in.)

Table 5.1 Values of Critical Load P_{CrT} (ACI) Using
Theoretical Panel Thickness

$t = 0.25$ in. (6.4 mm)

Plate	f'_c , psi	ϵ_0 , $\mu\epsilon$	f_a , psi	P_a , lb
1 to 4	7,420	3,100	326	978
8 to 11	7,100	3,200	318	956
12 to 16	6,300	2,600	300	900
5,6,7 and 17	7,300	2,900	323	969
15 and 20	6,400	2,800	302	906

Table 5.2 Values of P_{CrT} (ACI) Using Actual Panel Thickness

Plate	f'_c , psi	t , in*	F_a , psi	P_a , lb
1	7,420	0.266	369	1,177
2	7,420	0.248	320	954
3	7,420	0.268	374	1,204
4	7,420	0.258	347	1,074
8	7,100	0.233	277	774
9	7,100	0.282	405	1,372
10	7,100	0.276	388	1,286
11	7,100	0.263	353	1,113
12	6,300	0.247	293	868
16	6,300	0.247	293	868
15	6,400	0.240	279	803
5	7,300	0.274	388	1,276
6	7,300	0.272	382	1,248
7	7,300	0.287	426	1,467
17	7,300	0.262	355	1,116

* Average Thickness of a Bulldged Face of Each Plate

1 in = 25.4 mm
1 lb = 4.5 N
1 psi = 6.9 KPa

Table 5.3 Cylinder Compressive Load-Strain Data From Five Batches

Cylinder	Plate	Average Cylinder Strength f'_c , psi	Strain at Ultimate Stress ϵ_o , in./in. $\times 10^6$	Poisson's Ratio
I	1 to 4	7,420	3,100	0.19
II	8 to 11	7,100	3,200	0.21
III	12 and 16	6,300	2,600	0.18
IV	5,6,7 and 17	7,300	2,900	0.21
V	15 and 20	6,400	2,800	0.20
	Mean	6,900	2,900	0.19

1 psi = 6.9 KPa

Table 5.4 Theoretical Values of Critical Load
(P_{crT}) Using Design Panel Thickness

$$t = 0.25 \text{ in (6.4 mm)}$$

$$I = 15.62 \text{ in}^4 10^{-3} (6497.9 \text{ mm}^4)$$

Plate Number	Long Side Support Conditions*	n**	ϵ_{cr} , $\mu\epsilon$	f_{cr} , psi	P_{crT} , lb
1	SS	--	1,120.7	3,735.86	11,732
2	SS	--	1,120.7	3,735.86	11,732
3	2CA	2	280.1	1,280	3,962.6
4	2CA	2	280.1	1,280	3,962.6
8	SS	--	1,123.8	3,494.5	10,483
9	SS	--	1,135.7	3,523.6	11,645
10	2CA	2	271.1	1,152	3,696
11	2CA	2	289	1,224	3,673
12	Free	1	70.54	337	1,072.5
16	SS	--	1,072	3,505.6	11,523
15	SS	--	1,087.5	3,405	10,472
5	Free	1	70.83	352	1,117
6	2CA	2	27.3	1,305.6	4,151.5
7	Free	1	72.8	361.8	1,116.6
17	Free	1	72.8	361.8	1,116.6

$$1 \text{ psi} = 6.9 \text{ KPa}$$

$$1 \text{ lb} = 4.5 \text{ N}$$

*SS = Simply-Supported; 2CA = Two Double Clip Angles at Midheight & Free

**n = Number of Waves Panels Deflects

$$1 \text{ in} = 25.6 \text{ mm}$$

$$1 \text{ lb} = 4.5 \text{ N}$$

$$1 \text{ psi} = 6.9 \text{ KPa}$$

Table 5.5 Theoretical Values of Critical Load (P_{CrA}) Using Actual Panel Thickness

Plate Number	Long Support Type	Spacing (in)	n	Thickness t(in)*	I (in ⁴ x 10 ⁻³)	ϵ_0 ($\mu\epsilon$)	f'_c (psi)	ϵ_{cr} ($\mu\epsilon$)	f_{cr} (psi)	P_{CrC} (lb)
1	SS	1	--	0.266	18.82	3,100	7,420	1,126	4,002	13,342
2	SS	1	--	0.248	15.25	3,100	7,420	1,107	3,701	11,528
3	2CA	1	2	0.268	19.25	3,100	7,420	3,201	1,453	4,814
4	2CA	1	2	0.258	17.17	3,100	7,420	297.6	1,356	4,328.8
8	SS	0	--	0.233	12.65	3,200	7,100	1,008	3,204	8,958.7
9	SS	$\frac{1}{2}$	--	0.282	22.42	3,200	7,100	1,348	4,013	14,823
10	2CA	$\frac{1}{2}$	2	0.276	21.02	3,200	7,100	328.8	1,384	4,875.7
11	2CA	0	2	0.263	18.19	3,200	7,100	318.2	1,341.8	4,234.8
12	Free	$\frac{1}{2}$	1	0.247	15.07	2,600	6,300	68.86	329.3	1,035.5
16	SS	$\frac{1}{2}$	--	0.247	15.07	2,600	6,300	1,054	3,462	11,238
15	SS	2	--	0.240	13.82	2,800	6,400	1,024.8	3,253.5	9,808.6
5	Free	$\frac{1}{2}$	1	0.274	20.57	2,900	7,300	85.3	423	1,464
6	2CA	$\frac{1}{2}$	2	0.272	20.12	2,900	7,300	320.3	1,523.5	5,249
7	Free	1	1	0.287	23.64	2,900	7,300	95.88	474.7	1,676
17	Free	1	1	0.262	17.98	2,900	7,300	79.9	396.9	1,282

* Average Thickness Measured at Bulged Face of Each Plate

1 in = 25.4 mm
1 in⁴ = 416,230 mm⁴
1 psi = 6.9 KPa
1 lb = 4.5 N

Table 5.6 Evaluation of Experimental Buckling Load ($P_{Cr E_i}$) Using Different Approaches

Plate Number	Long Side Support	Spacing (in)	$P_{Cr E1}^*$ (lb)	$P_{Cr E2}^{**}$ (lb)	$P_{Cr E3}^{***}$ (lb)	Failure Load P_F (lb)	Buckling Location
1	SS	1	10,800	11,000	10,300	11,350	1/3 from top
2	SS	1	8,700	8,500	8,200	9,000	1/4 from top
3	2CA	1	4,500	6,200	5,000	6,400	1/4 from top and 1/4 from bottom (with cracks parallel to edges)
4	2CA	1	5,500	6,600	5,700	6,650	1/4 from top and bottom, middle (corresponding to cracks)
5	Free	1/2	2,000	3,400	2,250	3,460	1 wave largest deflection at 1/4 from bottom (thinner thickness)
6	2CA	1/2	7,000	7,750	7,200	8,000	1/4 from bottom, 1/4 from top
7	Free	1	--	1,200	--	1,260	damaged with small cracks before test
17	Free	1	1,200	1,400	1,100	1,450	middle toward bottom edge
9	SS	1/2	--	10,200	--	10,300	local fracture at top edge
10	2CA	1/2	8,000	9,500	8,400	9,500	1/4 from top, 1/4 from bottom (with cracks)
11	2CA	0	--	7,000	--	7,400	series of fractures in top half
8	SS	0	--	6,600	--	6,800	middle with hole of 10in x 3in
12	Free	1/2	--	3,150	--	3,180	cracks at 1/3 from top
16	SS	1/2	9,000	10,400	9,400	10,600	4in from bottom (trapezoidal yield line)
14	SS	2	5,300	5,500	5,300	5,600	1/8 from top
15	SS	2	5,800	5,800	5,500	5,960	bottom support (no indication of buckling)
18	Free	2	--	1,800	--	1,810	plate midheight toward top
19	2CA	2	3,000	3,000	3,000	3,300	local fracture at top

* $P_{Cr E1}$ = Evaluated from Mikhail of Guralnick Method** $P_{Cr E2}$ = Obtained from Vertical Deflection Profiles*** $P_{Cr E3}$ = Obtained from Average Stain Method

1 in = 25.4 mm

1 lb = 4.5 N

Table 5.7 Identification of the Buckling Loads

Plate number	Support Type & (Spacing, in)	Theoretical Buckling Load P _{crT} (lb)	Calculated Buckling Load P _{crC} (lb)	Experimental Buckling Load P _{crE} (lb)	Failure Load PF (lb)	$\frac{P_{crE}}{P_{crT}}$	$\frac{P_{crE}}{P_{crC}}$	$\frac{P_{crE}}{P_F}$
8	SS (0)	10,483	8,958+	6,600*	6,800	0.629	0.736	0.970
9	SS ($\frac{1}{2}$)	11,645	14,823	10,200*	10,300	0.876	0.688	0.990
16	SS ($\frac{1}{2}$)	11,523	11,238	9,000	10,600	0.781	0.800	0.849
1	SS (1)	11,732	13,342	10,800	11,350	0.92	0.809	0.951
2	SS (1)	11,732	11,528	8,700	9,000	0.74	0.754	0.967
15	SS (2)	10,472	9,808	5,800	5,960	0.553	0.591	0.973
14	SS (2)	--	--	5,000	--	--	--	--
11	2CA (0)	3,673	4,235++	7,000*	7,400	1.906	1.65	0.946
6	2CA ($\frac{1}{2}$)	4,151	5,249	7,000	8,000	1.686	1.33	0.875
10	2CA ($\frac{1}{2}$)	3,696	4,876	8,000	9,500	2.16	1.64	0.842
3	2CA (1)	3,963	4,814	4,500	6,400	1.13	0.93	0.703
4	2CA (1)	3,963	4,328	5,500	6,650	1.38	1.27	0.827
19	2CA (2)	--	--	3,000	--	--	--	--
5	Free ($\frac{1}{2}$)	1,117	1,464	2,000	3,460	1.79	1.36	0.578
12	Free ($\frac{1}{2}$)	1,072	1,035	3,150*	3,180	2.82	3.04	0.990
7	Free (1)	1,116	1,676	1,200*	1,260	1.07	0.716	0.952
17	Free (1)	1,116	1,282	1,200	1,450	1.07	0.936	0.827
18	Free (2)	--	--	1,800*	--	--	--	--

+ Theoretical Buckling Load Based on Plate Buckling Equation
++ Theoretical Buckling Load Based on Column Buckling Equation
* Values obtained from deflection profile P_{crE2}, all others are from strains P_{crE1}

1 in = 25.4 mm
1 lb = 4.5 N
1 psi = 6.9 kPa

Table 5.8 Buckling Ratio Results

Plate Number	Long Side Support Conditions	Spacing (in)	Predicted Buckling Load $P_{Cr C}$ (lb)	Observed Buckling Load $P_{Cr E}$ (lb)	$\frac{P_{Cr E}}{P_{Cr C}}$
8	SS	0	8,958+	6,600*	0.736
9	SS	$\frac{1}{2}$	14,823	10,200*	0.688
16	SS	$\frac{1}{2}$	11,238	9,000	0.800
1	SS	1	13,342	10,800	0.809
2	SS	1	11,528	8,700	0.754
15	SS	2	9,808	5,800	0.591
11	2CA	0	4,235++	7,000*	1.65
6	2CA	$\frac{1}{2}$	5,249	7,000	1.33
10	2CA	$\frac{1}{2}$	4,876	8,000	1.64
3	2CA	1	4,814	4,500	0.93
4	2CA	1	4,328	5,500	1.27
5	Free	$\frac{1}{2}$	1,464++	2,000	1.36
12	Free	$\frac{1}{2}$	1,035	3,150*	3.04
7	Free	1	1,676	1,200*	0.716
17	Free	1	1,282	1,200	0.936

+ $P_{Cr C}$ = From Plate Type Formula
 ++ $P_{Cr C}$ = From Column Type Formula
 * $P_{Cr E}$ = From Lateral Deflection Profiles

1 in = 25.4 mm
 1 lb = 4.5 N
 1 psi = 6.9 KPa

Table 5.9 Values of the Modulus of Elasticity of Concrete Based on Different Formulas

Plate Number	Support Type Condition (spacing, in)	$E_T = \frac{2f_c'}{\epsilon_o} (1 - \frac{\epsilon_{cr}}{\epsilon_o})$ (10^6 psi)	$E_C = 33w^{1.5}\sqrt{f_c'}$ (10^6 psi)	$E = \frac{Pl^3}{48\Delta I^*}$ (10^6 psi)
3	2CA(1)	4.21	4.46	3.51
4	2CA(1)	4.25	4.46	3.93
10	2CA($\frac{1}{2}$)	3.90	4.36	--
11	2CA(0)	3.92	4.36	4.29
6	2CA($\frac{1}{2}$)	4.38	4.42	6.038
7	Free(1)	4.84	4.42	2.974
17	Free(1)	4.87	4.42	4.528
5	Free($\frac{1}{2}$)	4.86	4.42	5.91
12	Free($\frac{1}{2}$)	4.69	4.11	5.084
Mean		4.43	4.38	4.533

*I Based on Actual Panel Thickness
(at the location of the bulged face)

1 in = 25.4 mm
1 psi = 6.9 KPa

BIBLIOGRAPHY

1. Aldridge, Weldon W., Breen John E., "Useful Techniques in Direct Modeling of Reinforced Concrete Structures," Paper SP 24-5, ACI Publications, pp. 125-140.
2. Anderson, Wayne G., "Analyzing Concrete Mixtures for Pumpability," Title No. 74-42, ACI Journal, September 1977, pp. 447-451.
3. Best, J. F., Lane, O. R., "Testing for Optimum Pumpability of Concrete," Concrete International, October 1980, pp. 9-17.
4. Browne, Roger D., Bamforth Phillip B., "Tests to Establish Concrete Pumpability," Title No. 74-19, ACI Journal, May 1977, pp. 193-203.
5. Carpenter, James E., Roll, Fredric, Zelman, Maier I., "Techniques and Materials for Structural Models," Paper SP 24-3, ACI Publications, pp. 41-63.
6. Committee 318, ACI, "Building Code Requirements for Reinforced Concrete (ACI 318-77)," October 1978, pp. 63-64.
7. Committee 533, ACI, "Design of Precast Concrete Wall Panels," ACI Journal, July 1971, pp. 504-513.
8. Ernst, G. C., Hromadik, J. J., and Riveland, A. R., "Inelastic Buckling of Plain and Reinforced Concrete Columns, Plates, Shells," Bulletin No.3, Engineering Experiment Station, University of Nebraska at Lincoln, August 1953, pp. 211.
9. Harris, Harry G., Sabnis, Gajanan M., White, Richard N., "Reinforcement for Small Scale Direct Models of Concrete Structures," Paper SP 24-6, ACI Publications, pp. 141-158.
10. Houghton, Donald L., Committee 304, "Placing Concrete by Pumping Methods," Title No. 68-33, ACI Journal, May 1971, pp. 327-345.
11. Litte, W. A., Cohen, E., Somerville, G., "Accuracy of Structural Models," Paper SP 24-4, ACI Publications, pp. 65-84.
12. Mikhail, Michael L., and Guralnick, Sidney A., "Buckling of Simply-Supported Folded Plates," Proceedings, ASCE, V. 97, EM5, October 1971, p. 1363.
13. Munoz, A., "Buckling Behavior of Reinforced Concrete Wall Panel Models," KSU, Manhattan, Master's Thesis, 1981.
14. Sabnis, Gajanan M., Mirza, Saeed M., "Size Effects in Model Concrete?" Journal of the Structural Division, ST6, June 1979, pp. 1007-1020.
15. Souza, M. A., Fok, W. C., Walker A. C., "Review of Experimental Techniques for Thin Walled Structures Liable to Buckling," Paper BSSM/RAeS Joint Conference, State of the Art' in Measurement Techniques, September 1982

16. Swartz, S. E., Rosebraugh, V. H., "Buckling of Reinforced Concrete Plates," Journal of the Structural Division, ASCE, January 1974, pp. 195-208.
17. Swartz, S. E., Rosebraugh, V. H., Berman, M., "Buckling Tests on Rectangular Concrete Panels," Title No. 71-5, ACI Journal, January 1974, pp. 33-39.
18. Swartz, S. E., Rosebraugh, V. H., Rogacki, S. A., "A Method of Determining the Buckling Strength of Concrete Panels," presented at the Third International Congress on Experimental Mechanics, Los Angeles, California, May 1973. (Paper No. 2120, Society for Experimental Stress Analysis, Westport, Conn.)
19. Zia, Paul, White, Richard N., Vanhorn, David A., "Principles of Model Analysis," Paper SP 24-2, ACI Publications, pp. 19-37.

COMPUTER PROGRAM

```

5  REM "THIS PROGRAM IS SAVED UNDER THE NAME YAYA..."
10 REM "THIS PROGRAM CALCULATES THE CRITICAL LOAD FOR PLATE SUBJECTED TO
    UNIFORM LOAD ON OPPOSITE SIDES.THE CALCULATION IS BASED ON COLUMN-TYPE
    OR PLATE-TYPE      BUCKLING FORMULAS PREVIOUSLY DISCUSSED IN THIS REPORT"

20 GOTO 50
30 INPUT  "ARE YOU DONE WITH THE CALCULATION (Y/N)?";Y$
40 IF Y$="Y" THEN 125
50 INPUT "Plate number=";IJ
60 INPUT "STRAIN AT ULTIMATE STRESS EO= ";EO
70 INPUT"ULTIMATE STRESS FO= ";FO
80 INPUT "IS THE BUCKLING OF COLUMN TYPE (Y/N)?";A$
90 IF A$="Y" THEN GOSUB 1000
100 REM IF A$=N, THEN THE BUCKLING IS PLATE TYPE
110 IF A$="N" THEN GOSUB 2000
120 GOTO 30
125 PRINT"
    "
130 PRINT "*****Good bye . Have a good day sir!*****"
    "
140 END

1000 REM COLUMN TYPE BUCKLING FORMULA
1010 INPUT "IS THE THICKNESS USED THEORETICAL(Y/N)";B$
1020 LPRINT"Column type buckling - Plate # ";IJ
1030 IF B$="Y" THEN 1040
1040 IF B$="N" THEN 1060
1050 LPRINT " (USING THEORETICAL THICKNESS) "
1055 GOTO 1065
1060 LPRINT " (USING ACTUAL THICKNESS) "
1065 LPRINT " "
1070 INPUT "AREA OF STEEL = ";AS
1080 INPUT "AREA OF CONCRETE = ";AC
1090 INPUT "NUMBER OF WAVES = ";N
1100 INPUT "MOMENT OF INERTIA = ";I
1110 P=29.129E-3
1120 ES=28.20E6
1130 REM :  $EC^2 - (P*(N^2)*I/AC + 2*EO + ES*AS*(EO^2)/(AC*FO))*EC + P*(N^2)*I*EO/AC = 0$ 
1140 D=-(P*(N^2)*I/AC+2*EO+ES*AS*(EO^2)/(AC*FO))
1150 C=(P*(N^2)*I*EO)/AC
1160 EC=(-D-((D^2)-4*C)^.5)/2
1170 FC=FO*((2*EC)/EO-(EC/EO)^2)
1180 PC=AC*FC + AS*ES*EC
1190 LPRINT "AREA OF STEEL ***** AS(Sq.in.)=";AS
1200 LPRINT "AREA OF CONCRETE ***** AC(Sq.in.)=";AC
1210 LPRINT "NUMBER OF WAVES ***** N =" ;N
1220 LPRINT "MOMENT OF INERTIA ***** I (in ^4) =" ;I
1230 LPRINT "STRAIN AT ULTIMATE STRESS ***** EO(in.) =" ;EO
1240 LPRINT "ULTIMATE STRESS ***** FO(psi) =" ;FO
1250 LPRINT "CRITICAL STRAIN IN CONCRETE ***** EC(in.) =" ;EC

```

```

1260 LPRINT "CRITICAL STRESS IN CONCRETE ***** FC(psi)   =";FC
1270 LPRINT "CRITICAL BUCKLING LOAD ***** PC(lbs.)   =";PC
1275 LPRINT " "
1280 RETURN
2000 REM PLATE TYPE FORMULA
2020 INPUT "IS THE THICKNESS USED THEORETICAL(Y/N)";B$

```

```

2030 LPRINT"Plate type buckling - Plate # ";IJ
2040 IF B$="Y" THEN 2060
2050 IF B$="N" THEN 2070
2060 LPRINT " (USING THEORETICAL THICKNESS) "
2065 GOTO 2080
2070 LPRINT " (USING ACTUAL THICKNESS) "
2080 LPRINT" "
2090 INPUT "PLATE THICKNESS = ";TH
2100 INPUT "STEEL RATIO = ";SR
2110 WH=12
2120 A= 6.5797363
2130 ES=28.20E6
2140 B=(A*(TH/WH)^2)/(EO*(1-SR))
2150 EC=EO*(1+0.5*(B-(4+B^2)^0.5))
2160 FC=0.425*F0*B*(-B+(4+B^2)^0.5)
2170 PC=1*WH*TH*(FC*(1-SR)+ES*EC*SR)
2180 LPRINT "PLATE THICKNESS ***** TH(in.)           = ";TH
2190 LPRINT "STEEL RATIO ***** SR(in./in.) = ";SR
2200 GOTO 1230
2210 RETURN

```

APPENDIX B:

NOTATION

- A_c, A_g = Gross cross-sectional area of concrete panel, sq. in.
 A_s = Area of steel reinforcement, sq. in.
 B = Parameter for buckling stress-strain calculations
 C_s = Factor of safety
 E = Modulus of elasticity for concrete, psi.
 E_s = Modulus of elasticity for steel reinforcement, psi.
 E_T = Tangent modulus for concrete, psi.
 e = ratio of ϵ_c to ϵ_o
 e_{cr} = ratio of ϵ_{cr} to ϵ_o
 F_a = Compressive stress, psi.
 f_c = Compressive concrete stress, psi.
 f'_c = Specified compressive strength of concrete, psi.
 f_{cr} = Critical stress of concrete, psi.
 f_y = Yield strength of reinforcement, psi.
 I = Moment of inertia about bending axis of panel, in.⁴
 L = Unsupported length of panel, in.
 l = Ratio of length to width of panel
 n = Number of waves panel deflects
 P_a, P_{cr}, P_{nw} = Critical axial load on panel, lbs., computed by various methods
 P_{crC} = Calculated critical panel load using actual thickness
 P_{crT} = Calculated critical panel load using theoretical thickness

P_{crE} = Experimentally-obtained panel buckling load

t = Thickness of panel, in.

w = Width of panel, in.

w_c = Unit weight of concrete, pcf.

ϵ_c = Concrete strain, in. per in.

ϵ_{cr} = Critical strain, buckling strain, in. per in.

ϵ_o = Strain at ultimate stress, in. per in.

ϵ_y = Yield strain of reinforcing steel, in. per in.

μ = Poisson's ratio

ρ = Ratio of reinforcing steel

ϕ = Strength reduction factor, 0.7 for buckling

BUCKLING BEHAVIOR OF REINFORCED CONCRETE
PLATE MODELS

by

Abdoulaye Yaya SECK

B.S., Ecole Nationale d'Ingenieurs
de Bamako, MALI, West Africa, 1974

AN ABSTRACT OF A MASTER'S THESIS
submitted in partial fulfillment of the
requirements for the degree

MASTER OF SCIENCE

Department of Civil Engineering

KANSAS STATE UNIVERSITY

Manhattan, Kansas

1983

ABSTRACT

The experimental study of this report consisted of making and testing, in uniaxial compression, a series of twenty reinforced microconcrete plate models. Three different ratios of steel wire reinforcement to concrete area were used and three different support conditions along the vertical edges were studied. The top and bottom edges of the plates were always simply-supported. A concrete pump was used to place the concrete in the mold.

The principal objective was to check published theoretical equations, for the buckling loads of plates, against experimental values. Also, a comparison of the results for models to those published for larger plates was undertaken.

Methods for evaluating the experimental buckling load included the use of Miknail and Guralnick method, and the Averaged Strain method, both based on the strain gages behavior at the location of the buckled surface of the plate.

The predicted experimental buckling loads with their ratios are presented for comparison. Depending upon how the unloaded edges were supported, the plate will buckle into single or biaxial curvature. It was concluded that more experimental investigations are needed to verify the proposed plate design formula.